Imatinib reduces non-alcoholic fatty liver disease in obese mice by targeting inflammatory and lipogenic pathways in macrophages and liver

Inauguraldissertation
zur
Erlangung der Würde eines Doktors der Philosophie vorgelegt
der Philosophisch-Naturwissenschaftlichen Fakultät der
Universität Basel
von

Shefaa AlAsfoor
Aus Diraz, Bahrain

Basel, 2019

Originaldokument gespeichert auf dem Dokumentenserver der Universität Basel
edoc.unibas.ch

Genehmigt von der Philosophisch-Naturwissenschaftlichen Fakultät auf Antrag von

Prof. Dr. med. Christoph Hess
Faculty representative and dissertation supervisor
Prof. Dr. med. Marc Donath
co-examiner

Basel, Feb 19th 2019

Prof. Dr. Martin Spiess

Dekan der Philosophisch-
Naturwissenschaftlichen Fakultät

Dedication

To whom their suffering inspired me
Imam Hussain & Dad

To whom is waiting for this moment
Mum

To whom spent their life for our happiness and success
Grandpa & Grandma

Basel, 2019

Acknowledgements

First and foremost, I would like to express my warm and sincere gratitude to my supervisor: PD Dr. Claudia Cavelti-Weder for her continuous and unlimited support during my PhD study. Her supervision guided me in all the time of research and writing this thesis. Thanks for her constructive comments, valuable feedbacks and inspiration.

Besides my supervisors, I am sincerely thankful to my best colleagues in the Translational Diabetes Lab: Theresa Rohm, Angela Jeanne Tamara Bosch, Thomas Dervos, Zora Baumann, Marc Stawiski, and Regula Fuchs. Thank you all for the unlimited support, optimal teamwork and intimate atmosphere.

I am deeply grateful to my PhD committee members for their valuable advices and precious inputs: Prof. Dr. med. Christoph Hess, Prof. Dr. med. Marc Donath, and Prof. Dr. Christoph Handschin

My thankfulness to Donath laboratory members: PD Dr. Marianne Böni for Friederike Schulze, Stéphanie Häuselmann, Erez Dror, Elise Dalmas, Constanze Thienel, Thierry Nordmann, Marcela Borsigova, Katharina Dembinski, Shuyang Traub, Daniel Zeman, Jousua Wehner, Leila Rachid and Sophia Wiedemann for their discussion, their big help, sharing knowledge and cooperation.

I deeply thank Hess laboratory members: for sharing knowledge; Sarah Dimeloe, Marco Fischer and Jasmin Grählert.

I warmly acknowledge my friends and colleagues in the Department of Biomedicine and clinics for their nice assistance and tips particularly: Dr. Matthias Betz, Jana Orellana Miguez, Marc Bigler, Dino Lüthi, Fabian Baldin, Benedikt Meyer, Sophia Thanei, Denise Dubler, Claudia Donat, Pascal Rabatscher, Marwa Almosailleakh, Katharina Leonards, Corina Frick, Annaise Jauch, Fabian Baldin, Berna Kaya, Philipp Wuggenig, Lucia Schirmbeck, Kinga Csorba and Robert Kölm.

I also would like to deeply thanks the animal facility members for the animal care

Special big thanks for our collaborators who participated in this work: Diego Calabrese, Mattias Matter, Michèle Baumann and Achim Weber.

I also would like to expresses my thankfulness to antelope team for their supports and encouragements.

Last but not least; I am most deeply indebted to my parents and grandparents, aunts, uncles, sisters, brothers and cousins. Mum thanks for your cherubic prayer and patience. Dad and granddad, your love from heaven was the cause of my successes. My grandmother grateful to your angelic prayer, I owe my sincere thanks to my uncle A.Al Jalil who I never forget his limitless love, tenderness and support forever in my life.

Finally,

The Federal Commission for Scholarships for Foreign
Thank you very much for funding my PhD study

"And say, My Lord, increase me in knowledge". Surat Taha-115

~Thanks Allah~

Table of content

1. Abstract

Macrophages have been recognized as key players in non-alcoholic fatty liver disease (NAFLD). Our aim was to assess whether pharmacological attenuation of macrophages can be achieved by imatinib, an anti-leukemia drug with known anti-inflammatory and anti-diabetic properties, and how this impact on NAFLD. We analyzed the pro- and anti-inflammatory gene expression of murine macrophages and human monocytes *in vitro* in the presence or absence of imatinib. In a time-resolved study, we characterized metabolic disease manifestations such as hepatic steatosis, systemic and adipose tissue inflammation as well as lipid and glucose metabolism in obese mice at one and three months of imatinib treatment. Our results showed that imatinib lowered pro-inflammatory markers in murine macrophages and human monocytes *in vitro*. In obese mice, imatinib reduced TNFα-gene expression in peritoneal and liver macrophages and systemic lipid levels at one month. This was followed by decreased hepatic steatosis, systemic and adipose tissue inflammation and increased insulin sensitivity after three months. As the transcription factor sterol regulatory element-binding protein (SREBP) links lipid metabolism to the innate immune response, we assessed the gene expression of SREBPs and their target genes, which was indeed downregulated in the liver and partially in peritoneal macrophages. In conclusion, targeting both inflammatory and lipogenic pathways in macrophages and liver as shown by imatinib could represent an attractive novel therapeutic strategy for patients with NAFLD.

List of Abbreviation

Abbreviation	
ATP	Adenosine triphosphate
CCL	Chemokine ligand
CCR	Chemokine receptor
CXCL	Chemokine ligand
DAMP	Damage-associated molecular patterns
FFA	Free fatty acids
GTT	Glucose tolerance test
PPAR-γ	Peroxisome proliferator-activated receptor-gamma
pS273	Phosphorylation at serine 273
PRR	Pattern recognition receptors
HDL	High-density lipoprotein
HFD	High fat diet
ITT	Insulin tolerance test
i.p.	Intraperitoneal
KC	Kupffer cell
NAFLD	Non-alcoholic fatty liver disease
ROS	Reactive oxygen species
SREBP	Sterol regulatory element binding protein
STZ	Streptozotocin
SVF	*Stromal vascular fraction*
T2D	Type 2 diabetes
TLR4	Toll-like receptor 4
TZDs	Thiazolidinediones
VLDL	Very low-density lipoprotein

2. Introduction

2.1 Normal physiology

2.1.1 Energy sources

The human body requires the three energy sources of carbohydrates, lipids and proteins. These biomaterials are metabolized into the smaller biomolecules glucose, fatty acids and amino acids, which can be used to generate adenosine triphosphate molecule (ATP). ATP is a nucleotide known as the "molecular currency" of intracellular energy transfer due to its ability to store and transfer energy in the cells[1].

2.1.2 The concept of glucose homeostasis

Glucose is the main source of energy in the body and is maintained in a physiological range of 3.5-5.5 mmol/L in the blood[2]. Glucose homeostasis is defined as the balance between glucose entering and removal from the circulation. Glucose is derived either exogenously with food intake or endogenously by breakdown of stored glycogen or by gluconeogenesis. The glucose metabolism is regulated by many gluco-regulatory hormones. The key regulators of glucose homeostasis are insulin and glucagon, but also other hormones impact on glucose homeostasis such as amylin, glucagon like peptide-1, glucose-dependent insulin tropic peptide, epinephrine, cortisol and growth hormones. After food intake, pancreatic beta cells sense elevated blood glucose levels via GLUT2 dependent glucose uptake with a subsequent increase in the ATP to ADP ratio, KATP channel closure, opening of voltage gated calcium channels causing insulin granule fusion and exocytosis. Secreted insulin increases glucose uptake by muscles and adipose. Subsequently, the absorbed glucose is converted into glycogen via glycogenesis in the muscles and into triglycerides via lipogenesis in adipose tissue. In the liver, insulin inhibits glucose production via activating glycogenesis and thereby increasing hepatic glycogen. Conversely during starvation, low blood glucose levels stimulate pancreatic alpha cells to release glucagon, which in turn increases glucose production by triggering glycogenolysis and gluconeogenesis in the liver[2, 3].

2.1.3 Fatty acids in homeostatic state

Fatty acid homeostasis is defined as the balance between lipid synthesis (lipogenesis) and lipid breakdown (lipolysis/ fatty acid oxidation). Fatty acids can be obtained exogenously from

nutrition or endogenously by lipogenesis via conversion of acetyl-CoA into triglycerides in both liver and adipose tissue. Normal fasting lipids levels are tightly regulated: Fasting and dietary unsaturated fatty acids prevent lipid synthesis by stimulating lipolysis in adipose tissue and inhibition of lipid synthesis enzymes in the liver, respectively[4, 5]. Moreover during fasting, low plasma insulin levels activate glycolytic and lipogenic enzymes and thereby increase glucose uptake and lipid synthesis[5]. In contrast, a diet rich in carbohydrates triggers lipogenesis in both adipose tissue and liver. Additionally, multiple factors contribute to the regulation of lipid metabolism including diet, hormones such as insulin, growth hormones and leptin as well as transcription factors including sterol regulatory element binding proteins (SREBPs) and peroxisome proliferator-activated receptor gamma (PPAR-γ) in both the liver and adipose tissue[5, 6].

2.2 Pathophysiology

2.2.1 Obesity

Obesity and overweight are global health problems and have increased dramatically over the last years. In 2016, the World Health Organization reported that more than 1.9 billion adults worldwide were overweight with a body mass index (BMI) of 25.0 to 29.9 kg/m² and 600 millions of patients were obese (BMI ≥30 kg/m²)[7-9]. Obesity and overweight are defined as abnormal fat accumulation in adipose tissue[10] and in other insulin sensitive tissues that are associated with insulin resistance[11]. Obesity is strongly linked to insulin resistance related diseases such as type 2 diabetes (T2D), hypertension, dyslipidemia and non-alcoholic fatty liver disease (NAFLD)[7, 8, 12]. Moreover, recent reports revealed that low-grade inflammation is also associated with insulin resistance in obesity and other metabolic diseases[13, 14].

2.2.2 Type 2 diabetes

While about 5% of diabetes cases are considered as type 1 diabetes (T1D) due to a loss in pancreatic β-cells[15, 16], 90-95% of patients are diagnosed with type 2 diabetes (T2D), which is strongly associated with obesity[16]. Interestingly, only one-third of all obese individuals develop T2D. Obesity can progress to T2D when the β-cells of the pancreatic islets fail to compensate for insulin resistance. Whereas insulin resistance defined as an inability of cells to properly respond to the insulin action, β-cell dysfunction refers to insulin deficiency due to impaired insulin secretion or a reduced β-cell mass caused by apoptosis[17, 18]. While T1D arises from

β-cell dysfunction/loss, T2D is a consequence of both insulin resistance and β-cell dysfunction[16]. Physical inactivity, overnutrition, genetics and epigenetics increase the risk for T2D by triggering different mechanisms such as glucotoxicity, lipotoxicity, oxidative stress, endoplasmic reticulum stress, altered gut microbiota and amyloid deposition, which eventually leads to T2D. These various stresses are associated with sterile inflammation during development of T2D[19-25].

2.2.3 Non-alcoholic fatty liver disease

Non-alcoholic fatty liver disease (NAFLD) has become the most frequent chronic liver disease in developed countries affecting more than 30% of the population[26-28]. Moreover, NAFLD is the main cause for liver transplantations nowadays[29]. NAFLD comprises of a wide spectrum of diseases ranging from simple fatty liver (NAFL) or steatosis to non-alcoholic steatohepatitis (NASH). NAFL is determined by the accumulation of more than 5% of fat droplets in hepatocytes[30]. NASH is characterized by different features of hepatocellular injury such as ballooning, apoptosis/necrosis, Mallory's hyaline bodies, giant mitochondria and inflammation/ fibrosis[31, 32].

NAFLD is classified into a primary and secondary form based of the underlying pathogenesis[33]: Primary NAFLD is strictly associated with insulin resistance and metabolic disease such as obesity and T2D. For example, 80 % of NAFLD subjects are obese[34] and around 61 % of NAFLD patients have T2D[35, 36]. Moreover, NAFLD in diabetic patients is linked to increased risk of cardiovascular disease[37] and chronic kidney diseases[38]. The secondary form of NAFLD is caused by underlying diseases such as hepatitis C[39], HIV[40], metabolic disorders i.e. hypopituitarism[41] or some drugs like tamoxifen[42] and methotrexate[43].

Pathogenesis of non-alcoholic fatty liver disease

The molecular etiology and mechanisms behind the pathophysiology of NAFLD are complicated as many factors and pathways contribute to the disease development[44]. Recently, a multiple-hit hypothesis was introduced to explain the development of NAFLD[45]. Diet, genetic polymorphisms[46], altered gut microbiota[47] and hormones secreted by adipose tissue[48] have been postulated as important contributors for NAFLD development. However, insulin resistance, hepatic lipid accumulation (lipotoxicity), inflammation and mitochondrial

dysfunction are key mechanisms for disease progression and they have been broadly studied in the context of NAFLD and metabolic syndrome[44].

The link between insulin resistance and lipid accumulation in NAFLD

In the physiological state, glucose is catabolized into fatty acids through the multi-enzyme process of de novo lipogenesis in the liver. In addition, fatty acids in the liver are either oxidized in the mitochondria or anabolized into triglycerides and released into the blood as very low-density lipoprotein (VLDL)[44, 49]. However, excessive food intake and insulin resistance result in alterations of fatty acid and glucose homeostasis, leading to an accumulation of lipids in the liver, also known as steatosis.

Hepatic lipid accumulation happens by three different ways during NAFLD progression: In the NAFL stage, steatosis occurs either due to an increased free fatty acids (FFA) influx originating from dysfunctional adipose tissue or an increased hepatic de novo lipogenesis resultant from excess dietary carbohydrate[30, 33, 44, 49-51]. In the NASH stage, decreased lipid exportation as VLDLs contributes to lipid accumulation in the liver[51] (Fig. 1).

Different mechanisms have been proposed behind abnormal lipid accumulation in the liver. In the adipose tissue, insulin resistance reduces the inhibitory action of insulin on the hormone sensitive lipase (HSL) and triggers the breakdown of triglycerides, which subsequently leads to an increase of FFA in the circulation.

In the liver, increased dietary FFA influx and lipogenesis result in hepatic lipotoxicity augmenting insulin resistance[33]. Hepatic insulin resistance is mediated by lipid intermediates particularly diacylglycerols and ceramides[44, 49, 52]. Accumulation of diacylglycerols and ceramides inhibits insulin signaling by activating Protein kinase Cε[53] and by suppression of protein kinase B[50], respectively. Moreover, under hyperinsulinemic conditions, hepatic glucose production is increased due to an increase in Forkhead box A2 (FOXA2) protein, a master regulator of gluconeogenesis. Paradoxically, insulin promotes increased de novo lipogenesis by enhancing SREBP1c through the stimulation of mTOR complex 1[44, 54]. An additionally postulated mechanism is the upregulation of hepatic PPAR-γ mRNA together with SREBP1c in obese NAFLD patients[55].

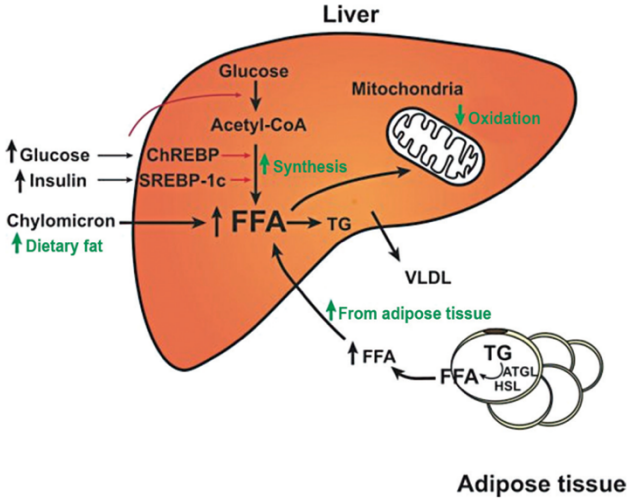

Figure 1| Development of steatosis in non-alcoholic fatty liver disease. In the homeostatic state, hepatic lipids are derived from dietary fat, hepatic *de novo* lipogenesis and peripheral adipose tissue. In insulin resistant individuals, lipid metabolism is altered resulting in increased steatosis. Adipose tissue lipases (i.e. HSL, ATGL) are not inhibited by insulin, leading to a continuous influx of free fatty acids (FFAs) to hepatocytes. Hyperglycemia and hyperinsulinemia stimulate both carbohydrate response element binding protein (ChREBP) and sterol regulatory element binding protein-1c (SREBP-1c) in the liver, causing increased *de novo* fatty acid synthesis. In hepatic mitochondria, fatty acid oxidation is reduced due to boosted acetyl-coenzyme A (CoA), which is generated from increased fatty acid synthesis. Thus, free fatty acids in the liver are favorably esterified to triglycerides (TG) with an increased exportation of very low-density lipoprotein (VLDL) into the blood stream. However, in the NASH stage, VLDL exportation is decreased resulting in an increase of TG in the liver and a decrease of VLDL in the plasma. Abbreviations: HSL; hormone sensitive lipase, ATGL; adipose triglyceride lipase. Figure was taken from Moon, Y.A., 2017[56].

Inflammation in NAFLD

The initial accumulation of triglycerides in hepatocytes is considered as benign and a physiological response to potentially toxic triglycerides metabolites. This was demonstrated in a NASH model where inhibition of triglycerides synthesis improved steatosis, but aggravated liver damage[57, 58]. However, accumulation of FFA and cholesterol in the mitochondria of hepatocytes is considered as a dangerous signal. This kind of accumulation leads to metabolic stress resulting in an increase of Tumor necrosis factor alpha (TNF-α) and reactive oxygen species (ROS) production mediating liver damage and inflammation, eventually resulting in NASH development[59, 60].

The progression of steatosis to NASH is associated with a chronic sterile inflammation, which is triggered by endogenous damage-associated molecular patterns (DAMPs) produced by cellular damage or stress i.e. high-mobility group box 1 (HMGB1), saturated fatty acids, cholesterol crystals, proteins, uric acid and ATP and exogenous gut-derived pattern-associated molecular patterns (PAMPs) such as lipopolysaccharide (LPS), bacterial DNA or

peptidoglycans, which reach the liver via the enterohepatic circulation[61-64]. DAMP and PAMP molecules subsequently activate immune cells of the liver, such as Kupffer cells, monocytes, neutrophils, dendritic cells, natural killer cells and NK T cells via pattern recognition receptors (PRRs)[65]. Activation of immune cells amplifies the hepatic inflammatory cascade by the release of cytokines such as TNF-α and IL1β, chemokines and ROS, thereby aggravating fibrosis and cirrhosis finally leading to hepatocellular carcinoma[61, 66].

2.2.4 Liver macrophages in health and NAFLD

Role of macrophages in the healthy liver

The liver is the organ with the largest reservoir of macrophages with macrophages accounting for 15% of total liver cells[67, 68]. The macrophages of the liver are a heterogeneous population including two main types of macrophages[62]: Yolk sac or fetal liver-derived tissue-resident Kupffer cells (KCs) and monocyte-derived macrophages. Whereas KCs are located along sinusoidal endothelial cells, monocyte-derived macrophages are normally found in the portal triad. In the published literature, F4/80 and CD68 have been used as typical markers for KCs, while Ly6C, F4/80 and CD11b were used to identify monocyte-derived macrophages in the liver[68, 69]. However, it seems that hepatic macrophages are heterogenous and surface markers of KCs and monocyte-derived macrophages are overlapping, which makes it hard to distinguish distinct populations[68].

As the macrophages in the liver cannot be properly distinguished, we will refer to them as "liver macrophages" in our study. Like other tissue macrophages, liver macrophages display a wide range of plasticity during homeostasis and diseases depending on the stimulus[68, 70]. Liver macrophages are activated by exogenous signals like LPS or endogenous danger signals such as necrotic cell debris via PRRs. They can exhibit either a pro- or anti-inflammatory phenotype[68, 71]. Pro-inflammatory macrophages are characterized by the expression of the chemokines CXCL1 and CCL2, the release of the cytokines i.e. TNF-α, interleukin-1β (IL-1β), Interleukin-6 (IL-6) and the production of reactive nitrogen species (iNOS) or ROS. In contrast, anti-inflammatory macrophages are typically characterized by effective phagocytic activity due to activation of scavenger (CD163), mannose (Mrc1) and galactose (Mgl1) receptors and the production of the cytokine IL-10.

Role of macrophages in NAFLD

Progression of NAFLD is often associated with the activation of KCs and macrophage recruitment[72, 73]. Different human and rodent studies underline the importance of macrophages for the development of steatosis, inflammation and fibrosis. A study conducted in patients with steatosis revealed recruitment of CD68+ macrophages in portal areas even before expression of pro-inflammatory cytokines[74]. Additionally, depletion of KCs by clodronate liposomes or gadolinium chloride rescues mice from steatosis[75, 76]. The pro-inflammatory phenotype of hepatic macrophages is correlated to the disease severity or progression[72]. It has been demonstrated that monocyte-derived macrophages releasing TNF-α are triggered by KCs in the later stage of steatohepatitis as shown in a NASH model[77]. Another study showed that the number of hepatic pro-inflammatory macrophages expressing CCR2 was increased in the portal zones of patients with fibrosis and cirrhosis[78].

In the setting of NAFLD and insulin resistance, KCs are activated by various immune signals: (i) hepatocytes damage molecules i.e. apoptotic bodies, (ii) lipid overload derived-DAMPs (i.e. FFA, free cholesterol and their metabolites, oxidized lipoproteins, ceramides, diacylglycerols) and PAMP molecules like LPS[72]. Upon activation, KCs release pro-inflammatory cytokines (e.g. TNF-α, IL-6, IL-1β) and thereby worsen the hepatocytes' injury. Consequently, KCs recruit monocytes via the chemokine pathways like CCL2/CCR2 or CCL5/CCR1 into the injured liver tissue. These recruited macrophages can develop into pro-inflammatory, angiogenic and fibrogenic macrophages and thus deteriorate NAFLD disease[79] (Fig. 2).

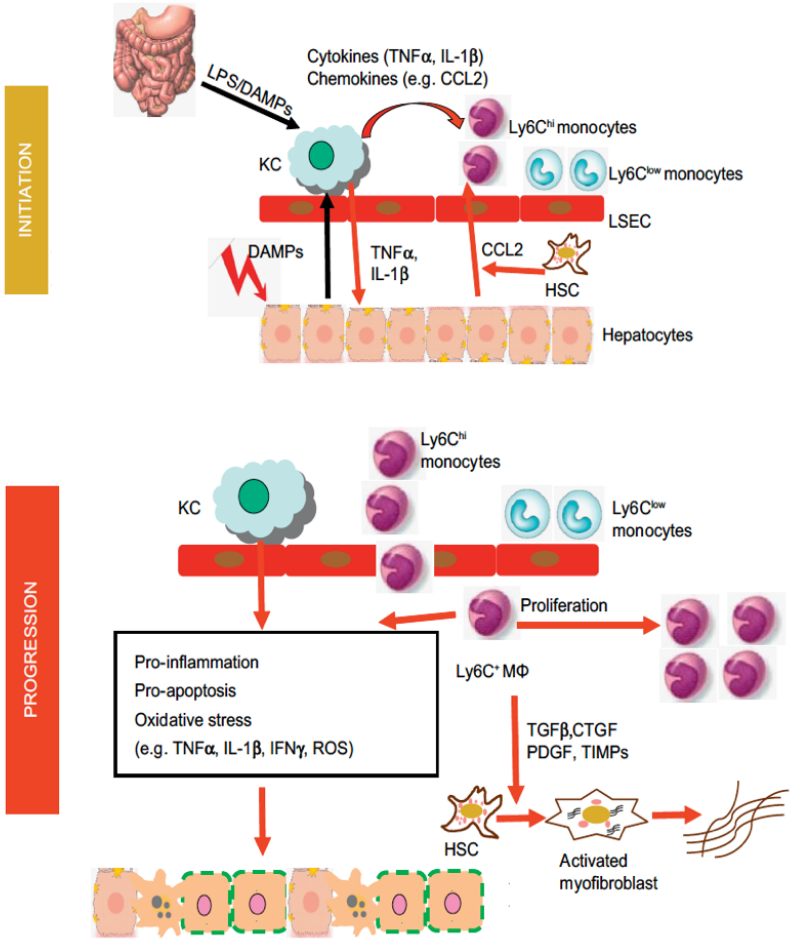

Figure 2| Activation of hepatic macrophages during initiation and progression of NAFLD. In the initiation stage, DAMPs induced by hepatocytic injury or gut-derived LPS activate KCs in the sinusoidal endothelium. KCs in turn produce pro-inflammatory cytokines (e.g. TNF-α, IL-1β). Furthermore, KCs, hepatocytes and hepatic stellate cells (HSC) release chemokines such as CCL2, triggering the recruitment of Ly6C^{hi} monocytes into the injured liver. In the progression stage (chronic injury), infiltrated monocytes develop and expand into Ly6C^{+} macrophages (Mϕ), thereby amplifying inflammation, apoptosis and oxidative stress resulting in increased hepatic damage. Additionally, Ly6C^{+}Mϕ stimulate HSC to develop into collagen-producing myofibroblasts by secreting pro-fibrotic mediators including tumor growth factor (TGF-β), connective tissue growth factor (CTGF), platelet-derived growth factor (PDGF) and tissue inhibitor of matrix metalloproteinase (TIMPs). Adapted from Ju, C. and F. Tacke, 2016[80].

Targeting macrophages in NAFLD

No approved effective drug is available to treat NAFLD. However, hepatic macrophages have been suggested as a potential therapeutic target to prevent or improve NAFLD due to their crucial contribution in NAFLD progression[79]. Pharmacological depletion of KCs indeed prevents the development of NAFLD in rodents[75, 81]. However, complete depletion of macrophages is not an appropriate approach in a clinical human setting due to the essential role of macrophages in the homeostatic state[82]. Several studies have been conducted with the aim to block the recruitment of monocyte-derived macrophages into liver. For instance, pharmacological or genetic ablation of different chemokine, cytokines and pattern recognition

receptors improves NAFLD characteristics (e.g. CCR2-CCL2[83-87], CCR2/5[78, 87], CXCR3-CXCL10[88, 89], CXCL16[90], IL-6[91], TNF-α[92], TLR4[93]). Treatment of NAFLD/diabetic patients with a CCR2/5 antagonist showed a significant improvement in fibrosis during a clinical trial phase IIb[72, 94]. Additionally, targeting differentiation of macrophages by a Galectin 3 antagonist improves fibrosis induced-liver damage in both NASH patients and in a mouse model[95, 96]. Besides blocking macrophage recruitment, pharmacological attenuation of pro-inflammatory macrophages could be an alternative strategy to treat NAFLD. As macrophage activation and chronic low-grade inflammation are linked to metabolic disease and insulin resistance[97], targeting pathologically activated macrophages might even have a broader impact than on NAFLD only, but also improve insulin resistance and inflammation.

Pharmacological attenuation of hepatic macrophages

PPARγ-agonists/thiazolidinediones (TZDs) have been proposed as a pharmacological agent targeting macrophages in NAFLD/NASH. TZDs are anti-diabetic drugs acting mainly on the adipose tissue. Additionally, PPARγ-agonists have been shown to dampen liver inflammation by attenuating macrophage infiltration and shifting macrophages towards an anti-inflammatory phenotype, thereby improving steatosis in the liver[98-100]. Besides that, a meta-analysis showed that TZDs could be an effective agent for targeting inflammation and steatosis in NASH[101]. However, TZDs have also been linked to many deleterious side effects such as weight gain and congestive heart failure, as well as an increased risk for bladder cancer[102, 103]. Therefore, they have been largely abandoned from clinical practice.

Intriguingly, the beneficial anti-diabetic/ anti-inflammatory action and unwanted side effects of TZDs are mechanistically distinct: Recent studies have revealed that the anti-diabetic/ anti-inflammatory effects are associated with post-translational modification of PPARγ[104, 105], which involves inhibition of phosphorylation at serine 273 (pS273) that is implicated in obesity and insulin resistance[105, 106]. In contrast, side effects of TZDs are due to transcriptional activation of PPARγ-related genes, known as classical PPARγ-agonism[104, 105]. Thus, uncoupling post-translational modification (anti-diabetic/anti-inflammatory effects) from transcriptional activation of PPARγ (side effects) could be a promising strategy for pharmacological macrophage attenuation.

Imatinib as an alternative to TZD

One potential candidate drug with anti-inflammatory properties is the tyrosine kinase inhibitor (TKI) imatinib, which was originally developed to target the tumor-associated fusion protein BCR-Abl in chronic myelogenous leukemia (CML). Over the years, several other targets of imatinib have been identified[107]. Most recently, imatinib has been shown to inhibit posttranslational phosphorylation of PPARγ without classical PPARγ-agonism[105]. Like TZDs, imatinib has also anti-diabetic/ anti-inflammatory properties. Regarding its anti-inflammatory effects, imatinib treatment polarizes tumor-associated macrophages towards an anti-inflammatory phenotype[108], suppresses glycolysis as an indication for anti-inflammatory polarization in leukemia cells[109], reduces acute liver injury[110] and attenuates adipose tissue inflammation in obese mice[105]. Furthermore, glucose-lowering effects have been observed as "side effects" in cancer patients treated with imatinib[111, 112]. In diabetic mouse models, these anti-diabetic effects have been attributed to reduced β-cell death and maintained β-cell function[113-115].

3. Aim of the study

Based on the anti-inflammatory and anti-diabetic effects of imatinib potentially involving PPARγ, the aim of our study was to assess whether imatinib directly attenuates macrophages and could therefore be used in disease states with pathological macrophage activation such as NAFLD. We set out a proof-of-concept study to addresses this novel therapeutic concept by testing the effect of imatinib on (i) macrophage activation *in vitro*, (ii) NAFLD and other insulin resistance related diseases such as diabetes and obesity in a time-resolved manner *in vivo* and (iii) human monocytes to assess its translational application. The concept of pharmacological macrophage attenuation in NAFLD is intriguing as restoring pathologically activated macrophages could potentially not only target the root cause of NAFLD progression, but also other metabolic disease manifestations such as adipose tissue and systemic inflammation and insulin resistance. A more profound understanding of macrophage modulation and the molecular pathways involved holds the promise for new treatment strategies in NAFLD and metabolic disease.

4. Materials and methods

4.1 Methods

4.1.1 Mice

Animals
C57BL/6N male mice (Charles River Laboratories, Sulzfeld, Germany) were maintained in our SPF-facility at 22 Celsius room temperature with a 12 hours light/12 hours dark cycle and housed in groups of 3-5 mice. Body weights were monitored once weekly. Mice used for metabolic experiments were allowed one week of acclimation after the arrival. All procedures were approved by the local Animal Care and Use Committee (Veterinary Office Basel, Switzerland) and carried out in accordance with relevant guidelines and regulations.

4.1.2 Cell isolation, culture and treatment

4.1.2.1 Cell isolation and culture

Peritoneal cells
Primary macrophages were obtained from 6-8 weeks old C57Bl/6N mice. To isolate peritoneal macrophages, peritoneal cells were harvested by intra-abdominal lavage: 10 mL of FACS buffer were injected into the peritoneal cavity using a 10 mL syringe with a 23Gx11/4 (0.6x32mm) needle (Terumo AGANI™ Needle, TERUMO®, Tokyo, Japan). The the peritoneal membrane was subsequently opened to collect the liquid containing the peritoneal cells through a glass funnnel placed in a 50 mL falcon tube. The collected liquid was filtered through a 70 µm filter (Sigma-Aldrich). Peritoneal cells were pelleted by centrifugation at 453x g for 5 minutes at 4 Celsius. The cells were used either for RNA isolation or proceessed further for macrophage enrichment.

Peritoneal macrophages
Peritoneal cells were cultured in 24-well plates (200000-700000 cells/ well) in RPMI-1640 medium without glucose and glutamin suplemented with 10 % FBS, 1 % Glutamax, (100 x, 200 mM), 1 % Penicillin/ Streptomycin (10000 U/10 mL), 0.1 % fungizone: Amphotericin B (250 µg/mL). Cells were incubated overnight at 37 Celsius supplied with 5 % CO_2 in a humidified atmosphere. On the next day, the cells were enriched for macrophages by washing

out the non-adherent cells twice using PBS and then treated as outlined in the section "cell treatment".

Bone marrow derived macrophages (BMDM)

To isolate murine bone marrow cells, an incision was longitudinally made in the hind leg and both of muscles and connective tissue were removed from femur and tibia. Then, the leg was cut at pelvic-hip joint and placed in a petri dish containing RPMI-1640 medium. Femur and tibia were separated and each of them was cut at one side under sterile conditions. To isolate bone marrow cells, the bone was flushed with 5 mL medium (into a 15 mL Falcon). The cells were washed (453x g, 5 minutes at 4 Celsius) and resuspended in 1 mL medium. Bone marrow cells (0.5 mL) were cultured in a petri dish (Falcon Corning® Dishes 100 x 20 mm style, Thermo Fisher Scientific) in RPMI-1640 medium containing HEPES (25 mM) and L-glutamin (2mM) suplemented with 10 % FBS, 2 % Penicillin/ Streptomycin, 1 % Sodium Pyruvate (100 mM), 1 % MEM Non-essential Amino Acids (100 x), and 0.055 mM β-mercapoethanol (1000 x). For macrophage differentiation, cells were cultured in the presence of M-CSF (10 ng/mL, PeproTech, London, UK) at 37 Celsius in an incubator supplied with 5 % CO_2 for 7- 9 days. The cells were washed with PBS two times at day 3 and 7. One day prior to treatment, the cells were washed, collected and seeded in a 96-well plate (60000-100000 cells/ well) in absence of M-CSF for 24 hours prior treatment.

Adipose tissue stromal vascular fraction (SVF)

Murine epididymal adipose tissue was isolated and the weight measured. The tissue was placed into a 50 mL falcon tube and minced using a curved scissor. The minced tissue was collected in 4 mL of HBSS (Gibco) and a 2x digestion mix containing HBSS, 10 mM HEPES, 8.25 µg/mL DNAse I, (Sigma- Aldrich) and collagenase IV (Worthington, OH, USA) was added. The tissue was digested at 37 Celsius for 25-30 minutes, shaking at 400x g using a ThermoMixer® C (Eppendorf, Germany). The digestion was stopped by adding 27 mL cold FACS buffer. Digested tissue was filtered through a gauze (HARTMANN Group, Heidenheim an der Brenz, Germany) placed on a glass funnel on a 50 mL falcon tube. Isolated cells were spun down at 453x g, 5 minutes at 4 Celsius, resuspended in 1 mL red cell lysis buffer to remove red blood cells and washed with 10 mL FACS buffer.

Cell treatment

Peritoneal macrophages and BMDM were polarized to a pro-inflammatory M1 (10 ng/mL IFNγ, PeproTech, 100 ng/mL Lipopolysaccharide (LPS) *E. coli* 0111: B4, Sigma-Aldrich, Saint Louis, MO, USA) or anti-inflammatory M2 phenotype (10 ng/mL IL-4 and IL-13, Thermo Fisher Scientific, Waltham, MA, USA) or left unstimulated (M0) in the presence or absence of imatinib (1 μM, Novartis, Basel, Switzerland) for 6 hours (material see Table 2). The supernatant from cells were collected and spun down at 2000x g for 5 minutes at 4 Celsius to and stored at -20 Celsius for further analysis. Additionally, the cells were lysed for RNA isolation using 350 µl RA1 lysis buffer supplemented with 3.5 µl 2-Mercaptoethanol (Sigma-Alderich, St. Louis, USA) per sample and stored at -80 Celsius.

Macrophage type	Cytokine/ drug	concentration	Source
Mouse cytokines			
M1	LPS *E. coli* 0111: B4	100ng/mL	Sigma-Aldrich
	IFNγ	10ng/mL	PeproTech
M2	IL-4	10ng/mL	Thermo Fisher Scientific
	IL-13	10ng/mL	Thermo Fisher Scientific
Human cytokines			
M1	LPS *E. coli* 0111: B4	100ng/mL	Sigma-Aldrich
	IFNγ	10 ng/mL	ImmunoTools
Tyrosin kinase inhibitor (TKI)	Imatinib	1μM	Novartis

Table 1: List of cytokines, LPS and TKI used for macrophage's polarization and treatment

4.1.3 Animal models

Acute inflammation model

A single intraperitoneal (i.p.) LPS injection (1mg/kg) was applied to mice that were pre-treated three times with either imatinib (100 mg/kg) or PBS during 24 hours prior to the LPS injection. The mice were analyzed 2 hours after the LPS injection.

Chronic inflammation models

High fat diet - streptozotocin model (HFD-STZ)

Mice were fed a high fat diet (HFD; containing 58% fat, 16.4% protein and 25.6% carbohydrate, Research diet, New Brunswick, NJ, USA) from 5 weeks onwards for up to 14 weeks. After 3 weeks of HFD, the mice were treated with a single i.p. injection of Streptozotocin (STZ ,130 mg/kg, Sigma-Aldrich) to induce beta cell death. Following 10 weeks of HFD, the mice were treated either with imatinib (100 mg/kg) or water for 1 month by oral gavage.

High fat diet model (HFD)

HFD is a well-established model for obesity, T2D and NAFLD. Mice were put on HFD for up to 13-17 weeks and then treated orally with imatinib (100mg/kg) or vehicle for 1 or 3 months, respectively.

Insulin and glucose tolerance tests

Insulin tolerance test (ITT) assess whole-body insulin resistance, while glucose tolerance test (GTT) test glucose tolerance along with insulin secretion. ITT and GTT tests were performed at 4 or 8 weeks of imatinib treatment. For ITT, mice were fasted 3 hours and i.p. injected with insulin (2 U/kg BW). Blood glucose levels were measured at 0, 15, 30, 60 and 120 minutes after insulin injection, using a glucometer (FreeStyle Freedom Lite, Abbott Laboratories, Illinois, USA).

For GTT, mice were fasted 6 hours. Blood samples from tail vein were collected prior to i.p. glucose (2 g/kg BW) injections at 0 minutes, or after injections at 15, 30, 60 and 90 minutes. Blood glucose levels at indicated time points were measured using glucometer (FreeStyle Freedom Lite, Abbott Laboratories, Illinois, USA).

4.1.4 Human study

To translate our findings to human, a study was conducted with 18 donors according to the Declaration of Helsinki and relevant guidelines and regulations. Study approval was obtained from the local ethics committee (Ethics Committee of northwest and central Switzerland, EKNZ).

Study design and patient's recruitment

18 subjects were grouped in healthy controls (He, n=6), adequately controlled diabetics (aDM, n=5) and inadequately controlled diabetics (iaDM, n=7). All diabetic subjects were recruited at the department of Endocrinology, Diabetes and Metabolism, at University Hospital of Basel and included into the study according to the following criteria: (i) age ≥18 years old; (ii) diabetes history for more than >3 months (American Diabetes Association criteria); (iii) no immunosuppressive treatment or immunodeficiency history; (iv) no immunotherapy treatment at the time of sample collection e.g. corticosteroids, antibodies or hemapheresis; (v) no psychiatric illness; and (vi) no pregnancy or breastfeeding. Healthy subjects were selected base on their age (≥ 18 years old) and their BMI (18-25 kg/m^2).

Study protocol

During the first screening visit, patients were informed about the study and screened for study inclusion and exclusion criteria by collecting the following data: date of birth, gender, medical history, date of diabetes diagnosis, other relevant diagnoses, concomitant therapies/drugs, family history (concerning diabetes, obesity and cardiovascular diseases), weight, BMI, waist-to-hip ratio and blood pressure. During the second visit, 49 mL of blood was collected using S-Monovette® 7.5 mL, K3 EDTA (Sarstedt, Nümbrecht, Germany). In addition, vital signs and long-term blood glucose levels (HbA1c) were measured.

Human peripheral blood mononuclear cells (PBMCs)

10 mL PBS (without Mg and Ca; Sigma-Aldrich) was added to 20 mL of the collected blood. The diluted blood was added to 16 mL of density gradient medium (Lymphoprep™, STEMCELL Technologies Inc., Vancouver, BC, Canada), centrifuged at 453x g, 25 minutes at 22 Celsius (acceleration: 4 and deacceleration: 1). The buffy coat layer containing PBMCs was collected and washed two times with isolation buffer (PBS, 3 % FBS, 10 mM EDTA) at 300x g, 10 minutes. The cells were resuspended in 20 mL of isolation buffer, diluted 1:1 and counted using cell counting slides by an automatic cell counter (EVE™ NanoEnTek, South Korea). Monocytes were enriched from PBMCs at $1x10^8$ cells/mL density using MagniSort® Human Pan-Monocyte Enrichment kit (Thermo Fisher Scientific) according to their protocol. Isolated monocytes were cultured for 2 hours in RPMI-1640 medium containing HEPES (25 mM) and L-glutamin (2 mM) suplemented with 1 % Penicillin/ Streptomycin, 1 % 100 mM Sodium Pyruvate and 1 % MEM Non-essential Amino Acids (100 x). After two hours, non-attached cells were washed away. Attached monocytes were cultured with the medium described above, additionally supplemented with 10 % FBS. The cells were polarized towards a pro-inflammatory phenotype (M1; 10 ng/mL IFNγ, ImmunoTools, Friesoythe, Germany, 100 ng/mL LPS *E. coli* 0111: B4) or left unstimulated (M0) in the presence or absence of imatinib (1 μM) for 24 hours (material see Table 2). Finally, supernatants and cells were analyzed as described in the section “cell treatment”.

4.1.5 Readout measures

RNA isolation

RNA was isolated from lysed cells or tissues using NucleoSpin RNA kit (Macherey Nagel, Düren, Germany) and RNeasy Plus Universal Mini kit (QIAGEN, Düsseldorf, Germany); respectively, according to the manufacturer's instructions.

Reverse transcription (cDNA synthesis)

Reverse transcription was performed using SuperScriptII Reverse Transcriptase kit (Thermo Fisher Scientific). To synthesize cDNA, 1µL deoxynucleotide triphosphates (dNTPs, 10 mM, Roch, Basel, Switzerland) and 1 µl random hexamers (50 ng/µL, Microsynth, Balgach, Switzerland) were added to 11.5 µl of total mRNA normalized to 50-100 ng. First, RNA was denatured at 65 Celsius for 5 minutes in TProfessional Standard PCR Thermocycler and then quickly chilled on ice. Second, a Master Mix containing 4µl 5x Buffer (250 mM Tris-HCl, pH 8.3 at room temperature; 375 mM KCl; 15 mM MgCl2), 2µl DTT (0.1M) and 0.5µl SuperScript II reverse transcriptase was added to each sample and incubated at room temperature for 10 minutes. Third, samples were placed back into thermocycler at 42 Celsius for 50 minutes and the reaction was inactivated at 70 Celsius for 15 minutes. Finally, cDNA product was diluted 1: 12 in nuclease free water and stored at -20 Celsius. RNaseOUT™ (40 units/µL) was added in case of low amount of RNA and in tissue samples.

Quantitative real time polymerase chain reaction (qRT-PCR)

QRT-PCR (ViiA™ 7 Real-Time PCR System, Thermo Fischer Scientific) was carried out to quantify gene expression. A mixture of 7.8 µl of GoTaq® qPCR Master Mix (Promega Corporation, Madison, USA) and 5.2 µl cDNA (1:12) was run in duplicate in a 384-well plate (VWR, Randor, Pennsylvania, USA). Gene expression of target genes was normalized to the geometric mean of two housekeeping genes: *B2M* (β-2-microglobulin) and *PPIA* (peptidylprolyl isomerase A). Relative gene expression was calculated by $2^{-\Delta\Delta CT}$ and the melting curves were assessed in each run to confirm primer specificity of the PCR reaction. Classical pro- and anti-inflammatory markers were obtained from (Microsynth, Balgach, Switzerland, see Table 2).

Gene	Forward Primer	Reverse Primer
Mouse hkg and m1- and m2 -–markers		
B2m	5′ TTCTGGTGCTTGTCTCACTGA	5′ CAGTATGTTCGGCTTCCCATTC
Ppia	5′ GAGCTGTTTGCAGACAAAGTTC	5′ CCCTGGCACATGAATCCTGG
Tnf-α	5′ ACTGAACTTCGGGGTGATCG	5′ TGAGGGTCTGGGCCATAGAA
Il-6	5′ GGATACCACTCCCAACAGACCT	5′ GCCATTGCACAACTCTTTTCTC
Il-1β	5′ GCAACTGTTCCTGAACTCAACT	5′ ATCTTTTGGGGTCCGTCAACT
Inos	5′ GTTCTCAGCCCAACAATACAAGA	5′ GTGGACGGGTCGATGTCAC
Kc	5′ CTGGGATTCACCTCAAGAACATC	5′ CAGGGTCAAGGCAAGCCTC
Mrc1	5′ CTCTGTTCAGCTATTGGACGC	5′ CGGAATTTCTGGGATTCAGCTTC
Mgl1	5′ TGAGAAAGGCTTTAAGAACTGGG	5′ GACCACCTGTAGTGATGTGGG
Rentla	5′ CCAATCCAGCTAACTATCCCTCC	5′ CCAGTCAACGAGTAAGCACAG
Chil3	5′ AGGAAGCCCTCCTAAGGACA	5′ CTCCACAGATTCTTCCTCAAAAGC
Il-10	5′ AGGCGCTGTCATCGATTTCTC	5′ GCCTTGTAGACACCTTGGTCTT
Cd68	5′ GCAGCACAGTGGACATTCAT	5′ AGAGAAACATGGCCC GAAGT
Adgre1 (f4/80 or emr1)	5′ GCC CAG GAGTGGAATGTCAA	5′ CAGACACTCATCAACATCTGCG
Mouse sterol regulatory element-binding protein (srebps) genes		
Srebp1a	5′ GCCGGCGCCATGGACGAGCTGGCC	5′ CAGGAAGGCTTCCAGAGAGGAGGC
Nlrp1a	5′ AGGCTCTTTACCCTCTTCTA	5′ ATGTGCTTCTTCTTCTGGTA
Nlrp1c	5′ GAATCTTTACTCCACCCAGC	5′ CTTTTCCTGGCAAATGTCTT
Srebp1c	5′ GGAGCCATGGATTGCACATT	5′ GGCCCGGGAAGTCACTGT
Elovl5	5′ CTGAGTGACGCATCGAAATG	5′ CTTGCACATCCTCCTGCTC
Scd2	5′ TGCCTTGTATGTTCTGTGGC	5′ TCCTGCAAGCTCTACACCTG
Fads1s	5′ TGGTGCCCTTCATCCTCTGT	5′ GGTGCCCAAAGTCATGCTGTA
Acc1	5′ CCTCCGTCAGCTCAGATACA	5′ TTTACTAGGTGCAAGCCAGACA
Scd1	5′ CTGTACGGGATCATACTGGTTC	5′ GCCGTGCCTTGTAAGTTCTG
Fasn	5′ AGCGGCCATTTCCATTGCCC	5′ CCATGCCCAGAGGGTGGTTG
Acacb	5′ CCCAGGAGGCTGCATTGA	5′ AGACATGCTGGGCCTCATAGTA
Ldlr	5′ ACCTGCCGACCTGATGAATTC	5′ GCAGTCATGTTCACGGTCACA
Hmgcs1	5′ TTTGATGCAGCTGTTTGAGG	5′ CCACCTGTAGGTCTGGCATT
Fdps	5′ GAGTCTGCCCGATCTCTGTC	5′ TGAACCTGCTGGAGCTCTTT
Mvk	5′ GAAGACATCGTCCCTTGCTG	5′ AAC CCT TCT GGT GTGGACA
Pmvk	5′ GCTCGCATCCAGAAGTCTCT	5′ GCTCTCTGGTCCACTCAAGG
Hmgcr	5′ GGCCTCCATTGAGATCCG	5′ CACAATAACTTCCCAGGGGT
Mouse ppar-γ phosphorylation-related genes		
Rarres2	5′ GCCTGGCCTGCATTAAAATGG	5′ CTTGCTTCAGAATTGGGCAGT
Txnip	5′ TCTTTTGAGGTGGTCTTCAACG	5′ GCTTTGACTCGGGTAACTTCACA
Nr1d1	5′ TACATTGGCTCTAGTGGCTCC	5′ CAGTAGGTGATGGTGGGAAGTA
Cd24a	5′ GTTGCACCGTTTCCCGGTAA	5′ CCCCTCTGGTGGTAGCGTTA
Peg10	5′ TGCTTGCACAGAGCTACAGTC	5′ AGTTTGGGATAGGGGCTGCT
Acyl	5′ CAGCCAAGGCAATTTCAGAGC	5′ CTCGACGTTTGATTAACTGGTCT
Cidec	5′ ATGGACTACGCCATGAAGTCT	5′ CGGTGCTAACACGACAGGG
Nr1d2	5′ TGAACGCAGGAGGTGTGATTG	5′ GAGGACTGGAAGCTATTCTCAGA
Ddx17	5′ TCTTCAGCCAACAATCCCAATC	5′ GGCTCTATCGGTTTCACTACG
Rybp	5′ CGACCAGGCCAAAAAGACAAG	5′ CACATCGCAGATGCTGCATT
Nr3c1	5′ AGCTCCCCCTGGTAGAGAC	5′ GGTGAAGACGCAGAAACCTTG
Aplp2	5′ GTGGTGGAAGACCGTGACTAC	5′ TCGGGGGAACTTTAACATCGT
Slenbp2	5′ ATGGCTACAAAATGCACAAAGTG	5′ CCTGTGTTCCGGTAAATGCAG
Cycp2f2	5′ GTCGGTGTTCACGGTGTACC	5′ AAAGTTCCGCAGGATTTGGAC
Car3	5′ TGACAGGTCTATGCTGAGGGG	5′ CAGCGTATTTTACTCCGTCCAC
Adipsin	5′ CATGCTCGGCCCTACATGG	5′ CACAGAGTCGTCATCCGTCAC
Adiponectin	5′ TGTTCCTCTTAATCCTGCCCA	5′ CCAACCTGCACAAGTTCCCTT
Mouse adipose tissue browning markers		
Cpt1b	5′ TGCCTTTACATCGTCTCCAA	5′ GGCTCCAGGGTTCAGAAAGT
Ucp1	5′ CTTTGCCTCACTCAGGATTGG	5′ ACTGCCACACCTCCAGTCATT

Pgc1α	5′ TATGGAGTGACATAGAGTGTGCT	5′ CCACTTCAATCCACCCAGAAAG
Dio2	5′ AATTATGCCTCGGAGAAGACCG	5′ GGCAGTTGCCTAGTGAAAGGT
Cox5b	5′ ATCAGCAACAAGAGAATAGTGGG	5′ GTAATGGGTTCCACAGTTGGG
Human HKG and M1- and M2- markers		
B2M	5′ GCTCGCGCTACTCTCTCTTT	5′ TGTCGGATGGATGAAACCCA
PPIA	5′ GCATACGGGTCCTGGCATCTTGTCC	5′ ATGGTGATCTTCTTGCTGGTCTTGC
TNF-A	5′ CAGAGGGCCTGTACCTCATC	5′ GGAAGACCCCTCCCAGATAG
MCP-1	5′ CCCCAGTCACCTGCTGTTAT	5′ TGGAATCCTGAACCCACTTC
MRC1	5′ CGAGGAAGAGGTTCGGTTCACC	5′ GCAATCCCGGTTCTCATGGC
CD163	5′ TTGCCAGCAGCTTAAATGTG	5′ AGGACAGTGTTTGGGACTGG

Table 2: Primers sequences used for quantitative real time-PCR

qRT-PCR reaction program

Stage 1: denaturation

Step 1 50 Celsius 2 minutes

Step 2 95 Celsius 10 minutes

Stage 2: annealing

Step 1 95 Celsius 15 second

Step 2 60 Celsius 1 minutes

Number of cycles 40x

Stage 3: dissociation

Step 1 95 Celsius 15 second

Step 2 60 Celsius 1 minutes

Step 3 95 Celsius 15 second

Hold

MesoScale technology (MSD)

For insulin measurement, blood samples were collected in EDTA and centrifuged at 12000x g, 5 minutes at 4 Celsius. Isolated plasma was stored at -20 Celsius or -80 Celsius and later analyzed using MSD mouse/rat insulin kit. For cytokines secretion analysis, plasma and supernatants were diluted 2- and 6-fold, respectively, and then analyzed using mouse pro-inflammatory V-PLEX custom kit for TNFα & IL-6 (MSD, MesoScale Diagnostics, Maryland, USA). Plasma insulin, TNFα and IL-6 cytokines were quantified according to manufactures' instruction by electrochemiluminescence (MESO SECTOR S 600) using a standard curve approach.

Flow cytometry of adipose tissue macrophages

SVF cells were blocked with anti-mouse CD32/16 antibody (BioLegend, Pacific Heights Blvd San Diego, CA San Diego, USA) for 15 minutes and then stained with the following surface markers 30 minutes on ice in the dark: CD45 (30-F11), Siglec-F (E50-2440), F4/80 (BM8), CD11b (M1/70), CD206 (C068C2) and CD11c (N418) (antibodies see Table 3). To discriminate between live and dead cells, DAPI was added prior to analysis. SVF cells were analyzed using BD LSRII instrument (BD Biosciences, Franklin Lakes, NJ, USA) and FlowJo software (TreeStar Inc., Ashland, OR, USA). ATM identification was achieved using the following gating strategy: leukocytes ($CD45^+$) were gated on single-live cells population (Singlets $DAPI^-$). Eosinophils ($CD45^+F4/80^{low}SiglecF^+$) were excluded and ATM (non-eosinophils $CD11b^+F4/80^+$) were further classified into double negative (DN), monocyte-derived M1a ($CD11c^+CD206^-$), inflammatory M1b ($CD11c^+CD206^{mid}$) and anti-inflammatory M2 ($CD11c^{-\text{ to low}}CD206^{high}$) macrophages as shown in supplementary Fig. 4a-c.

Antibody	Clone	Fluorophore	Source
CD45	30-F11	PerCP/Cy5.5	Biolegend
Siglec-F	E50-2440	BV510	BD Biosciences
CD11b	M1/70	BV421	Biolegend
F4/80	BM8	PE	Biolegend
CD11c	N418	PE/Cy7	Biolegend
CD206	C068C2	A647	Biolegend

Table 3: List of Antibodies for flow cytometry in adipose tissue

Liver enzymes and lipids

Liver enzymes and lipids were measured in mouse plasma using a Cobas 8000 modular analyzer (Roche Diagnostics, Basel, Switzerland) according to the manufacturer's protocol. The assay was performed by Mirjam Jaeggy and Fausta Chiaverio from the Biochemistry laboratory, University hospital of Basel, Switzerland.

Seahorse XF flux analysis

Seahorse metabolic assay was performed to evaluate imatinib's effect on the metabolic status of macrophages. One day prior to the assay, a seahorse sensor cartridge was hydrated using Seahorse XF Calibrant solution (200 µl/ well) at 37 Celsius in a non- CO_2 incubator overnight. On the following day, peritoneal macrophages isolated from obese mice were seeded (100000 /well) in a seahorse XF 96-well microplate plate and incubated for 2 hours at 37 Celsius supplied with 5 % CO_2 in RPMI-1640 medium (without glutamin), suplemented with 10 % FBS, 1 % Glutamax, 1 % Penicillin/ Streptomycin, 0.1 % fungizone. After incubation, cells

were washed two times with 150 µl warm medium (RPMI1640-medium with L-glutamine, without glucose and sodium bicarbonate, Sigma -Aldrich) followed by addition of 175 µl of the same medium. For metabolic flux measurement, 25 µl of each Seahorse XF compound was loaded in the corresponded injection port (Table 4) and the sensor cartridge calibrated for 20 minutes in the XF96 Seahorse Metabolic Analyzer (Seahorse Bioscience, North Billerica, MA, USA) followed by microplate placement according to the instructions. Glycolysis was measured by ECAR (extracellular acidification rate) and mitochondrial respiration by OCR (oxygen consumption rate) following each reagent injection for two hours. The following glycolysis stress compounds were used: Glucose to induce glycolysis; oligomycin to inhibit mitochondrial ATP synthase (complex V). The following mitochondrial stress reagents were used: FCCP to uncouple oxygen consumption from ATP production; sodium pyruvate (simultaneously with FCCP) to fuel maximal respiration upon uncoupling; and rotenone to inhibit mitochondrial complex 1. The assay was performed according to the manufacturer's instructions and as described in [116].

Port	Injection	Reagents	Stock	Initial concentration	Final concentration	Injection (µl)
A	8x	Glucose	-	200 mM	25 mM	25
B	9x	Oligomycin	50 µM	13.5 µM	1.5 µM	25
C	10x	FCCP	15 mM	15 µM	1.5 µM	25
		Sodium pyrvate	100 mM	10 mM	1 mM	
D	11x	Rotenone	13.75 mM	13.75 µM	1.25 µM	25

Table 4: Seahorse XF reagents and injections.

Seahorse program

Basal	4 cycles	24 minutes
Injection port A	4 cycles	24 minutes
Injection port B	4 cycles	24 minutes
Injection port C	4 cycles	24 minutes

Liver histology

Fixation, embedding and cutting

Liver samples were isolated and fixed in 4 % formalin (Formafix AG, Hittnau, Switzerland) for 24-48 hours. The samples were the placed between two layers of sponge (MEDITE GmbH, Burgdorf, Germany) in a cassette (MEDITE) in PBS. Tissue samples were processed in a closed linear Tissue Processing System (TPC 15 Duo, MEDITE). The tissue was embedded in paraffin using tissue embedding system; *TES Valida*® (MEDITE) and stored at room

temperature. Paraffin blocks were cut by HM355S Microtome (Thermo Fisher Scientific) into 5 µm sections by Diego Calabrese (Hepatology Group, Department of Biomedicine, University Hospital of Basel) and Michelle Baumann (from the Institute of Pathology, University Hospital of Basel).

H&E staining

Hematoxylin-eosin (H&E) staining was performed by a staining machine (Tissue Tek Prisma, Sakura) using a standard automatic staining protocol. Images were acquired using a Nikon inverted microscope system (ECLIPSE Ti with DS-Qi2 camera, Tokyo, Japan) and NIS-Elements AR-4.6 software (Nikon). The NAFLD activity score (NAS)[117] was assessed in a blinded fashion (Table 5) by Dr. Matthias Matter (Institute of Pathology, University Hospital of Basel).

Criteria	Score Range	Score
Grade low- to medium-power evaluation of parenchymal involvement by steatosis	0-3	0= <5%
		1= 5%-33%
		2= 33%-66%
Location Predominant distribution pattern	0-3	0= Zone 3
		1= Zone 1
		2= Azonal
		3=Panacinar
Inflammation lobular inflammation overall assessment of all inflammatory foci	0-1	0= No foci
		1= 2 foci per 200 ^{L} field
Ballooning	0-1	0= None
		1= few balloon cells

Table 5: Non-alcoholic fatty liver disease score (NAS).

Immunohistochemistry

Livers sections were deparaffinized, rehydrated and stained with primary antibodies of different immune cells for 44 minutes as follows: macrophage marker F4/80, T cell marker CD3, B cell marker B220 and neutrophil maker Ly-6G (antibodies see Table 6). Samples were washed and stained with secondary antibody for half an hour (anti-rabbit HRP). Slides were counterstained with hematoxylin for 8 minutes and bluing reagent was added for 4 minutes. The slides were scanned by a Prior robot/Nikon slide scanner. To quantify immune cells, three independent visual fields were semi-automatically quantified for area fraction (F4/80) or number of cells per nuclei (CD3, B220, Ly-6G) using the Nikon software (NIS) tool (Table 5).

IHC	Primary antibody	Diluent	Visualization
F4/80	F4/80 T-2006 clone BM8 BMA Biomedicals	1/50	Performed on Discovery Ventana UltraMap anti Rat DAB Kit
B220	B220 553084 clone RA3-6B2, BD Biosciences	1/4000	Performed on Discovery Ventana UltraMap anti Rat DAB Kit
CD3	CD3 MA1-90582 clone SP7, Thermo Fisher Scientific	1/300	Performed on Bond Leica DAB Kit
Ly-6G	Ly-6G 551459 clone 1A8, BD Biosciences	1/600	Performed on Bond Leica DAB Kit

Table 6: Antibodies for IHC of immune cells in paraffin liver sections

In situ hybridization (ISH)

ISH was used to co-localize the RNA of both TNF α and Emr1in hepatic macrophages after imatinib treatment. The assay was performed by Diego Calabrese (Hepatology Group, Department of Biomedicine, University Hospital of Basel) as previously described [118] and according to the manufacturer's instructions with some modifications.

Tissue Processing

Formalin-Fixed and Paraffin-Embedded Liver Tissue (FFPE) were deparaffinized, rehydrated and pre-treated by boiling the tissues at 85-95 Celsius for 15 minutes, followed by protease digestion for 15 minutes at 40 Celsius to unmask target mRNAs and to allow probe accessibility.

Hybridization

TNF-α (20 oligonucleotide, TYPE 1, VB1-10175-06, Panomics-Affymetrix) and Emr1 (20 oligonucleotide, TYPE 2, VB6-12917-VT, Panomics-Affymetrix) probe sets were diluted 1:30 and 1:40, respectively, in hybridization buffer and then hybridized at 40 Celsius in ThermoBrite oven for 2.5 hours.

Amplification & detection

Multiple series of hybridization steps were performed at 40 Celsius in a ThermoBrite oven, using PreAmplifier Mix QT and Amplifier Mix QT to amplify the signal before the detection. The detection was performed incubating the tissues with alkaline phosphates (AP) labeled probes for 45 minutes at 40 Celsius. Slides were then incubated with AP chromogenic substrates (i.e. Fast Red and Fast Blue), respectively, at 40 Celsius. in the ThermoBrite oven and room temperature in a humidified chamber.

Counterstaining, slides mounting and visualization

Each slide was counterstained with Gill's hematoxylin. Slides were then mounted with water based mounting media containing DAPI, covered with No. 1 glass coverslip, air-dried for 15 minutes and finally stored at 4 Celsius. Brightfield and fluorescent images were acquired using a laser scanning confocal microscope (LSM710, Carl Zeiss Microscopy, Göttingen, Germany) and the Zen2 software (Carl Zeiss Microscopy, Göttingen, Germany) and processed further by ImageJ software.

4.1.6 Data analysis

Data from independent experiments were analyzed using GraphPad Prism™ Software, (version 7; GraphPad Software Inc, San Diego, CA). All data are presented as mean±SEM. Non-parametric unpaired Mann-Whitney test was used for statistical significance. A p-value <0.05 was considered as statistically significant. Grubbs (Extreme Studentized Deviate) test was used to identify outliers among at least three samples.

4.2 Materials

4.2.1 Buffers and media

0.5M EDTA (4 Celsius.)

186.1 g	EDTA x 2H20 MW 372.2	Sigma-Aldrich	E6635-1kg
1 L	dH20		

FACS Buffer (4 Celsius.)

445 mL	dH20		
50 mL	10x DPBS	Gibco	14200067-500ML
2.5 g	BSA	VWR	441555J-100 G
5 mL	0.5 M EDTA	Sigma-Aldrich	03690-100 ML

Red Cell Lysis Buffer (4 Celsius.)

8.237 g	NH4Cl (154 mM)	Sigma-Aldrich	A9434-500 G
1 g	KHC03 (10 mM)	Sigma-Aldrich	P9144-500 G
0.2 mL	0.5 M EDTA pH 8 (0.1 mM)	Sigma-Aldrich	03690-100 ML
1 L	dH20		

Adipose tissue 2x Digestion mix (V_{Total}= 8mL*sample)

$V_{Total}/2$	1x HBSS	Gibco	24020-091
0.01 mL/mL	1 M HEPES pH 7.5 (10 mM HEPES)	Sigma-Aldrich	H0887-100 ML
1.5 mg/mL	Collagenase IV ACT: 280 u/mg	Worthington	LS004189
0.33 µl/mL	DNAse I	Roche	11284932001

Peritoneal Macrophages medium (4 Celsius.)

RPMI-1640 medium	-Glutamin	Gibco	31870025-500 ML
10 %	FBS	Gibco	10500064-500 ML
1 %	Glutamax (100 X, 200 mM)	Gibco	35050038-100 ML
1 %	Pen/ Strep (10 000 U/10 mL)	Gibco	15140122-100 ML
0.1 %	Amphotericin B (250 µg/mL)	Gibco	04195780F-50 ML
0.1 %	Gentamycin	Gibco	15750037-20 ML

Bone Marrow Derived Macrophages medium (4 Celsius.)

RPMI-1640 medium	HEBES 25 mM L-Glutamin 2 mM	Gibco	52400025-500 ML
10 %	FBS	Gibco	10500064-500 ML
1 %	Glutamax (100 X, 200 mM)	Gibco	35050038-100 ML
2 %	Pen/ Strep (10 000 U/10 mL)	Gibco	15140122-100 ML
1 %	MEM Non-Essential Amino acids 100 x	Gibco	11140035-100 ML
1 %	Sodium Pyruvate (100mM)	Gibco	11360039-100 ML
0.055 mM	β-mercapoethanol (1000 x)	Gibco	31350010-20 ML

Human Monocytes medium (4 Celsius.)

RPMI-1640 medium	HEBES 25 mM L-Glutamin 2 mM	Gibco	52400025-500 ML
10 %	FBS	Gibco	10500064-500 ML
1 %	Glutamax (100 X, 200 mM)	Gibco	35050038-100 ML
1 %	Pen/ Strep (10 000 U/10 mL)	Gibco	5140122-100 ML

1 %	MEM Non-Essential Amino acids 100x	Gibco	11140035-100 ML
1 %	Sodium Pyruvate (100mM)	Gibco	11360039-100 ML

Affymetrix Isolation Buffer (4 Celsius.)

1 x	PBS -Mg, -Ca	Sigma-Aldrich	D8537-500ML
3 %	FBS	Gibco	10500064-500 ML
10mM	EDTA	Sigma-Aldrich	03690-100ML

Seahorse Unbuffered Free Glucose medium (4 Celsius.)

1 Bottle	RPMI-1640 medium with L-glutamine pH 7.4	Sigma-Aldrich	R1383-10x1L
Add to 1 L	dH20		

Seahorse XF Compounds (-20 Celsius.)

200 mM	D (+) Glucose	Sigma-Aldrich	G7021-1KG
50 μM	Oligomycin	Sigma-Aldrich	75351-5MG
15 mM	FCCP	Sigma-Aldrich	C2920-10MG
100 mM	Sodium Pyruvate (100mM)	Gibco	11360039-100 ML
13.75 mM	Rotenone.	Sigma-Aldrich	R8875-1G

5. Publication

SCIENTIFIC REPORTS

OPEN

Imatinib reduces non-alcoholic fatty liver disease in obese mice by targeting inflammatory and lipogenic pathways in macrophages and liver

Received: 6 June 2018
Accepted: 17 September 2018
Published online: 17 October 2018

Shefaa AlAsfoor[1,2], Theresa V. Rohm[1,2], Angela J. T. Bosch[1,2], Thomas Dervos[1,2], Diego Calabrese[2], Matthias S. Matter[3], Achim Weber[4] & Claudia Cavelti-Weder[1,2]

Macrophages have been recognized as key players in non-alcoholic fatty liver disease (NAFLD). Our aim was to assess whether pharmacological attenuation of macrophages can be achieved by imatinib, an anti-leukemia drug with known anti-inflammatory and anti-diabetic properties, and how this impacts on NAFLD. We analyzed the pro- and anti-inflammatory gene expression of murine macrophages and human monocytes *in vitro* in the presence or absence of imatinib. In a time-resolved study, we characterized metabolic disease manifestations such as hepatic steatosis, systemic and adipose tissue inflammation as well as lipid and glucose metabolism in obese mice at one and three months of imatinib treatment. Our results showed that imatinib lowered pro-inflammatory markers in murine macrophages and human monocytes *in vitro*. In obese mice, imatinib reduced TNFα-gene expression in peritoneal and liver macrophages and systemic lipid levels at one month. This was followed by decreased hepatic steatosis, systemic and adipose tissue inflammation and increased insulin sensitivity after three months. As the transcription factor sterol regulatory element-binding protein (SREBP) links lipid metabolism to the innate immune response, we assessed the gene expression of SREBPs and their target genes, which was indeed downregulated in the liver and partially in peritoneal macrophages. In conclusion, targeting both inflammatory and lipogenic pathways in macrophages and liver as shown by imatinib could represent an attractive novel therapeutic strategy for patients with NAFLD.

As a result of the increasing prevalence of obesity, non-alcoholic fatty liver disease (NAFLD) has become one of the most common chronic liver diseases worldwide[1]. NAFLD comprises a wide spectrum of diseases ranging from simple fatty liver (NAFL) to non-alcoholic steatohepatitis (NASH), which is characterized by infiltration of immune cells in the liver. In recent years, evidence has accumulated that macrophages play a key role in the onset and progression of NAFLD: Liver injury activates resident liver macrophages leading to cytokine and chemokine release, which induces the recruitment of bone marrow-derived macrophages (BMDM) into the liver, further amplifying the disease process[2–4]. We use the term "liver macrophages" for both bone marrow-derived and resident liver macrophages as their markers strongly overlap[5]. Targeting liver macrophages has been postulated as a therapeutic strategy for NAFLD[3], especially as currently no specific treatment exists. Pharmacological macrophage depletion indeed prevents the development of NAFLD in mouse models[2,6,7]. Similarly, blocking bone marrow-derived macrophage recruitment to the liver by pharmacological or genetic ablation of different chemokine or cytokine pathways improves NAFLD characteristics (e.g. CCR2-CCL2[4,8–10], CCR2/5[11,12], CXCR3-CXCL10[13,14], CXCL16[15], IL-6[16], TNFα[17]). A CCR2/5 antagonist has been tested in a clinical trial with promising results regarding fibrosis in NASH patients[18]. Besides macrophage depletion and blocking macrophage

[1]Clinic of Endocrinology, Diabetes and Metabolism, University Hospital Basel, Basel, Switzerland. [2]Department of Biomedicine, University of Basel and University Hospital Basel, Basel, Switzerland. [3]Institute of Pathology, University Hospital of Basel, Basel, Switzerland. [4]Department of Pathology and Molecular Pathology, University and University Hospital of Zurich, Zurich, Switzerland. Correspondence and requests for materials should be addressed to C.C.-W. (email: claudia.cavelti-weder@usb.ch)

recruitment, pharmacological attenuation of pro-inflammatory macrophages could be an alternative strategy to treat NAFLD. As macrophage activation and chronic low-grade inflammation are linked to metabolic disease and insulin resistance[19], targeting pathologically activated macrophages might even have a broader impact on metabolic disease manifestations.

A potential candidate drug with anti-inflammatory properties is the tyrosine kinase inhibitor (TKI) imatinib, which was originally developed to target the tumor-associated fusion protein BCR-Abl in chronic myelogenous leukemia (CML). Over the years, several other targets of imatinib have been identified[20]. Most recently, imatinib was shown to inhibit posttranslational phosphorylation of PPARγ[21], which is an important regulator of macrophage polarization[22]. Anti-inflammatory effects upon imatinib treatment include adoption of an anti-inflammatory phenotype in tumor-associated macrophages[23], suppressed glycolysis as an indication for anti-inflammatory polarization in leukemia cells[24], reduced acute liver injury[25], and attenuated adipose tissue inflammation in obese mice[21]. Additionally, glucose-lowering effects have been observed as "side effects" in cancer patients treated with imatinib[26,27]. In diabetic mouse models, these anti-diabetic effects have been attributed to reduced β-cell death and maintained β-cell function[28–30]. The combination of anti-inflammatory and anti-diabetic effects is reminiscent of PPARγ-agonists/thiazolidinediones (TZDs), which are anti-diabetic drugs also known to dampen macrophage activation[31,32]. TZDs were even implicated in reduced hepatic steatosis via modulation of liver macrophages[33]. However, due to side effects such as fluid retention, congestive heart failure, weight gain and bone fractures, TZDs have been largely abandoned from clinical practice.

Based on the anti-inflammatory and anti-diabetic effects of imatinib potentially involving PPARγ, the aim of our study was to assess whether imatinib directly attenuates macrophages and could therefore be used in disease states with pathological macrophage activation such as NAFLD. We set out a proof-of-concept study to addresses this novel therapeutic concept by testing the effect of imatinib on (1) macrophage activation *in vitro*, (2) NAFLD and other metabolic disease manifestations in a time-resolved manner *in vivo*, and (3) human monocytes to assess its translational application. The concept of pharmacological macrophage attenuation in NAFLD is intriguing as restoring pathologically activated macrophages could potentially not only target the root cause of NAFLD, but also other metabolic disease manifestations such as adipose tissue and systemic inflammation and insulin resistance. A more profound understanding of macrophage modulation and the molecular pathways involved holds the promise for new treatment strategies in NAFLD and metabolic disease.

Results

Imatinib lowers pro-inflammatory macrophage activation *in vitro*. Imatinib was tested in differentially activated peritoneal macrophages *in vitro* (M0, M1, M2) after the optimization of housekeeping genes (HKGs), the timing of macrophage activation and the dose of imatinib (Supplementary Fig. S1): In peritoneal M1-activated macrophages, imatinib lowered multiple pro-inflammatory genes, most consistently TNFα. Accordingly, TNFα and IL-6 protein were lower in the supernatants of imatinib-treated M1-macrophages (Fig. 1a). In contrast, pro-inflammatory genes were not altered in unstimulated M0- and anti-inflammatory M2-peritoneal macrophages (Fig. 1b). To confirm this immune-dampening effect in a different macrophage population, imatinib was tested in BMDM, where it exerted a similar immune-dampening effect, although less pronounced than in peritoneal cells (Fig. 1c). To find out whether imatinib only dampens pro-inflammatory genes or also promotes anti-inflammatory gene expression, anti-inflammatory genes were similarly assessed in differentially activated macrophages. We found higher Mgl1 in M2- and Mrc1 in M1-, but no change in M0-macrophages upon imatinib (Fig. 1d). This demonstrates that imatinib primarily lowers pro-inflammatory markers in M1-activated macrophages *in vitro* and does not promote up-regulation of anti-inflammatory genes.

Imatinib lowers peritoneal macrophage activation in acute inflammation and metabolic disease models. Next, we asked whether this immune-dampening effect of imatinib on macrophages also occurs *in vivo*. To validate peritoneal macrophages as a direct readout for macrophage attenuation, we tested an acute inflammation model by inducing a highly inflammatory response by intraperitoneal (i.p.) Lipopolysaccharide (LPS-) injection in mice pretreated with imatinib or water. Imatinib pretreatment lowered TNFα gene expression in peritoneal macrophages (Fig. 2a), while anti-inflammatory genes were not altered (Supplementary Fig. S2a). To test imatinib in chronic metabolic disease models, diabetic (high fat diet and streptozocin (HFD + STZ)) and obese mice (HFD) were treated with imatinib (IM) or vehicle for up to three months. In diabetic mice, TNFα gene expression was significantly lower in peritoneal cells (0.64 ± 0.05 fold) and less induced by additional LPS/IFNγ-stimulation when compared to untreated controls (1.8 ± 0.5 and 2.3 ± 0.4 fold, respectively, Fig. 2b). Likewise, TNFα gene expression was lower in peritoneal cells of obese mice after one and three months of imatinib treatment (both time points 0.58 ± 0.1 fold) and less induced in peritoneal macrophages upon additional LPS/IFNγ-stimulation (1.2 ± 0.1 and 2.0 ± 0.3 fold, Fig. 2c). Similar to the acute inflammation model, anti-inflammatory genes were not altered (Supplementary Fig. S2b,c). As an additional readout for macrophage activation, we used Seahorse analysis, which showed lower metabolic oxidation (OCR) in peritoneal macrophages from imatinib-treated mice with significantly lower non-mitochondrial and maximum respiration (Supplementary Fig. S2d), while only minor effects were found for glycolysis. Thus, imatinib lowers pro-inflammatory activation of peritoneal macrophages in acute inflammation and metabolic disease models *in vivo* as assessed by gene expression and metabolic flux.

Imatinib reduces liver macrophages via modulation of the TNFα-pathway. To assess whether imatinib also affects liver macrophages, which are key drivers of NAFLD, we performed a time-resolved study with HFD-induced obese mice (data summarized in Table 1): Concurrent with TNFα-reduction in peritoneal macrophages, imatinib lowered TNFα gene expression in liver tissue after one month. This was followed by a reduction in macrophage gene expression after three months of imatinib treatment (Fig. 2e). Co-localization of

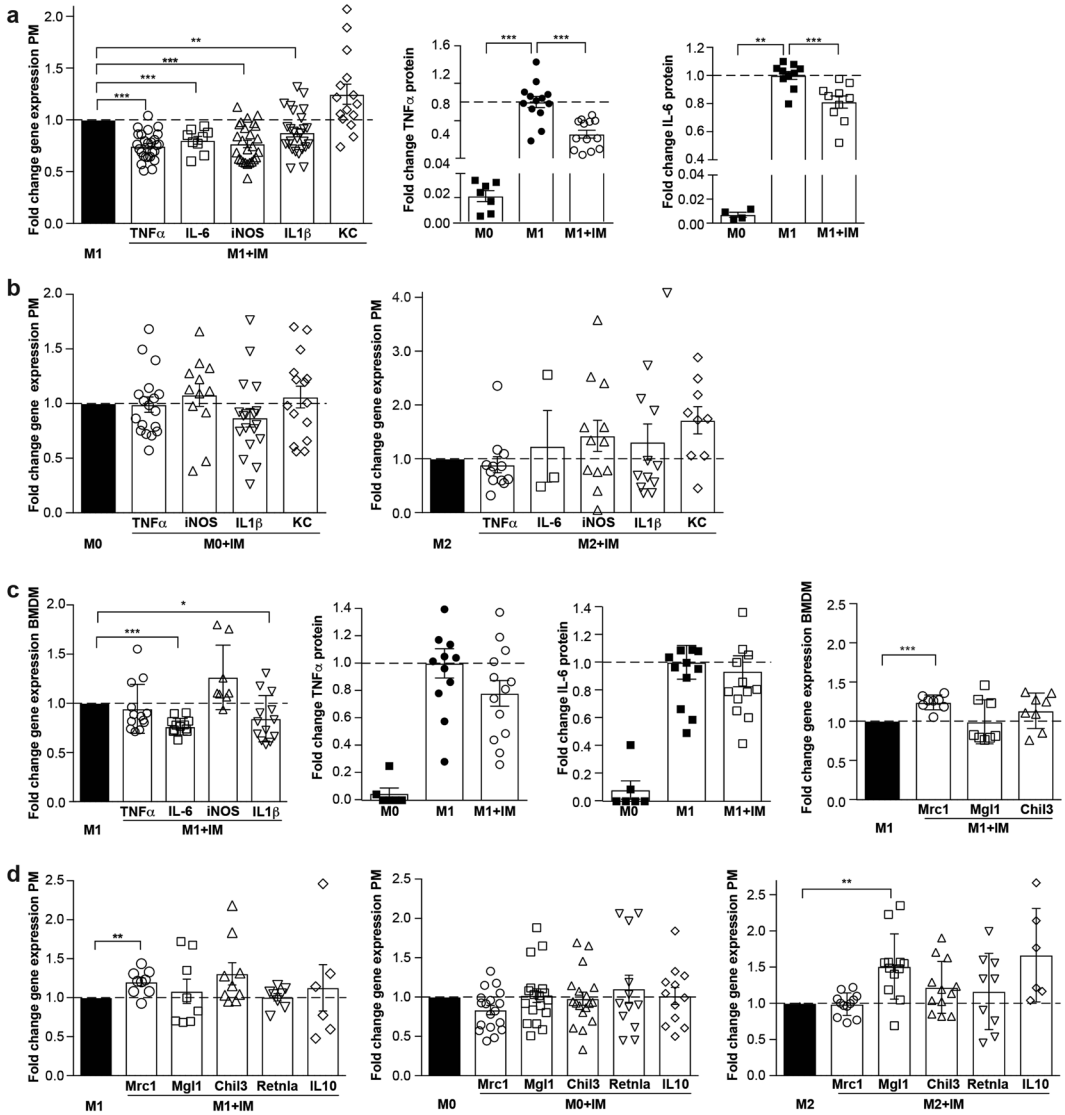

Figure 1. Imatinib lowers pro-inflammatory macrophage activation *in vitro*. (**a**) Fold change gene expression of pro-inflammatory markers in M1-peritoneal macrophages treated with 1 μM of imatinib (M1 + IM, open bars) compared to non-treated M1-controls (M1, closed bar) (n = 8–26). Fold change of TNFα and IL-6 protein in the supernatant of unstimulated (M0), activated (M1) and concomitantly activated/imatinib-treated (M1 + IM) peritoneal macrophages (n = 4–13). (**b**) Fold change of pro-inflammatory gene expression in unstimulated/imatinib-treated (M0 + IM, n = 12–18) and anti-inflammatory/imatinib-treated macrophages (M2 + IM, n = 3–12) compared to their respective controls (M0 or M2). (**c**) Fold change of pro-inflammatory gene expression in activated/imatinib-treated BMDM (M1 + IM) and controls (M1) (n = 8–13). Fold change of TNFα and IL-6 protein in the supernatant of unstimulated (M0), activated (M1) and concomitantly activated/imatinib-treated (M1 + IM) BMDM (n = 6–13). Gene expression of anti-inflammatory genes in BMDM (n = 6–9) treated with imatinib compared to non-treated M1-controls. (**d**) Gene expression of anti-inflammatory genes in M1-activated (n = 6–9), unstimulated M0 (n = 12–18) and anti-inflammatory M2-peritoneal macrophages (n = 6–12) treated with imatinib compared to their respective controls (M1, M0, M2). Data are presented as mean ± SEM. *$p < 0.05$, **$p < 0.01$, ***$p < 0.001$.

TNFα and Emr1 (macrophage marker) mRNA in the liver indicated that TNFα-reduction occurred in liver macrophages (Fig. 2d). Consistent with gene expression, F4/80 area fraction showed no change after one month, but prevention of the HFD-induced increase in liver macrophages after three months of imatinib treatment (Fig. 2f,g). The immune-modulation was specific to macrophages, as other immune cells such as B- and T-lymphocytes and neutrophils were not affected in the liver (Fig. 2h,i). Thus, imatinib leads to early TNFα-reduction in liver macrophages, which later prevents the HFD-induced increase in liver macrophages.

Early TNFα-reduction in macrophages is accompanied by changes in lipid metabolism, followed later by markedly decreased hepatic steatosis. We used our time-resolved approach to address the question whether and in what time frame liver macrophage attenuation by imatinib impacts on liver

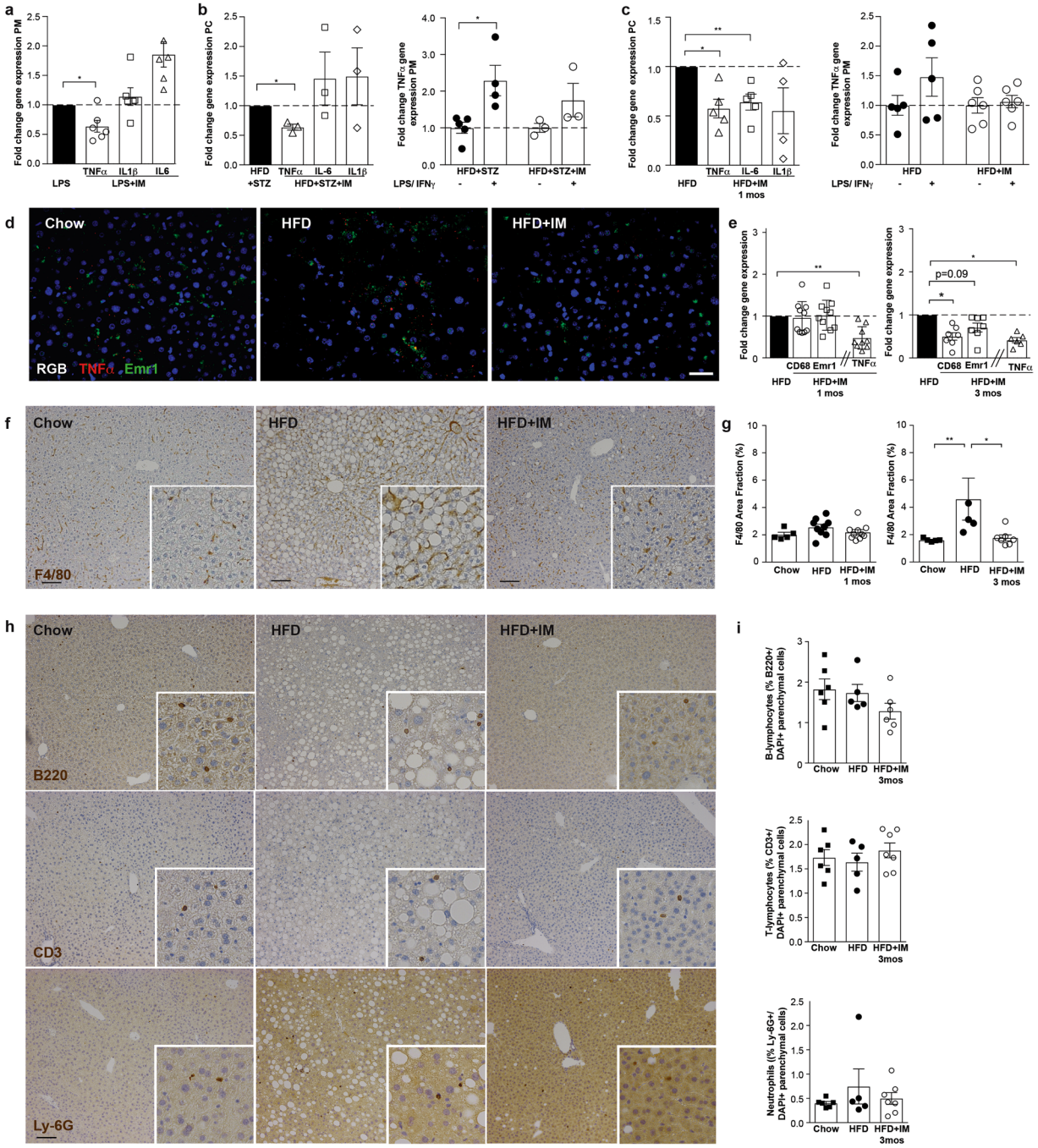

Figure 2. Imatinib lowers pro-inflammatory activation in peritoneal and liver macrophages *in vivo*. (**a**) Fold change of pro-inflammatory genes in peritoneal macrophages in the acute inflammation model (LPS + IM: imatinib pretreated mice; LPS: water treated controls; n = 4–6). (**b**) Fold change of pro-inflammatory genes in peritoneal cells and in peritoneal macrophages upon *ex vivo* stimulation with LPS/IFNγ from diabetic mice treated for one month with imatinib (HFD + STZ + IM) compared to water-treated controls (HFD + STZ) (n = 3–6). (**c**) Fold change of pro-inflammatory genes in peritoneal cells and in peritoneal macrophages upon *ex vivo* LPS/IFNγ-stimulation from obese mice (HFD + IM) treated with imatinib compared with water-treated controls (HFD) (n = 4–10). (**d**) *In situ* hybridization for TNFα (red) and Emr1 (green) mRNA and DAPI nuclear staining (blue) in liver sections from chow, HFD and HFD + IM-treated mice. (**e**) Fold change gene expression of macrophage markers CD68 and Emr1 and TNFα in HFD + IM-treated mice compared to HFD controls after one and three months of imatinib (n = 5–7). (**f,g**) Representative liver sections stained for F4/80 from chow, HFD-fed and HFD + IM-treated mice and quantification by macrophage area fraction (%) at one and three months of imatinib treatment. (**h,i**) Representative liver sections stained for B220, CD3, Ly-6G and DAPI from chow, HFD-fed and HFD + IM-treated mice and quantification by % of cells/ DAPI + parenchymal cells at three months of imatinib. HFD: High fat diet, IM: imatinib, mos: months, PC: peritoneal cells, PM: peritoneal macrophages. Scale bar represents 100μm. Data expressed as mean ± SEM, *$p < 0.05$, **$p < 0.01$.

	1 month IM	3 months IM
Peritoneal cells		
TNFα gene expression	**0.58 ± 0.1**	0.58 ± 0.1
SREBP1c target genes	**1/4 reduced**	0/4 reduced
pS273 PPARγ-related genes	0/12 induced	1/12 induced
Liver		
TNFα gene expression	**0.48 ± 0.1**	**0.41 ± 0.1**
SREBP1a target genes	**1/3 reduced**	
SREBP1c target genes	**3/8 reduced**	1/8 reduced
SREBP2 target genes	**2/6 reduced**	1/6 reduced
CD68 gene expression	0.95 ± 0.1	**0.50 ± 0.1**
F4/80 gene expression	1.0 ± 0.1	0.71 ± 0.1 (trend)
F4/80 area fraction	0.86 ± 0.1	**0.38 ± 0.1**
NAS-score	0.9 ± 0.2	**0.42 ± 0.2**
Alkaline phosphatase	not detected	**0.59 ± 0.1**
Systemic		
Cholesterol	**0.75 ± 0.05**	**0.7 ± 0.1**
HDL	**0.77 ± 0.05**	**0.76 ± 0.1**
Triglycerides	1.05 ± 0.1	**0.8 ± 0.1**
TNFα	0.9 ± 0.05	**0.43 ± 0.1**
Adipose tissue		
TNFα gene expression	0.55 ± 0.2	**0.39 ± 0.1**
CD68 gene expression	0.93 ± 0.2	0.57 ± 0.2
F4/80 gene expression	0.88 ± 0.1	**0.48 ± 0.1**
pS273 PPARγ-related genes	0/17 induced	5/17 induced
Metabolic tests		
ITT	ns	**s**
GTT	ns	ns

Table 1. Summary time resolved study (1 and 3 months imatinib) in obese mice. Statistical differences between one and three months data are indicated in bold font. Data presented as mean ± SEM.

outcomes: Besides TNFα-reduction in the liver, the earliest change we observed were lowered systemic lipid levels after one month of imatinib treatment, also persisting at three months (Fig. 3a,b). All other tissue changes were only observed after three months of imatinib treatment (Table 1): The stark increase in hepatic steatosis in mice on HFD compared to chow was almost completely resolved after three months of imatinib treatment as histologically quantified by the NAFLD activity score (NAS-)score (Fig. 3c,d; Supplementary Fig. S3). Fibrosis was not induced by our obesity model and therefore did not affect the NAS-score. These morphological changes also affected liver function as shown by lower alkaline phosphatase after three months of imatinib (Fig. 3e). Additionally, three months of imatinib prevented the HFD-induced increase in plasma TNFα-levels (Fig. 3f). Thus, besides TNFα-reduction in the liver imatinib leads to early changes in lipid metabolism, which is later followed by markedly decreased hepatic steatosis.

Imatinib lowers adipose tissue inflammation and increases insulin sensitivity after three months. We also studied the effect of imatinib on other metabolic disease manifestations such as adipose tissue inflammation and glucose metabolism in a time-resolved manner (Table 1): While there was no change in adipose tissue inflammation after one month of imatinib, the HFD-induced increase in macrophages and pro-inflammatory markers in adipose tissue was reversed by three months of imatinib treatment (Fig. 4a). Flow cytometry confirmed a higher frequency of macrophages in the adipose tissue of HFD-fed animals compared to mice treated for 3 months with imatinib. However, absolute numbers of adipose tissue subpopulations were unchanged (Supplementary Fig. S4). In terms of glucose metabolism, diabetic mice had slightly increased insulin sensitivity after one month of imatinib when compared to vehicle-treated mice, while glucose tolerance was unaltered (Fig. 4b). After one month of treatment, obese mice showed no change in body weight or glucose and insulin tolerance. However, after three months a comparable pattern as in the diabetic model was observed with increased insulin sensitivity, yet unchanged glucose tolerance (Fig. 4c). Taken together, reduced adipose tissue inflammation and increased insulin sensitivity occur after up to three months of imatinib treatment.

Time-resolved assessment of transcription factors suggests that imatinib targets SREBP, while restoration of PPARγ-phosphorylation is a secondary phenomenon. As the transcription factor sterol regulatory element-binding protein (SREBP) links lipid metabolism to the innate immune response[34] that were both early affected with imatinib treatment, we assessed the target genes of the three isoforms SREBP1a, SREBP1c and SREBP2: Imatinib downregulated SREBP1c gene expression in cultures of peritoneal macrophages, which was corroborated *in vivo* after one month of imatinib treatment (Fig. 5a,b). SREBP1a and its target genes

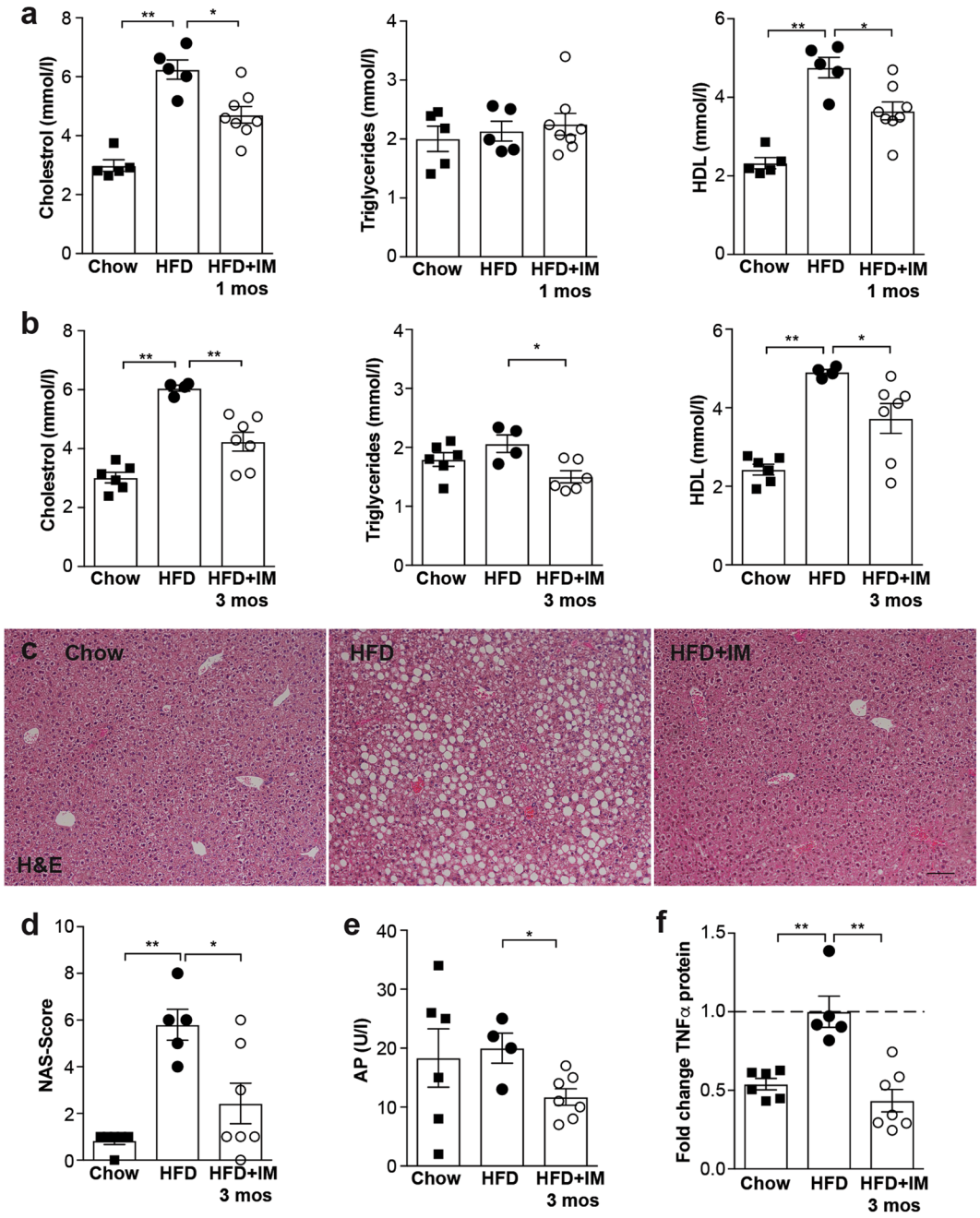

Figure 3. Early TNFα-reduction in macrophages is accompanied by changes in lipid metabolism, followed later by markedly decreased hepatic steatosis. (**a**,**b**) Plasma cholesterol, triglycerides and High-density lipoprotein (HDL) in chow, HFD and HFD + IM-treated mice after one (**a**) and three months of imatinib treatment (**b**; n = 4–7). (**c**) Representative H&E liver stainings from chow, HFD-fed and HFD + IM-treated mice. (**d**) Quantification of NAFLD features by the NAS-score in chow, HFD and HFD + IM-treated mice. (**e**) Alkaline phosphatase (AP) in chow, HFD and HFD + IM-treated mice (n = 4–7). (**f**) Fold change of systemic TNFα protein in chow, HFD and HFD + IM-treated mice (n = 5–7). HFD: High fat diet, IM: imatinib, mos: months. Scale bar represents 100 μm. Data expressed as mean ± SEM, *$p < 0.05$, **$p < 0.01$.

Nlrp1a and Nlrp1c, in contrast, were not altered in peritoneal cells. In the liver, 3/8 SREBP1c and 2/6 SREBP2 target genes were significantly downregulated after one month imatinib (Fig. 5d). Interestingly, after three months of imatinib treatment, SREBP target gene expression was mostly normalized to baseline in both peritoneal cells and liver tissue (Fig. 5c,e), suggesting that compensatory mechanisms might occur over time.

Another transcription factor that has been shown to control both inflammatory responses and lipid metabolism is PPARγ[35]. In the context of metabolic disease, PPARγ has been shown to become phosphorylated at serine273, leading to dysregulation of a large number of metabolically important genes[36]. Imatinib was shown to inhibit PPARγ-phosphorylation at serine273, thereby reducing insulin resistance and promoting browning

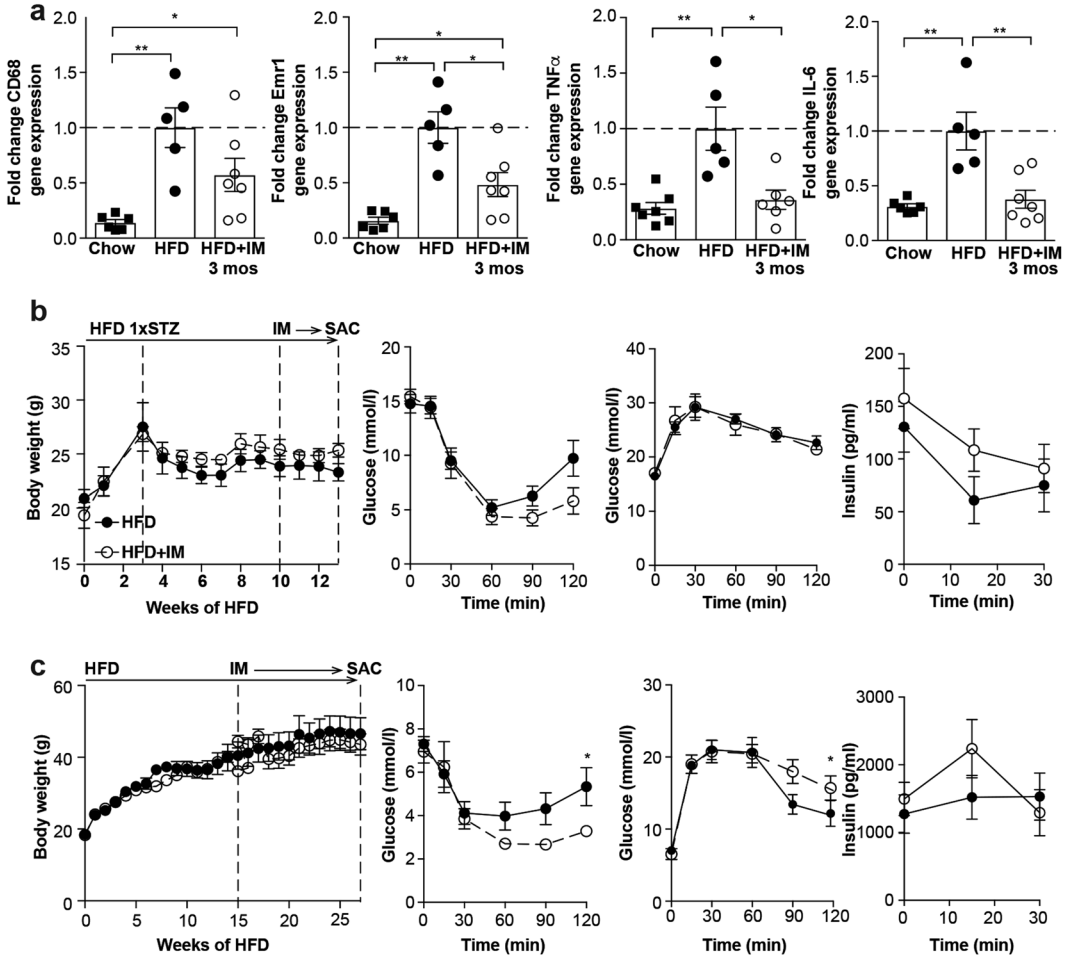

Figure 4. Imatinib reduces adipose tissue inflammation and increases insulin sensitivity over time. (**a**) Fold change gene expression of macrophage markers (CD68, F4/80) and pro-inflammatory M1-markers (TNFα, IL-6) in whole adipose tissue of chow, HFD and HFD + IM-treated animals (n = 5–7). (**b**) Body weight, insulin sensitivity and glucose tolerance with insulin in diabetic mice treated for one month with imatinib (HFD + STZ + IM) and controls (HFD + STZ; n = 4–5). (**c**) Body weight, insulin sensitivity and glucose tolerance with insulin in obese mice treated for three months with imatinib (HFD + IM) and controls (HFD; n = 5–6). HFD: High fat diet, IM: imatinib, mos: months, SAC: sacrifice, STZ: Streptozocin. Data expressed as mean ± SEM, *$p < 0.05$, **$p < 0.01$.

of white adipose tissue[21]. We therefore assessed genes related to PPARγ-phosphorylation at serine273 in our time-resolved study. In white adipose tissue, PPARγ-phosphorylation-related genes were dysregulated (lowered) by HFD mainly at the three months' time point (Supplementary Fig. S5a) when also restoration of these genes occurred by imatinib (upregulation of 5/17 PPARγ-phosphorylation-related genes; Fig. 5f). In peritoneal cells, no changes in PPARγ-phosphorylation-related genes were found at both one and three months of imatinib (Supplementary Fig. S5b), suggesting that phosphorylation at serine273 (pS273) is not directly affected in macrophages. Thus, the early immune-dampening effect in macrophages precedes restored PPARγ-phosphorylation in adipose tissue, indicating that restoration of PPARγ-phosphorylation-related genes might be a secondary phenomenon.

As a last potential mechanism, we assessed genes involved in thermogenesis as imatinib has previously been shown to induce browning of adipose tissue[21]. However, we did not find upregulation of cold-induced thermogenesis genes Pcg1α, Ucp-1, Cox5b, Cpt1b and Dio2 in inguinal adipose tissue of HFD-fed mice upon imatinib treatment (Supplementary Fig. S5c). In sum, our time-resolved assessment of potential pathways suggests that SREBP-signaling is affected in liver and partially in macrophages, while restoration of PPARγ-phosphorylation at pS273 seems to be a secondary phenomenon upon imatinib.

Imatinib lowers pro-inflammatory activation in human monocytes, but hyperglycemia alters their responsiveness. Finally, we assessed whether immune-modulation by imatinib could also be achieved in human monocytes. As hyperglycemia is known to impact on monocyte activation[37] and our *in vitro* data showed a differential response to imatinib depending on the activation state, we tested the effect of imatinib on monocytes from subjects with markedly distinct glycemia, including healthy controls (He), diabetics with

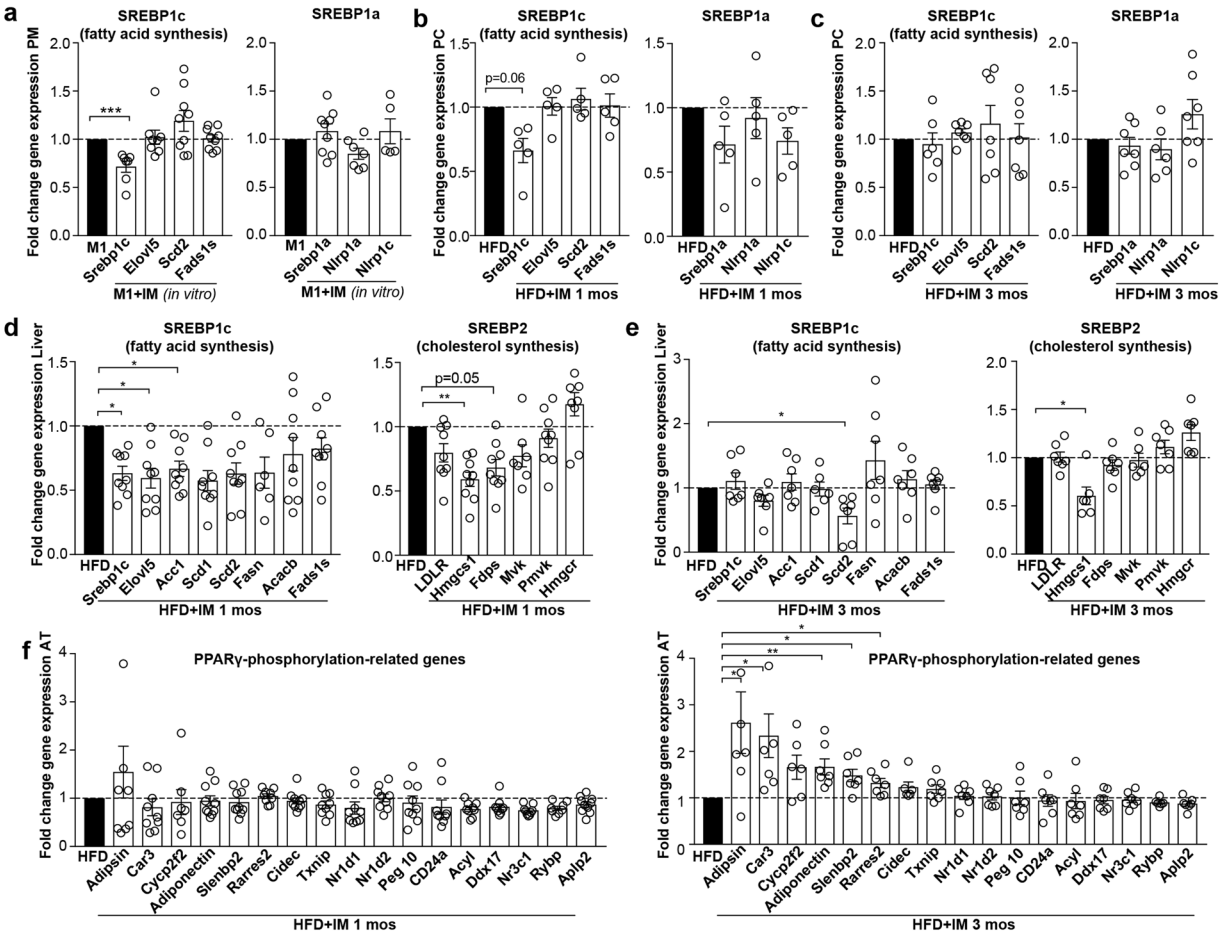

Figure 5. SREBP target genes are downregulated upon imatinib treatment, while PPARγ-phosphorylation seems to be a secondary phenomenon. (**a**) Fold change gene expression of SREBP target genes in M1-stimulated peritoneal macrophages treated with or without imatinib (IM) *in vitro* (n = 9). (**b**,**c**) Fold change gene expression of SREBP target genes in peritoneal cells after one and three months of imatinib treatment (n = 4–7). (**d**,**e**) Fold change gene expression of SREBP target genes in whole liver tissue after one and three months of imatinib (n = 5–9). (**f**) Fold change gene expression of PPARγ-phosphorylation-regulated genes in obese mice treated with imatinib (HFD + IM) compared with water-treated controls (HFD) after one (left) and three months of imatinib treatment (right; n = 5–10). AT: adipose tissue, HFD: High fat diet, IM: imatinib, mos: months, PC: peritoneal cells, PM: peritoneal macrophages. Data expressed as mean ± SEM, *p < 0.05, **p < 0.01, ***p < 0.001.

adequate (aDM) or inadequate glycemic control (iaDM). Supplementary Table S4 shows the baseline characteristics with the intended main differences between aDM and iaDM patients concerning their glycemic control (HbA1c aDM 52.6 ± 5.5 mmol/mol (7.0 ± 0.5%), iaDM 114.5 ± 6.5 mmol/mol (12.6 ± 0.6%)). Imatinib lowered the pro-inflammatory markers TNFα, MCP-1 and CD163 in unstimulated monocytes of all groups, while this immune-dampening effect was gradually lost in M1-activated monocytes with deranged glycemic control (Fig. 6a,b). Increasing the dose of imatinib did not restore the immune-dampening effect in iaDM patients (Fig. 6c). In sum, unstimulated human monocytes respond to imatinib treatment by down-regulation of pro-inflammatory markers. However with deranged glycemic control, the immune-dampening effect of imatinib is lost in activated monocytes, suggesting altered susceptibility to the drug with hyperglycemia.

Discussion

When first testing the notion of an immune-dampening effect of imatinib on macrophages *in vitro*, we found lower pro-inflammatory gene and protein expression, most consistently TNFα, while anti-inflammatory genes were not upregulated. This was slightly less pronounced in BMDM, most likely due to the artificial differentiation by exogenous Macrophage colony-stimulating factor (M-CSF) over one week. To translate our findings *in vivo*, we performed a time-resolved study assessing the effects of imatinib on macrophages and metabolic disease manifestations in HFD-induced obese mice: Reduction of TNFα in peritoneal and liver macrophages occurred most rapidly upon imatinib. Activated peritoneal macrophages are known to have both enhanced glycolysis and mitochondrial oxidation[38]. Metabolic flux as another measure for macrophage activation confirmed altered polarization by lower metabolic oxidation upon imatinib. In the liver, we were able to localize TNFα in liver macrophages, which decreased over time as shown by lower F4/80 area fraction and CD68 gene expression.

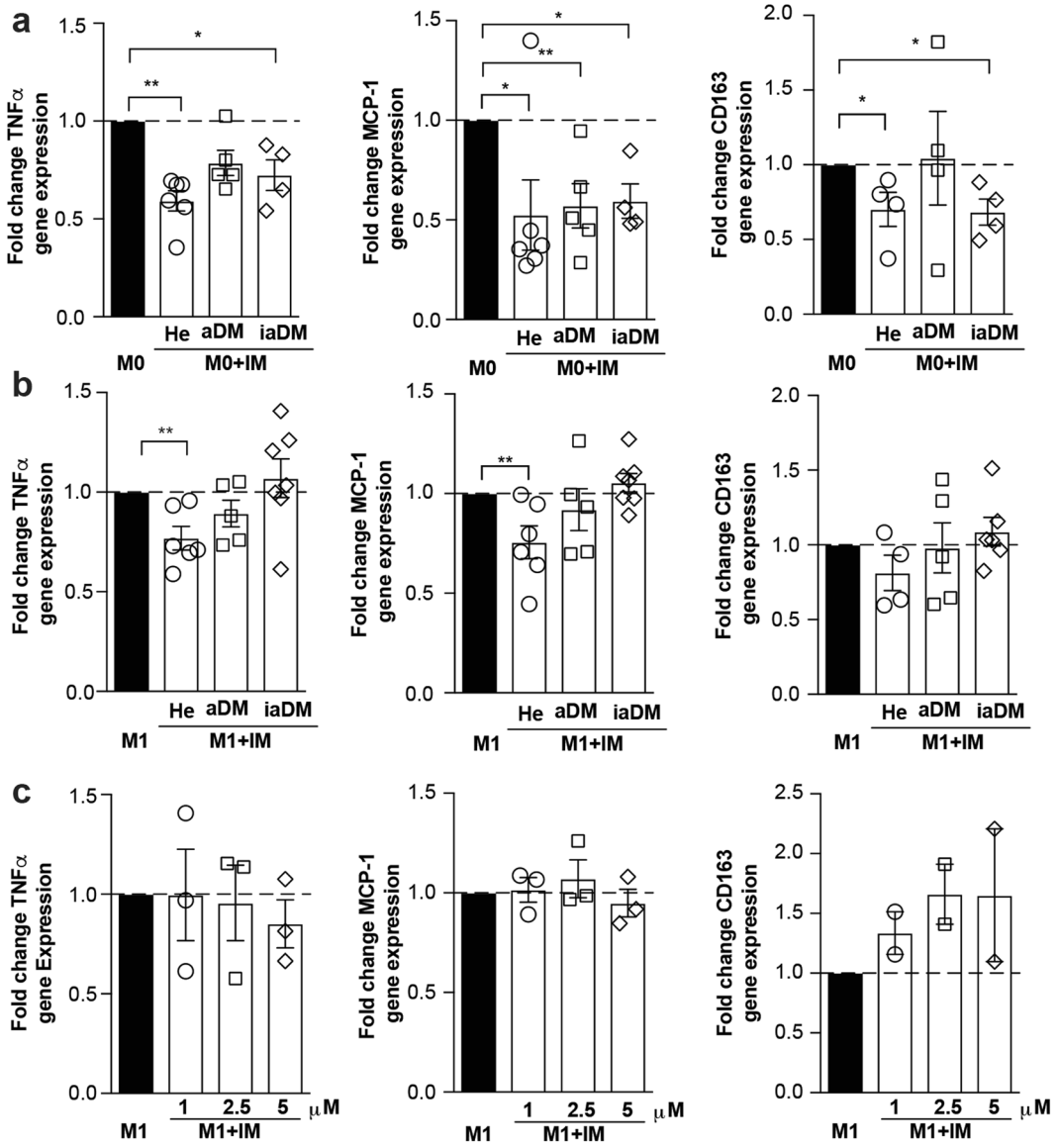

Figure 6. Imatinib lowers pro-inflammatory activation in human monocytes, but hyperglycemia alters their responsiveness. (**a,b**) Fold change gene expression of TNFα, MCP-1 and CD163 in human M0- (**a**) or M1-monocytes (**b**) treated with 1 μM of imatinib (M0 + IM or M1 + IM, open bars) compared to non-treated M0- or M1-monocytes (M0 or M1, closed bar) from healthy controls (He, n = 6), adequately controlled diabetics (aDM, n = 5) and inadequately controlled diabetics (iaDM, n = 5). (**c**) Fold change of gene expression of TNFα, MCP-1 and CD163 with increasing doses of imatinib (1, 2.5, 5 μM) in inadequately controlled diabetics (n = 3). Data expressed as mean ± SEM, *$p < 0.05$, **$p < 0.01$.

Thus, it is conceivable that down-regulation of TNFα by imatinib interrupts the vicious cycle of resident liver macrophage activation and/or bone marrow-derived macrophage recruitment to the liver, subsequently lowering their activation and/or number.

Concomitant with early TNFα-reduction in macrophages, imatinib led to lipid lowering effects, indicative for a mechanism that integrates both innate immunity and lipid metabolism. To assess a common mechanism involving both inflammation and lipogenesis, we first focused on the SREBP transcription factor family, which is known to activate lipogenic transcriptional programs, but has also been shown to control transcriptional regulation that extends beyond lipid synthesis[39]: For example, SREBP1a is highly expressed in immune cells such as macrophages and dendritic cells, where it not only activates genes required for lipogenesis but also a gene encoding Nlrp1, a core component of the inflammasome[34]. Thus, SREBP links lipid metabolism and the innate immune response and could therefore explain the simultaneous effects on inflammation and lipid levels we observed upon imatinib treatment. We found early reductions of SREBP1c-target genes in the liver and partially in peritoneal macrophages. These downregulations were gone after three months of imatinib treatment, most likely due to compensatory mechanisms. We speculate that the SREBP transcriptional program of the target cell determines the phenotypic alteration induced by imatinib: In macrophages, imatinib has preferentially an immune-dampening

effect, while in the liver also lipogenesis is affected. Thus, improvements in metabolic disease manifestations likely arise from a combination of the immune-dampening effect on macrophages and lowered lipogenesis induced by imatinib. Hence, in the long-term, lower SREBP target gene expression upon imatinib was associated with reduced hepatic steatosis, systemic and adipose tissue inflammation and increased insulin sensitivity.

Another transcription factor involved in both inflammation and lipid metabolism is PPARγ[35]. In obesity and insulin resistance, PPARγ was shown to become phosphorylated at serine273 with subsequent dysregulation of metabolically important genes[36]. Interestingly, PPARγ-phosphorylation at serine273 was blocked by imatinib, thereby restoring dysregulated diabetes-genes and reducing insulin resistance[21]. However, in our time-resolved assessment the early immune-dampening effect on macrophages and reduction in lipid levels clearly preceded restoration of PPARγ-phosphorylation-related genes in adipose tissue, indicating that restored PPARγ-phosphorylation might be a secondary phenomenon. Restoration of PPARγ-phosphorylation-related genes in adipose tissue potentially develops as less TNFα is available to engage in PPARγ-phosphorylation and its deleterious metabolic downstream effects. A recent study demonstrated that imatinib interferes with the interaction between the histone H3 lysine 4 methyltransferase MLL4 and PPARγ, thereby dampening steatotic target genes in short-term experiments[40]. Thus, dampened SREBP transcriptional programs as observed in our study could ultimately be due to imatinib interfering with the MLL4-PPARγ axis with subsequently reduced transcription of SREBP target genes.

As a third potential mechanistic pathway, we assessed browning of adipose tissue by imatinib, however, we were not able to find consistent upregulation of cold-induced thermogenesis genes. This is in contrast to the publication by Choi and colleagues[21], which could be explained by differences in the study set-up (administration of imatinib i.p. versus oral; treatment duration and genetic background (C57BL/6 J versus C57BL/6 N)). The latter is insofar important as genetic variability is known to affect cold-induced thermogenesis[41].

To translate our findings to human disease, we probed the effect of imatinib on human monocytes. Especially, as previous studies showed a heightened inflammatory state in human myeloid cells with hyperglycemia[37,42], diabetic patients could exhibit altered susceptibility to immune-modulatory drugs like imatinib. Human monocytes responded to imatinib treatment by down-regulation of pro-inflammatory markers also in a non-activated state. This is consistent with previous studies showing that monocytes have a "pre-activated" basal condition that requires only a single stimulation, while macrophages depend on a second signal to be activated[43]. In activated monocytes, however, the immune-dampening effect of imatinib was lost with deranged glycemic control, suggesting altered susceptibility to the drug with hyperglycemia, and could not be overcome with increasing doses of imatinib. Although the extreme stimulation as achieved by *ex vivo* LPS/IFNγ-stimulation might not represent the *in vivo* situation, it uncovers altered susceptibility to immune-modulation with hyperglycemia.

The strength of our study is that the long-term follow-up and time-resolved approach allowed us to distinguish early from later effects of imatinib on different cells and organs. Hence, it became clear that imatinib simultaneously affects inflammatory and lipogenic signals in macrophages and in the liver before reducing metabolic disease manifestations such as NAFLD, systemic and adipose tissue inflammation or insulin resistance. Our findings expand on previous literature by linking SREBP-signaling not only to lipogenesis, but also to innate immunity in the context of NAFLD. A more profound understanding of integrated pathways between inflammation and lipid metabolism could pave the way for the development of novel therapeutics in NAFLD.

The clinical significance of our findings lies in the scarcity of therapeutic measures available for NAFLD patients. Imatinib has generally a mild adverse effect profile and long-term safety record. In rare instances, however, imatinib has been associated with acute liver injury often in connection with hepatotoxic agents interfering with cytochrome P450 enzymes, leading to increased imatinib concentrations[44]. Thus, taking this into account, clinical trials could be envisaged in the context of NAFLD. Imatinib has already been tested in the setting of type 1 diabetes mellitus, however, the results have not yet been published[45]. In the light of our findings that imatinib exerts effects both on innate immunity and lipid metabolism, clinical studies involving patients with metabolic disease – preferentially with chronic low-grade inflammation and NAFLD – could yield promising results in the future.

Materials and Methods

Animals. Male C57BL/6 N mice (Charles River Laboratories, Sulzfeld, Germany) were maintained in our SPF-facility at 22 °C room temperature with 12 h light/12 h dark cycle and were housed in groups of 3–5 mice. Body weights were monitored once weekly. Mice used for metabolic experiments were kept for 1 week of acclimation period upon arrival. All procedures were approved by the local Animal Care and Use Committee (Veterinary Office Basel, Switzerland) and carried out in accordance with relevant guidelines and regulations.

Murine macrophages. Peritoneal cells were harvested from 6–8-week old male C57BL/6 N mice by intra-abdominal lavage, cultured overnight and enriched for macrophages by washing away non-adherent peritoneal cells. For BMDM, bone marrow cells were isolated from murine femur and tibia and differentiated by M-CSF (10 ng/mL, PeproTech, London, UK) for 7–9 days. Peritoneal macrophages or BMDM were polarized to a pro- (M1; 10 ng/mL IFNγ, PeproTech, 100 ng/mL LPS *E. coli* 0111:B4, Sigma-Aldrich, Saint Louis, MO, USA) or anti-inflammatory phenotype (M2; 10 ng/mL IL-4 and IL-13, Thermo Fisher Scientific, Waltham, MA, USA) or left unstimulated (M0) in the presence or absence of imatinib (1 μM, Novartis, Basel, Switzerland) for 6 hours.

Gene expression analysis. RNA was isolated using NucleoSpin RNA kit (Macherey Nagel, Düren, Germany) and RNeasy Plus Universal Mini kit (QIAGEN, Düsseldorf, Germany). Reverse transcription was performed with SuperScriptII Reverse Transcriptase kit (Thermo Fisher Scientific). GoTaq qPCR Master Mix (Promega, Madison, WI, USA) was used for real-time PCR (ViiA7, Thermo Fisher Scientific). Primer sequences (Microsynth, Balgach, Switzerland) are listed in Supplementary Table S1.

Protein expression analysis. Plasma insulin, TNF-α and IL-6 were quantified by electrochemiluminescence (MESO SECTOR S 600) using kits from MesoScale Diagnostics (MSD, Rockville, MD, USA).

Acute *in vivo* inflammation model. Imatinib (100 mg/kg) or water was administered by gavage three times during 24 h prior to a single i.p. LPS-injection (1 mg/kg). Analysis was performed 2 h post LPS and peritoneal cells and macrophages assessed by PCR.

Chronic *in vivo* inflammation model. Mice on high fat diet (HFD containing 58% fat, 16.4% protein and 25.6% carbohydrate, Research diet, New Brunswick, NJ, USA; start at 4–5 weeks of age for 14–27 weeks) and mice on HFD with a single i.p. injection of streptozocin (at week three of HFD STZ 130 mg/kg, Sigma-Aldrich) were treated with oral imatinib (gavage 100 mg/kg) or water for one or three months. A dose of 100 mg/kg imatinib has been reported to reach slightly lower steady state plasma concentrations (1 μM at 8 hours[46]) compared to humans treated with 400 mg imatinib daily (1.46 μM at 24 hours[47]) due to faster clearance in mice. Insulin and glucose tolerance tests (ITT/ GTT) were performed at 4 or 8 weeks of imatinib treatment with blood samplings from the tail vein before and 15, 30, 60 and 90 minutes after i.p. injection of 2 g/kg body weight glucose or 2U/kg body weight insulin. Peritoneal cells and macrophages were harvested as described for *in vitro* experiments. Other readout measures are specified below.

Seahorse XF flux analysis. Glycolysis (ECAR; extracellular acidification rate) and mitochondrial respiration (OCR, oxygen consumption rate) were measured by XF96 Seahorse Metabolic Analyzer (Seahorse Bioscience, North Billerica, MA, USA) in peritoneal macrophages *ex vivo* as previously described[48].

Flow cytometry of adipose tissue macrophages. Epididymal adipose tissue was minced and digested using collagenase IV (Worthington, OH, USA) and DNAse I (Sigma-Aldrich) at 37 °C for 25–30 min. To identify adipose tissue macrophages (ATMs), cells were stained with specific surface markers (Supplementary Table S2) and analyzed using the BD LSRII instrument (BD Biosciences, Franklin Lakes, NJ, USA) and FlowJo software (TreeStar Inc., Ashland, OR, USA). Among single (Singlets), live ($DAPI^-$) leukocytes ($CD45^+$) and after excluding eosinophils ($CD45^+F4/80^{low}SiglecF^+$) ATMs (non-eosinophils $CD11b^+F4/80^+$) were classified as double negative (DN), monocyte-derived M1a ($CD11c^+CD206^-$), inflammatory M1b ($CD11c^+CD206^{mid}$) and anti-inflammatory M2 ($CD11c^{-\text{ to low}}CD206^{high}$) (gating strategy: Supplementary Fig. S4a–c).

Liver histology. Hematoxylin-eosin (H&E) was performed according to established protocols and the NAS-score[49] assessed in a blinded fashion. Immunohistochemistry (IHC) for F4/80, CD3, B220, and Ly-6G (antibodies in Supplementary Table S3) was performed on paraffin-embedded liver sections. For quantification of immune cells, liver sections were scanned by a Prior robot/Nikon slide scanner. Three independent visual fields were semi-automatically quantified for area fraction (F4/80) or number of cells per DAPI-positive parenchymal cells (CD3, B220, Ly-6G) using the Nikon software (NIS) tool.

***In situ* hybridization (ISH).** Mouse TNFα (VB1-10175-VT) and Emr1 (VB6-12917-VT) genes were detected in formalin fixed, paraffin embedded (FFPE), 5μm liver sections using the ViewRNA ISH system (Affymetrix, Santa Clara, CA, USA) as previously described[50]. Brightfield and fluorescent images were acquired using a laser scanning confocal microscope (LSM710, Zeiss, Oberkochen, Germany) and Zen2 software (Zeiss) and subjected to image processing with ImageJ software.

Liver enzymes and lipids. Liver enzymes and blood lipids were measured in mouse plasma using a Cobas 8000 modular analyzer (Roche Diagnostics, Basel, Switzerland) according to the manufacturer's protocol.

Human monocytes. Study approval was obtained from the local ethics committee (Ethics Committee of northwest and central Switzerland, EKNZ). The human study was conducted in accordance with the Declaration of Helsinki and relevant guidelines and regulations. All diabetic subjects (HbA1c > 6.5%) and healthy volunteers (BMI 18–25 kg/m^2) gave written, informed consent. Detailed medical history and baseline characteristics were obtained at the day of the blood draw. Monocytes were enriched using MagniSort® Human Pan-Monocyte Enrichment kit (Thermo Fisher Scientific) from peripheral blood mononuclear cells (PBMCs). Human monocytes were kept for 2 h to attach and then activated towards a pro-inflammatory phenotype (M1; 10 ng/mL IFNγ, ImmunoTools, Friesoythe, Germany, 100 ng/mL Lipopolysaccharide (LPS) *E. coli* 0111:B4, Sigma-Aldrich, Saint Louis, MO, USA) or left unstimulated (M0) in the presence or absence of imatinib (1 μM) for 24 h.

Data analysis. Data are expressed as mean ± SEM. Unpaired Mann-Whitney test was used for statistical significance (GraphPad Prism). A p-value < 0.05 was considered as statistically significant.

References

1. Tilg, H., Moschen, A. R. & Roden, M. NAFLD and diabetes mellitus. *Nat Rev Gastroenterol Hepatol* **14**, 32–42, https://doi.org/10.1038/nrgastro.2016.147 (2017).
2. Tosello-Trampont, A. C., Landes, S. G., Nguyen, V., Novobrantseva, T. I. & Hahn, Y. S. Kuppfer cells trigger nonalcoholic steatohepatitis development in diet-induced mouse model through tumor necrosis factor-alpha production. *J Biol Chem* **287**, 40161–40172, https://doi.org/10.1074/jbc.M112.417014 (2012).
3. Tacke, F. Targeting hepatic macrophages to treat liver diseases. *J Hepatol* **66**, 1300–1312, https://doi.org/10.1016/j.jhep.2017.02.026 (2017).
4. Baeck, C. *et al*. Pharmacological inhibition of the chemokine CCL2 (MCP-1) diminishes liver macrophage infiltration and steatohepatitis in chronic hepatic injury. *Gut* **61**, 416–426, https://doi.org/10.1136/gutjnl-2011-300304 (2012).
5. Krenkel, O. & Tacke, F. Liver macrophages in tissue homeostasis and disease. *Nat Rev Immunol* **17**, 306–321, https://doi.org/10.1038/nri.2017.11 (2017).

6. Huang, W. *et al*. Depletion of liver Kupffer cells prevents the development of diet-induced hepatic steatosis and insulin resistance. *Diabetes* **59**, 347–357, https://doi.org/10.2337/db09-0016 (2010).
7. Reid, D. T. *et al*. Kupffer Cells Undergo Fundamental Changes during the Development of Experimental NASH and Are Critical in Initiating Liver Damage and Inflammation. *PLoS One* **11**, e0159524, https://doi.org/10.1371/journal.pone.0159524 (2016).
8. Tamura, Y. *et al*. Inhibition of CCR2 ameliorates insulin resistance and hepatic steatosis in db/db mice. *Arterioscler Thromb Vasc Biol* **28**, 2195–2201, https://doi.org/10.1161/ATVBAHA.108.168633 (2008).
9. Kanda, H. *et al*. MCP-1 contributes to macrophage infiltration into adipose tissue, insulin resistance, and hepatic steatosis in obesity. *J Clin Invest* **116**, 1494–1505, https://doi.org/10.1172/JCI26498 (2006).
10. Miura, K., Yang, L., van Rooijen, N., Ohnishi, H. & Seki, E. Hepatic recruitment of macrophages promotes nonalcoholic steatohepatitis through CCR2. *American journal of physiology. Gastrointestinal and liver physiology* **302**, G1310–1321, https://doi.org/10.1152/ajpgi.00365.2011 (2012).
11. Lefebvre, E. *et al*. Antifibrotic Effects of the Dual CCR2/CCR5 Antagonist Cenicriviroc in Animal Models of Liver and Kidney Fibrosis. *PLoS One* **11**, e0158156, https://doi.org/10.1371/journal.pone.0158156 (2016).
12. Krenkel, O. *et al*. Therapeutic Inhibition of Inflammatory Monocyte Recruitment Reduces Steatohepatitis and Liver Fibrosis. *Hepatology*, https://doi.org/10.1002/hep.29544 (2017).
13. Zhang, X. *et al*. CXC chemokine receptor 3 promotes steatohepatitis in mice through mediating inflammatory cytokines, macrophages and autophagy. *J Hepatol* **64**, 160–170, https://doi.org/10.1016/j.jhep.2015.09.005 (2016).
14. Zhang, X. *et al*. CXCL10 plays a key role as an inflammatory mediator and a non-invasive biomarker of non-alcoholic steatohepatitis. *J Hepatol* **61**, 1365–1375, https://doi.org/10.1016/j.jhep.2014.07.006 (2014).
15. Wehr, A. *et al*. Pharmacological inhibition of the chemokine CXCL16 diminishes liver macrophage infiltration and steatohepatitis in chronic hepatic injury. *PLoS One* **9**, e112327, https://doi.org/10.1371/journal.pone.0112327 (2014).
16. Park, E. J. *et al*. Dietary and genetic obesity promote liver inflammation and tumorigenesis by enhancing IL-6 and TNF expression. *Cell* **140**, 197–208, https://doi.org/10.1016/j.cell.2009.12.052 (2010).
17. Tomita, K. *et al*. Tumour necrosis factor alpha signalling through activation of Kupffer cells plays an essential role in liver fibrosis of non-alcoholic steatohepatitis in mice. *Gut* **55**, 415–424, https://doi.org/10.1136/gut.2005.071118 (2006).
18. Friedman, S. L. *et al*. A Randomized, Placebo-Controlled Trial of Cenicriviroc for Treatment of Nonalcoholic Steatohepatitis with Fibrosis. *Hepatology*, https://doi.org/10.1002/hep.29477 (2017).
19. McNelis, J. C. & Olefsky, J. M. Macrophages, immunity, and metabolic disease. *Immunity* **41**, 36–48, https://doi.org/10.1016/j.immuni.2014.05.010 (2014).
20. Hantschel, O., Rix, U. & Superti-Furga, G. Target spectrum of the BCR-ABL inhibitors imatinib, nilotinib and dasatinib. *Leukemia & lymphoma* **49**, 615–619, https://doi.org/10.1080/10428190801896103 (2008).
21. Choi, S. *et al*. PPARgamma antagonist Gleevec improves insulin sensitivity and promotes the browning of white adipose tissue. *Diabetes*. https://doi.org/10.2337/db15-1382 (2016).
22. Chawla, A. Control of macrophage activation and function by PPARs. *Circ Res* **106**, 1559–1569, https://doi.org/10.1161/CIRCRESAHA.110.216523 (2010).
23. Cavnar, M. J. *et al*. KIT oncogene inhibition drives intratumoral macrophage M2 polarization. *J Exp Med* **210**, 2873–2886, https://doi.org/10.1084/jem.20130875 (2013).
24. Klawitter, J. *et al*. Time-dependent effects of imatinib in human leukaemia cells: a kinetic NMR-profiling study. *Br J Cancer* **100**, 923–931, https://doi.org/10.1038/sj.bjc.6604946 (2009).
25. Wolf, A. M. *et al*. The kinase inhibitor imatinib mesylate inhibits TNF-{alpha} production *in vitro* and prevents TNF-dependent acute hepatic inflammation. *Proc Natl Acad Sci USA* **102**, 13622–13627, https://doi.org/10.1073/pnas.0501758102 (2005).
26. Breccia, M., Muscaritoli, M., Aversa, Z., Mandelli, F. & Alimena, G. Imatinib mesylate may improve fasting blood glucose in diabetic Ph+ chronic myelogenous leukemia patients responsive to treatment. *J Clin Oncol* **22**, 4653–4655, https://doi.org/10.1200/JCO.2004.04.217 (2004).
27. Agostino, N. M. *et al*. Effect of the tyrosine kinase inhibitors (sunitinib, sorafenib, dasatinib, and imatinib) on blood glucose levels in diabetic and nondiabetic patients in general clinical practice. *Journal of oncology pharmacy practice: official publication of the International Society of Oncology Pharmacy Practitioners* **17**, 197–202, https://doi.org/10.1177/1078155210378913 (2011).
28. Morita, S. *et al*. Targeting ABL-IRE1alpha Signaling Spares ER-Stressed Pancreatic beta Cells to Reverse Autoimmune Diabetes. *Cell Metab* **25**, 883–897 e888, https://doi.org/10.1016/j.cmet.2017.03.018 (2017).
29. Hagerkvist, R., Sandler, S., Mokhtari, D. & Welsh, N. Amelioration of diabetes by imatinib mesylate (Gleevec): role of beta-cell NF-kappaB activation and anti-apoptotic preconditioning. *FASEB J* **21**, 618–628, https://doi.org/10.1096/fj.06-6910com (2007).
30. Han, M. S. *et al*. Imatinib mesylate reduces endoplasmic reticulum stress and induces remission of diabetes in db/db mice. *Diabetes* **58**, 329–336, https://doi.org/10.2337/db08-0080 (2009).
31. Jiang, C., Ting, A. T. & Seed, B. PPAR-gamma agonists inhibit production of monocyte inflammatory cytokines. *Nature* **391**, 82–86, https://doi.org/10.1038/34184 (1998).
32. Ricote, M., Li, A. C., Willson, T. M., Kelly, C. J. & Glass, C. K. The peroxisome proliferator-activated receptor-gamma is a negative regulator of macrophage activation. *Nature* **391**, 79–82, https://doi.org/10.1038/34178 (1998).
33. Luo, W., Xu, Q., Wang, Q., Wu, H. & Hua, J. Effect of modulation of PPAR-gamma activity on Kupffer cells M1/M2 polarization in the development of non-alcoholic fatty liver disease. *Sci Rep* **7**, 44612, https://doi.org/10.1038/srep44612 (2017).
34. Im, S. S. *et al*. Linking lipid metabolism to the innate immune response in macrophages through sterol regulatory element binding protein-1a. *Cell Metab* **13**, 540–549, https://doi.org/10.1016/j.cmet.2011.04.001 (2011).
35. Varga, T., Czimmerer, Z. & Nagy, L. PPARs are a unique set of fatty acid regulated transcription factors controlling both lipid metabolism and inflammation. *Biochimica et biophysica acta* **1812**, 1007–1022, https://doi.org/10.1016/j.bbadis.2011.02.014 (2011).
36. Choi, J. H. *et al*. Anti-diabetic drugs inhibit obesity-linked phosphorylation of PPARgamma by Cdk5. *Nature* **466**, 451–456, https://doi.org/10.1038/nature09291 (2010).
37. Gonzalez, Y. *et al*. High glucose concentrations induce TNF-alpha production through the down-regulation of CD33 in primary human monocytes. *BMC Immunol* **13**, 19, https://doi.org/10.1186/1471-2172-13-19 (2012).
38. Artyomov, M. N., Sergushichev, A. & Schilling, J. D. Integrating immunometabolism and macrophage diversity. *Semin Immunol* **28**, 417–424, https://doi.org/10.1016/j.smim.2016.10.004 (2016).
39. Shao, W. & Espenshade, P. J. Expanding roles for SREBP in metabolism. *Cell Metab* **16**, 414–419, https://doi.org/10.1016/j.cmet.2012.09.002 (2012).
40. Kim, D. H. *et al*. Critical Roles of the Histone Methyltransferase MLL4/KMT2D in Murine Hepatic Steatosis Directed by ABL1 and PPARgamma2. *Cell reports* **17**, 1671–1682, https://doi.org/10.1016/j.celrep.2016.10.023 (2016).
41. Guerra, C., Koza, R. A., Yamashita, H., Walsh, K. & Kozak, L. P. Emergence of brown adipocytes in white fat in mice is under genetic control. *Effects on body weight and adiposity. J Clin Invest* **102**, 412–420, https://doi.org/10.1172/JCI3155 (1998).
42. Lee, H. M. *et al*. Upregulated NLRP3 inflammasome activation in patients with type 2 diabetes. *Diabetes* **62**, 194–204, https://doi.org/10.2337/db12-0420 (2013).
43. Netea, M. G. *et al*. Differential requirement for the activation of the inflammasome for processing and release of IL-1beta in monocytes and macrophages. *Blood* **113**, 2324–2335, https://doi.org/10.1182/blood-2008-03-146720 (2009).
44. Tonyali, O. *et al*. Imatinib mesylate-induced acute liver failure in a patient with gastrointestinal stromal tumors. *Med Oncol* **27**, 768–773, https://doi.org/10.1007/s12032-009-9284-y (2010).

45. https://clinicaltrials.gov/ct2/show/NCT01781975?term=imatinib+and+diabetes&rank=1.
46. Wolff, N. C. *et al*. Imatinib mesylate efficiently achieves therapeutic intratumor concentrations *in vivo* but has limited activity in a xenograft model of small cell lung cancer. *Clin Cancer Res* **10**, 3528–3534, https://doi.org/10.1158/1078-0432.CCR-0957-03 (2004).
47. Druker, B. J. *et al*. Efficacy and safety of a specific inhibitor of the BCR-ABL tyrosine kinase in chronic myeloid leukemia. *N Engl J Med* **344**, 1031–1037, https://doi.org/10.1056/NEJM200104053441401 (2001).
48. Van den Bossche, J., Baardman, J. & de Winther, M. P. Metabolic Characterization of Polarized M1 and M2 Bone Marrow-derived Macrophages Using Real-time Extracellular Flux Analysis. *J Vis Exp*. https://doi.org/10.3791/53424 (2015).
49. Kleiner, D. E. *et al*. Design and validation of a histological scoring system for nonalcoholic fatty liver disease. *Hepatology* **41**, 1313–1321, https://doi.org/10.1002/hep.20701 (2005).
50. Calabrese, D. & Wieland, S. F. Highly Sensitive Detection of HBV RNA in Liver Tissue by *In Situ* Hybridization. *Methods Mol Biol* **1540**, 119–134, https://doi.org/10.1007/978-1-4939-6700-1_10 (2017).

Acknowledgements

We thank M. Braendle for inspiring this project, Michèle Baumann and André Fitsche for technical assistance, Alina Liedtke for help with the human study and members of the Donath and Hess laboratories for advice and feedback. This study was supported by grants from the Swiss National Science Foundation (PZ00P3_161135), Goldschmidt-Jacobson Foundation, Novartis Foundation for medical-biological research, Gottfried und Julia Bangerter-Rhyner award, Jubiläumsstiftung Swiss Life, Olga Mayenfisch Foundation, Foundation Basler Diabetesgesellschaft, Foundation Freiwillig Akademische Gesellschaft (all to CCW), Swiss Government Excellence Scholarship (SAA).

Author Contributions

Experimental design: S.A.A., T.R., A.B., T.D., C.C.W. Experimental execution: S.A.A., T.R., A.B., T.D., D.C., M.S.M., A.W., C.C.W. Data analyses: S.A.A., T.R., C.C.W. Figure preparation, manuscript writing and editing: S.A.A., T.R., A.B., T.D., D.C., M.S.M., A.W., C.C.W. C.C.W. is the guarantor of this work.

Additional Information

Supplementary information accompanies this paper at https://doi.org/10.1038/s41598-018-32853-w.

Competing Interests: The authors declare no competing interests.

Publisher's note: Springer Nature remains neutral with regard to jurisdictional claims in published maps and institutional affiliations.

Open Access This article is licensed under a Creative Commons Attribution 4.0 International License, which permits use, sharing, adaptation, distribution and reproduction in any medium or format, as long as you give appropriate credit to the original author(s) and the source, provide a link to the Creative Commons license, and indicate if changes were made. The images or other third party material in this article are included in the article's Creative Commons license, unless indicated otherwise in a credit line to the material. If material is not included in the article's Creative Commons license and your intended use is not permitted by statutory regulation or exceeds the permitted use, you will need to obtain permission directly from the copyright holder. To view a copy of this license, visit http://creativecommons.org/licenses/by/4.0/.

© The Author(s) 2018

August 5th, 2018

Imatinib reduces non-alcoholic fatty liver disease in obese mice by targeting inflammatory and lipogenic pathways in macrophages and liver

Imatinib in non-alcoholic liver disease

Shefaa AlAsfoor[1], Theresa V. Rohm[1], Angela J. T. Bosch[1], Thomas Dervos[1], Diego Calabrese[2], Matthias S. Matter[3], Achim Weber[4], Claudia Cavelti-Weder[1]

[1]Clinic of Endocrinology, Diabetes and Metabolism, University Hospital Basel, Basel, Switzerland, and Department of Biomedicine, University of Basel, Basel, Switzerland
[2]Department of Biomedicine, University of Basel, Basel, Switzerland
[3]Institute of Pathology, University Hospital of Basel, Basel, Switzerland
[4]Department of Pathology and Molecular Pathology, University and University Hospital of Zurich, Zurich, Switzerland

Corresponding author:
Claudia Cavelti-Weder MD MPH
University Hospital of Basel, Department of Biomedicine
Hebelstrasse 20, 4031 Basel, Switzerland
Phone: +41 61 328 63 23, Fax: +41 61 265 51 00
claudia.cavelti-weder@usb.ch

SUPPLEMENTARY TABLES

Gene	Forward Primer	Reverse Primer
Mouse HKG and M1- and M2 -markers		
B2m	5′ TTCTGGTGCTTGTCTCACTGA	5′ CAGTATGTTCGGCTTCCCATTC
Ppia	5′ GAGCTGTTTGCAGACAAAGTTC	5′ CCCTGGCACATGAATCCTGG
TNF-α	5′ ACTGAACTTCGGGGTGATCG	5′ TGAGGGTCTGGGCCATAGAA
IL-6	5′ GGATACCACTCCCAACAGACCT	5′ GCCATTGCACAACTCTTTTCTC
IL-1β	5′ GCAACTGTTCCTGAACTCAACT	5′ ATCTTTTGGGGTCCGTCAACT
iNOS	5′ GTTCTCAGCCCAACAATACAAGA	5′ GTGGACGGGTCGATGTCAC
KC	5′ CTGGGATTCACCTCAAGAACATC	5′ CAGGGTCAAGGCAAGCCTC
Mrc1	5′ CTCTGTTCAGCTATTGGACGC	5′ CGGAATTTCTGGGATTCAGCTTC
Mgl1	5′ TGAGAAAGGCTTTAAGAACTGGG	5′ GACCACCTGTAGTGATGTGGG
Rentla	5′ CCAATCCAGCTAACTATCCCTCC	5′ CCAGTCAACGAGTAAGCACAG
Chil3	5′ AGGAAGCCCTCCTAAGGACA	5′ CTCCACAGATTCTTCCTCAAAAGC
IL-10	5′ AGGCGCTGTCATCGATTTCTC	5′ GCCTTGTAGACACCTTGGTCTT
CD68	5′ GCAGCACAGTGGACATTCAT	5′ AGAGAAACATGGCCC GAAGT
Adgre1 (F4/80 or Emr1)	5′ GCC CAG GAGTGGAATGTCAA	5′ CAGACACTCATCAACATCTGCG
Mouse sterol regulatory element-binding protein (SREBPs) genes		
Srebp1a	5′ GCCGGCGCCATGGACGAGCTGGCC	5′ CAGGAAGGCTTCCAGAGAGGAGGC
Nlrp1a	5′ AGGCTCTTTACCCTCTTCTA	5′ ATGTGCTTCTTCTTCTGGTA
Nlrp1c	5′ GAATCTTTACTCCACCCAGC	5′ CTTTTCCTGGCAAATGTCTT
Srebp1c	5′ GGAGCCATGGATTGCACATT	5′ GGCCCGGGAAGTCACTGT
Elovl5	5′ CTGAGTGACGCATCGAAATG	5′ CTTGCACATCCTCCTGCTC
Scd2	5′ TGCCTTGTATGTTCTGTGGC	5′ TCCTGCAAGCTCTACACCTG
Fads1s	5′ TGGTGCCCTTCATCCTCTGT	5′ GGTGCCCAAAGTCATGCTGTA
Acc1	5′ CCTCCGTCAGCTCAGATACA	5′ TTTACTAGGTGCAAGCCAGACA
Scd1	5′ CTGTACGGGATCATACTGGTTC	5′ GCCGTGCCTTGTAAGTTCTG
Fasn	5′ AGCGGCCATTTCCATTGCCC	5′ CCATGCCCAGAGGGTGGTTG
Acacb	5′ CCCAGGAGGCTGCATTGA	5′ AGACATGCTGGGCCTCATAGTA
LDLR	5′ ACCTGCCGACCTGATGAATTC	5′ GCAGTCATGTTCACGGTCACA
Hmgcs1	5′ TTTGATGCAGCTGTTTGAGG	5′ CCACCTGTAGGTCTGGCATT
Fdps	5′ GAGTCTGCCCGATCTCTGTC	5′ TGAACCTGCTGGAGCTCTTT
mvk	5′ GAAGACATCGTCCCTTGCTG	5′ AAC CCT TCT GGT GTGGACA
Pmvk	5′ GCTCGCATCCAGAAGTCTCT	5′ GCTCTCTGGTCCACTCAAGG
Hmgcr	5′ GGCCTCCATTGAGATCCG	5′ CACAATAACTTCCCAGGGGT
Mouse PPAR-γ phosphorylation-related genes		
Rarres2	5′ GCCTGGCCTGCATTAAAATGG	5′ CTTGCTTCAGAATTGGGCAGT
Txnip	5′ TCTTTTGAGGTGGTCTTCAACG	5′ GCTTTGACTCGGGTAACTTCACA
Nr1d1	5′ TACATTGGCTCTAGTGGCTCC	5′ CAGTAGGTGATGGTGGGAAGTA
CD24a	5′ GTTGCACCGTTTCCCGGTAA	5′ CCCCTCTGGTGGTAGCGTTA
Peg10	5′ TGCTTGCACAGAGCTACAGTC	5′ AGTTTGGGATAGGGGCTGCT
Acyl	5′ CAGCCAAGGCAATTTCAGAGC	5′ CTCGACGTTTGATTAACTGGTCT
Cidec	5′ ATGGACTACGCCATGAAGTCT	5′ CGGTGCTAACACGACAGGG
Nr1d2	5′ TGAACGCAGGAGGTGTGATTG	5′ GAGGACTGGAAGCTATTCTCAGA
Ddx17	5′ TCTTCAGCCAACAATCCCAATC	5′ GGCTCTATCGGTTTCACTACG
Rybp	5′ CGACCAGGCCAAAAAGACAAG	5′ CACATCGCAGATGCTGCATT
Nr3c1	5′ AGCTCCCCCTGGTAGAGAC	5′ GGTGAAGACGCAGAAACCTTG
Aplp2	5′ GTGGTGGAAGACCGTGACTAC	5′ TCGGGGGAACTTTAACATCGT
Slenbp2	5′ ATGGCTACAAAATGCACAAAGTG	5′ CCTGTGTTCCGGTAAATGCAG
Cycp2f2	5′ GTCGGTGTTCACGGTGTACC	5′ AAAGTTCCGCAGGATTTGGAC
Car3	5′ TGACAGGTCTATGCTGAGGGG	5′ CAGCGTATTTTACTCCGTCCAC
Adipsin	5′ CATGCTCGGCCCTACATGG	5′ CACAGAGTCGTCATCCGTCAC
Adiponectin	5′ TGTTCCTCTTAATCCTGCCCA	5′ CCAACCTGCACAAGTTCCCTT

Mouse adipose tissue browning markers		
CPT1b	5′ TGCCTTTACATCGTCTCCAA	5′ GGCTCCAGGGTTCAGAAAGT
UCP1	5′ CTTTGCCTCACTCAGGATTGG	5′ ACTGCCACACCTCCAGTCATT
PGC1α	5′ TATGGAGTGACATAGAGTGTGCT	5′ CCACTTCAATCCACCCAGAAAG
Dio2	5′ AATTATGCCTCGGAGAAGACCG	5′ GGCAGTTGCCTAGTGAAAGGT
Cox5b	5′ ATCAGCAACAAGAGAATAGTGGG	5′ GTAATGGGTTCCACAGTTGGG
Human HKG and M1- and M2- markers		
B2m	5′ GCTCGCGCTACTCTCTCTTT	5′ TGTCGGATGGATGAAACCCA
Ppia	5′ GCATACGGGTCCTGGCATCTTGTCC	5′ ATGGTGATCTTCTTGCTGGTCTTGC
TNF-α	5′ CAGAGGGCCTGTACCTCATC	5′ GGAAGACCCCTCCCAGATAG
MCP-1	5′ CCCCAGTCACCTGCTGTTAT	5′ TGGAATCCTGAACCCACTTC
Mrc1	5′ CGAGGAAGAGGTTCGGTTCACC	5′ GCAATCCCGGTTCTCATGGC
CD163	5′ TTGCCAGCAGCTTAAATGTG	5′ AGGACAGTGTTTGGGACTGG

Supplementary Table 1: Primers sequences used for quantitative real time-PCR

Antibody	Clone	Fluorophore	Source
CD45	30-F11	PerCP/Cy5.5	Biolegend
Siglec-F	E50-2440	BV510	BD Biosciences
CD11b	M1/70	BV421	Biolegend
F4/80	BM8	PE	Biolegend
CD11c	N418	PE/Cy7	Biolegend
CD206	C068C2	A647	Biolegend

Supplementary Table 2: List of Antibodies for flow cytometry in adipose tissue

IHC	Primary antibody	Diluent	Visualization
F4/80	F4/80 T-2006 clone BM8 BMA Biomedicals	1/50	Performed on Discovery Ventana UltraMap anti Rat DAB Kit
B220	B220 553084 clone RA3-6B2, BD Biosciences	1/4000	Performed on Discovery Ventana UltraMap anti Rat DAB Kit
CD3	CD3 MA1-90582 clone SP7, Thermo Fisher Scientific	1/300	Performed on Bond Leica DAB Kit
Ly-6G	Ly-6G 551459 clone 1A8, BD Biosciences	1/600	Performed on Bond Leica DAB Kit

Supplementary Table 3: Antibodies for IHC of immune cells in paraffin liver sections

	Healthy Controls (n=6)	Diabetics, adequate control (n=5)	Diabetics, inadequate control (n=7)
General parameter			
Sex (M/F)	6/0	3/2	4/3
Age (years)	29.5±3.3	57.0±5.0	52.7±5.5
BMI (kg/m^2)	22.8±1.5	33.5±1.9	37.4±4.5
Weight (kg)	74.8±4.6	100.0±7.6	111.3±16.8
Waist-to-hip Ratio	0.86±0.02	0.99±0.05	1.04±0.05
Glc metabolism			
HbA1c (mmol/mol (%))	na	**52.6±5.5 (7.0±0.5)**	**114.5±6.5(12.6±0.6)****
Fasting plasma glucose (mmol/l), average	na	**8.3±1.2**	**16.0±1.3****
Diabetes duration (years)	na	7.2±3.9	12.9±4.9
Antidiabetics			
- Oral/GLP1-Anal. (%)	na	80	85.7
- Insulin (%)	na	20	85.7
Inflammation			
CRP (mg/dl)		3.9±0.6	10.0±4.6
Leukocytes (x10^9/l)		**6.4±0.4**	**8.3±0.7***
Other Cv-Risks			
Blood Pressure			
- Antihypertensive drug (%)	0	40	85.7
- Systolic (mmHg)	125±4	126±9	143±7
- Diastolic (mmHg)	72±4	80±6	83±5
Family History			
- Diabetes (%)	16.7	100	57.1
- Obesity (%)	16.7	80	57.1
- CV disease (%)	16.7	40	42.9
Smoking (%)	0	0	42.9

Supplementary Table 4: Baseline characteristics of healthy, adequately and inadequately controlled diabetics. Statistical differences between adequately and inadequately controlled diabetics are indicated in bold font. Data presented as mean±SEM, na: not applicable, *p<.05, **p<.01.

SUPPLEMENTARY FIGURES

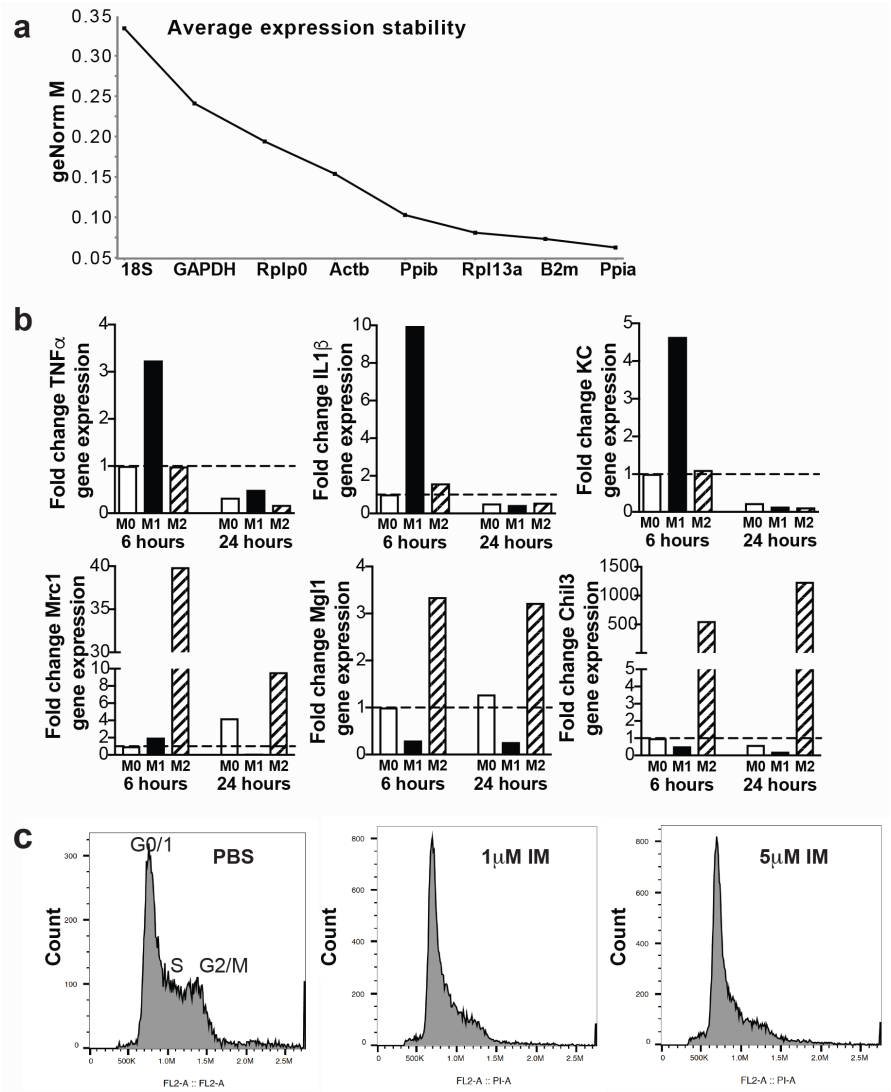

Supplementary Figure 1. Optimization of *in vitro* set-up. Due to the highly dynamic behavior of macrophages, *in vitro* readouts were optimized for macrophage housekeeping genes (HKGs), the optimal time point for macrophage activation and imatinib dose. (**a**) Average expression stability of HKGs 18S, GAPDH, Rplp0, Actb, Ppib, Rpl13a, B2m, Ppia according to the geNorm algorithm with B2m and Ppia most stably expressed. (**b**) The 6-hour time point was chosen for peritoneal macrophages when fold gene expression of pro-inflammatory M1-markers was most pronounced, while fold gene expression of anti-inflammatory M2-markers was similar at 6 and 24 hours after stimulation. (**c**) Flow cytometry for cell cycle with G1-phase arrest of the CML-cell line K562 at both 1uM and 5uM imatinib compared to PBS-treated cells.

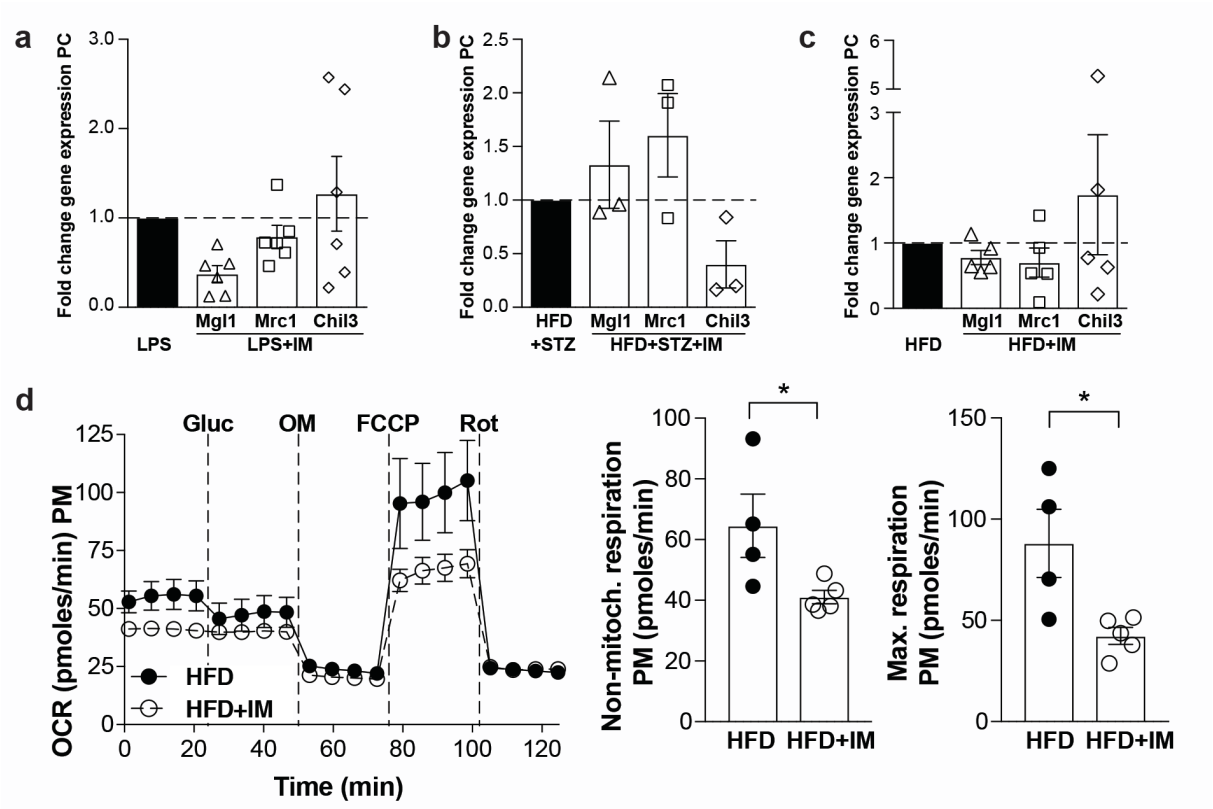

Supplementary Figure 2. Anti-inflammatory gene expression and metabolic flux in peritoneal macrophages of imatinib-treated mice. Fold change of anti-inflammatory genes in peritoneal macrophages of the acute inflammation model (**a**), diabetic (**b**) and obese mice (**c**) treated with imatinib compared to their respective controls. (**d**) Seahorse flux analysis with OCR (metabolic oxidation) and calculated non-mitochondrial and maximum respiration (pmoles/min) in peritoneal macrophages of HFD-fed mice treated for 3 months with imatinib or vehicle. Gluc: Glucose, HFD: High fat diet, IM: imatinib, OM: oligomycin, PC: peritoneal cells, PM: peritoneal macrophages, Rot: rotenone, STZ: Streptozocin. Data expressed as mean±SEM, *=p<.05.

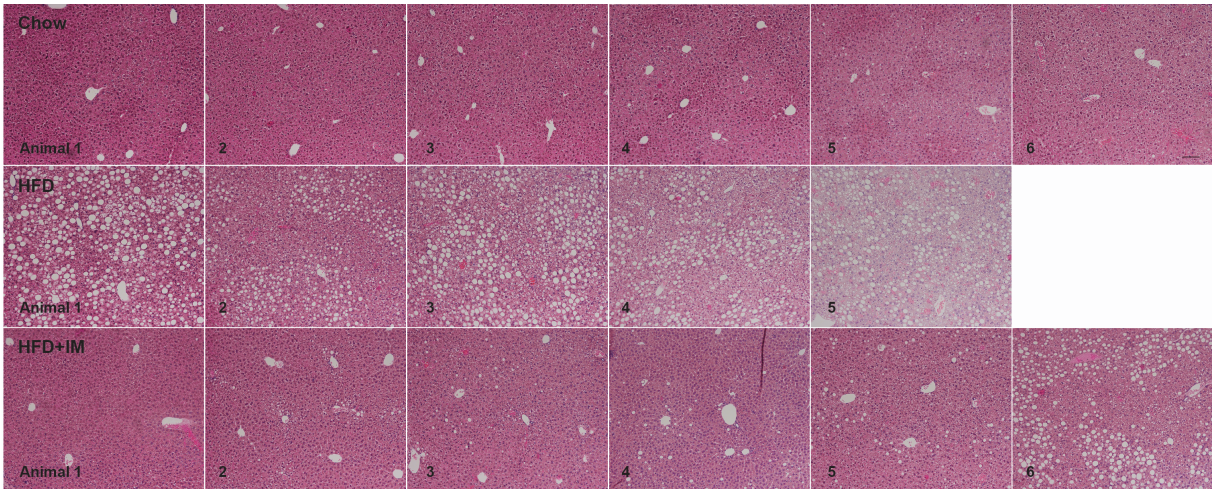

Supplementary Figure 3. Liver sections of individual mice regarding steatosis. Representative H&E liver sections of 5-6 individual mice of the chow, HFD and HFD+IM-groups. HFD: high fat diet; IM: imatinib. Scale bar represents 100µm.

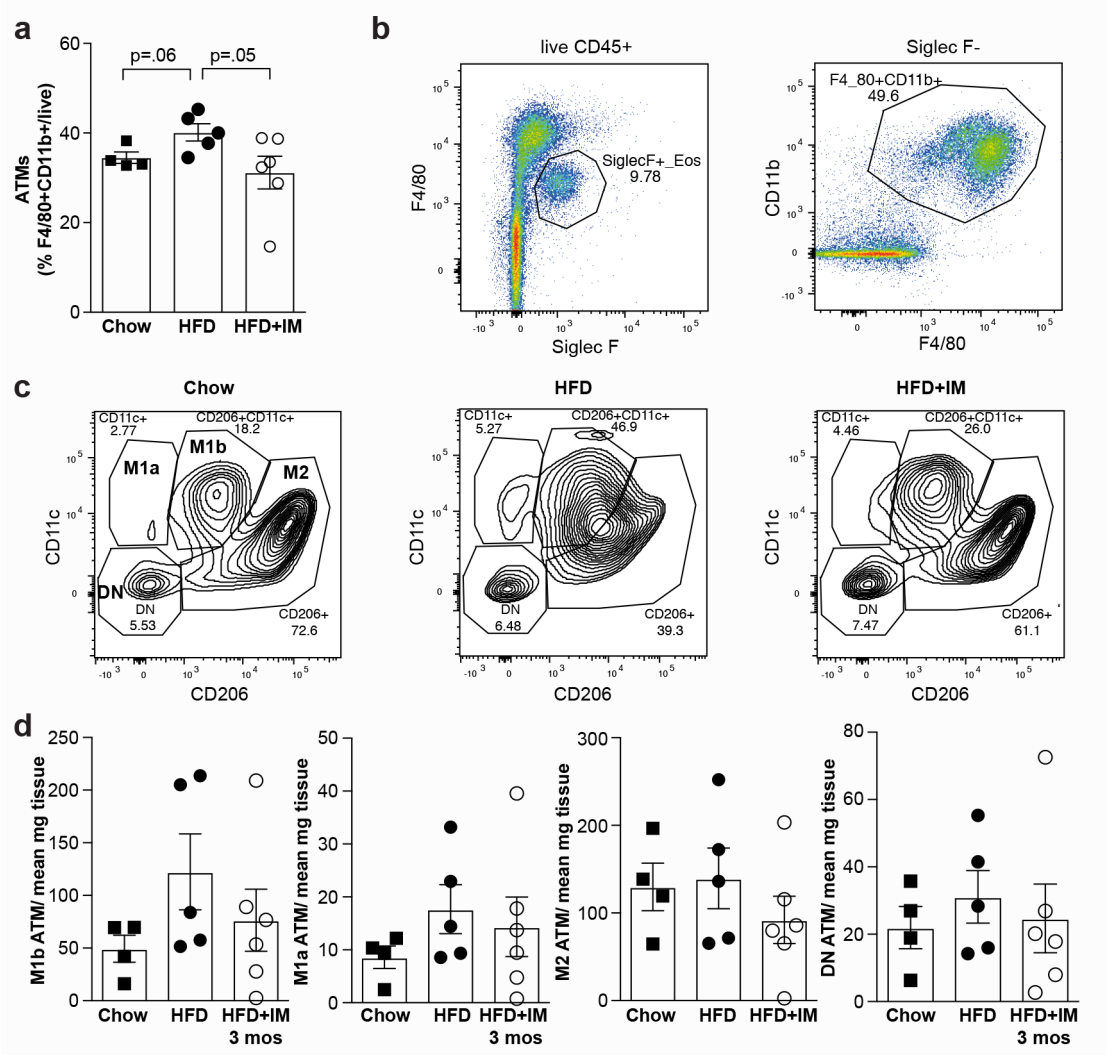

Supplementary Figure 4. Adipose tissue macrophages upon imatinib treatment. (**a**) Quantification of adipose tissue macrophages (ATMs) as percentage of live cells by flow cytometry of chow, HFD and HFD+IM-treated mice (n = 4-6). (**b**) Gating strategy to identify ATMs (single live non-eosinophils CD45+CD11b+F4/80+) by flow cytometry. (**c**) Representative flow cytometry plots for ATM subpopulations (DN: $CD11c^{-}CD206^{-}$; monocyte-derived M1a: $CD11c^{+}CD206^{-}$; inflammatory M1b: $CD11c^{+}CD206^{mid}$; anti-inflammatory M2: $CD11c^{-to\ low}CD206^{high}$). (**d**) Quantification of absolute cell numbers of ATM subpopulations M1a, M1b and M2 in chow, HFD and HFD+IM-treated mice (n = 4-6). ATM: adipose tissue macrophage, HFD: high fat diet, IM: imatinib, DN: double-negative.

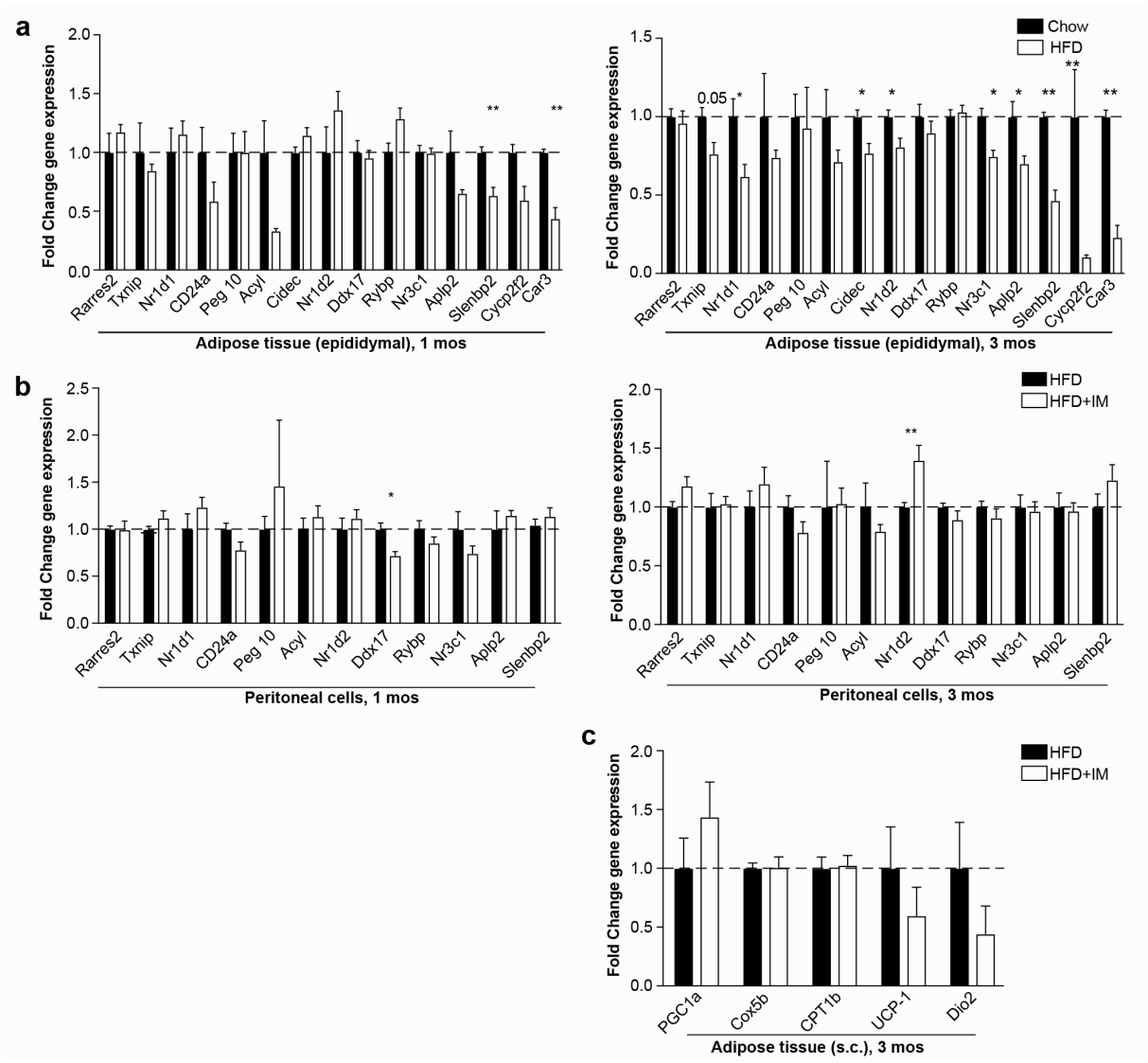

Supplementary Figure 5. PPARγ-phosphorylation-regulated genes in adipose tissue and peritoneal cells. (**a**) Effect of HFD on PPARγ-phosphorylation-regulated genes in adipose tissue compared to chow after one (left) and three (months) (n=3-9). (**b**) Effect of imatinib on PPARγ-phosphorylation-regulated genes in peritoneal cells in mice on HFD after one (left) and three months of imatinib treatment (right) (n= 5-10). (**c**) Fold change gene expression of genes related to adipose tissue browning after three months of imatinib treatment. HFD: High fat diet, IM: imatinib. Data are presented as mean±SEM. *p<.05, **=p<.01.

6. Discussion

NAFLD has developed to a serious growing health problem in recent years. So far, no therapeutic drug has been approved for NAFLD. NAFLD has been linked to insulin resistance related diseases such as obesity and diabetes. Due to the role of macrophages in NAFLD development, recent studies postulate that targeting of immune cells – especially macrophages – could be a potential treatment strategy for NAFLD. One promising therapeutic approach would be to attenuate macrophage activation during NAFLD onset and progression, thereby limiting inflammation and as a consequence improving liver function. Imatinib, a tyrosine kinase inhibitor that was originally developed to treat CML, has shown to have anti-diabetic and anti-inflammatory effects. Therefore, we hypothesized that imatinib could potentially be such a therapeutic drug to target macrophage activation in NAFLD. In this study, we assessed whether imatinib attenuates liver macrophages and thereby improves NAFLD outcomes. To test our hypothesis, we used well-established *in vitro* and *in vivo* models as well as human cells.

6.1 Imatinib modulates pro-inflammatory macrophage activation *in vitro*

Imatinib was shown to exert anti-inflammatory effects in tumor-associated macrophages in a gastrointestinal stromal tumor model[1]. To test the concept of an immune-modulatory effect of imatinib directly on macrophages primed to either a pro- or anti-inflammatory phenotype in *vitro*, we used two different types of macrophages: peritoneal macrophages and BMDM. We found that pro-inflammatory macrophages responded to imatinib as shown by reduced pro-inflammatory gene and protein expression, most prominently TNF-α. In contrast, unstimulated and anti-inflammatory macrophages were not affected by imatinib. As in metabolic disease including obesity and diabetes macrophages predominantly exhibit a pro-inflammatory phenotype[2], targeting specifically pro-inflammatory - but not unstimulated or anti-inflammatory - macrophages seems to be a favorable strategy as their homeostatic function is left unaltered. The attenuation of pro-inflammatory phenotype by imatinib was slightly less pronounced in BMDMs, most likely due to the artificial differentiation by exogenous M-CSF over one week in BMDM.

6.2 Imatinib attenuates activation of peritoneal macrophages in acute inflammation and metabolic disease models

Next, we asked whether this immune-dampening effect of imatinib on macrophages also occurs *in vivo*. To address this question, we used an LPS-induced acute inflammation model and two chronic low-grade inflammation models, one inducing inflammation by HFD-induced obesity, the other by a combination of the beta-cell toxin STZ and HFD (diabetes model).

Imatinib has been reported to reduce inflammation in a LPS-induced liver injury model as shown by lowering systemic TNF-α and IL-6[3, 4]. However, the cell type responsible for the reduction in these inflammatory markers was not assessed. When specifically testing peritoneal macrophages/ cells in our LPS-induced inflammation model with imatinib pretreatment, we observed a significantly diminished TNF-α gene expression in peritoneal macrophages already 2 hours after the LPS injection. Similarly, TNF-α was reduced in peritoneal macrophages/ cells in both diabetic and obese models treated with imatinib.

In contrast, IL-6 was not affected by imatinib in the peritoneal macrophages/ cells in the acute inflammation model and diabetic mice, respectively. It is believed that imatinib exerts its anti-inflammatory effect via inhibition of NF- κB[5], a downstream signaling of the LPS/TLR4 pathway. IL-6 can be induced via the activation of LPS/ TLR4 or IL-6/ sIL-6R (IL-6 receptor)/ STAT3 trans signaling pathways in the LPS-induced inflammation model[6]. Therefore, IL-6 might evade imatinib action via IL-6/ sIL-6R / STAT3 trans signaling pathways (Fig. 3).

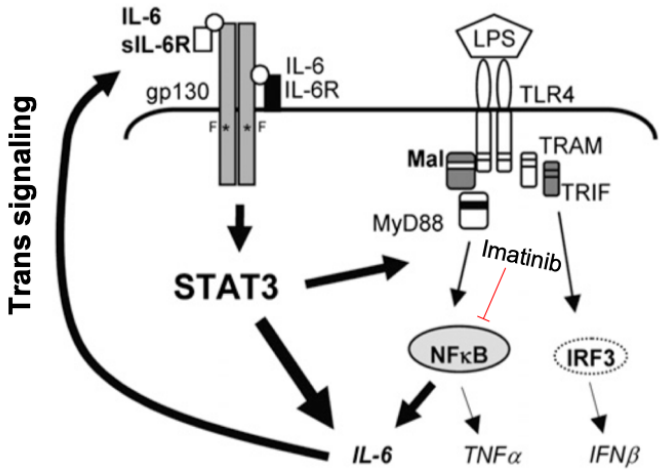

Figure 3| Model of IL-6 upon LPS stimulation. LPS can induce IL-6 via LPS/TLR4 pathway or through upregulation of IL-6 / sIL-6R complexes (trans signaling) and the gp130Y757F receptor, which in turn boosts STAT3 activation. Hyperactivation of STAT3 directly upregulates IL-6 production or indirectly via

LPS/TLR4 pathway. We speculate that LPS-induced IL-6 might evade imatinib action through IL-6 trans signaling pathway. Adapted from Greenhill, C. J et al[6].

Imatinib has been shown to decrease glycolysis in human leukemia BCR-ABL-positive cells[7]. A recent study reported that immunometabolism of macrophages depends on the cell type and tissue localization. For example, BMDMs or peritoneal macrophages have a distinct immunometabolism despite both being macrophages: Peritoneal macrophages activated *in vitro* with LPS enhance both glycolysis and mitochondrial oxidation, while activated BMDMs shows increased glycolysis and reduced mitochondrial oxidation[8]. Thus, we assessed immunometabolism upon imatinib treatment as another readout measure for macrophage activation and found that imatinib decreased metabolic oxidation in peritoneal macrophages from the chronic low-grade inflammation HFD model, confirming an altered activation state upon imatinib treatment.

6.3 Imatinib reduces the number of liver macrophages via modulation of the TNF-α pathway

Hepatic macrophages are crucial contributors to the development of fatty liver in obesity and NAFLD[9, 10]. KCs that accumulate lipids exhibit a pro-inflammatory phenotype characterized by secretion of TNF-α at an early stage of steatohepatitis in the HFD model[11]. In the liver, TNF-α is released by both hepatocytes and KCs[13]. To study the effect of imatinib on the pro-inflammatory macrophages in the fatty liver, we performed a time-resolved study up to three months, which allowed us to study the impact of imatinib over time. We found early down-regulation of TNF-α in liver tissue. TNF-α co-localized with liver macrophages, which decreased at the later time points as shown by lower F4/80 area fraction and CD68 gene expression. Thus, it is likely that the down-regulation of TNF-α by imatinib interferes with the vicious cycle of monocyte recruitment and/or macrophage activation in the liver, subsequently lowering their number and/or activation.

Several studies have shown that imatinib also inhibits T-cell proliferation[14] and increases the number of circulating B-cells and neutrophils in CML patients and infectious models, respectively[15, 16]. However, in our study, we did not observe any changes in T-cells (CD3), B-cells (B220) and neutrophils (Ly6-G) in liver tissue after 3 months of treatment. Thus, 3 months of imatinib treatment in mice suffering from NAFLD results first in a reduction of TNF-α in the liver, which is later followed by a decrease in liver macrophages, while other immune cells of the liver are not affected.

6.4 Imatinib alters lipid metabolism early on, followed later by markedly decreased hepatic steatosis

HFD-induced obesity and NAFLD often go along with hyperlipidemia, which is characterized by an increase in triglycerides and low-density lipoprotein (LDL) and a decrease in high-density lipoprotein HDL in the plasma[17, 18]. Besides early reduction of TNF-α in the liver, the other earliest change we found in our time-resolved study upon imatinib treatment was a reduction in systemic lipids, such as cholesterol and high-density lipoprotein (HDL) followed by a reduction in triglycerides.

Increased hepatic fatty acids synthesis (triglycerides) in obesity results in increased steatosis and thus NAFLD[19]. Therefore, we asked whether the reduced lipid levels by imatinib improves liver steatosis in the obese model. The liver sections from obese mice revealed that imatinib indeed reduced steatosis and NAFLD severity, which occurred at the late time point together with decreased systemic triglycerides and TNF-α. Thus, the simultaneous action of imatinib on TNF-α and systemic lipid levels could be an indication for an interplay between innate immunity and lipid metabolism, which eventually leads to a reduction in hepatic steatosis.

6.5 Imatinib lowers adipose tissue inflammation and increases insulin sensitivity after three months of treatment

Different studies support a role of adipose tissue inflammation in the development of NAFLD through an increased influx of FFAs to the liver, recruitment of pro-inflammatory macrophages and secretion of cytokines and adipokines[20, 21]. Accordingly, we have investigated the effect of imatinib on adipose tissue macrophages (ATMs) and inflammatory cytokines. As reported by Choi et al.[22], imatinib significantly reduced macrophages and pro-inflammatory markers in the adipose tissue. However, we observed this only after 3 months of treatment in our obese cohort. Our findings suggest that the beneficial effect of imatinib treatment first starts in the liver as TNF-α was reduced after one month of treatment in the liver, which was only later followed by reduced adipose tissue inflammation at three months.

Like inflammation, insulin resistance is also a crucial hit for the development of NAFLD[23]. In previous studies, imatinib was shown to increase both insulin sensitivity and insulin secretion in obesity[22] and diabetic[24] mouse models within a treatment duration ranging from 7 days[22] to 1 month[24]. In the present study, we found an improvement in insulin resistance in both diabetic

and obese model after 1 month and 3 months of imatinib treatment, respectively. As TNF-α is associated with insulin resistance in the HFD-induced obesity model[25, 26], it is likely that TNF-α reduction overtime in both liver and adipose tissue and blunted hepatic steatosis led to the improvement of insulin resistance. In contrast to the previous studies mentioned above, however, we could not detect an improvement in insulin secretion. This difference might be explained by differences in the experimental set-up like different routes of administration (oral in our study verus i.p. administrations[22, 24]), drug concentration (100 mg/kg in our study versus 25 mg/kg in[22, 24]), treatment period (1-3 months in our study versus 1 week[22]) and animal models (HFD model versus db/db mice in[24]).

6.6 Time-resolved assessment of transcription factors suggests that imatinib targets SREBP, while restoration of PPARγ-phosphorylation is a secondary phenomenon

As we found that imatinib affected innate immunity and steatosis in a time dependent manner, we assessed common mechanisms involving both inflammation and lipogenesis. We first focused on the SREBP transcription factor family, which is known to activate lipogenic transcriptional programs, but has also been shown to control transcriptional regulation that extends beyond lipid synthesis[27]: For example, SREBP1a is highly expressed in immune cells such as macrophages and dendritic cells, where it not only activates genes required for lipogenesis but also a gene encoding Nlrp1, a core component of the inflammasome[28]. Thus, SREBP links lipid metabolism and the innate immune response and could therefore explain the simultaneous effects on inflammation and lipid levels we observed upon imatinib treatment.

Indeed, we found early reductions of SREBP1c-target genes in the liver and partially in peritoneal macrophages. These downregulations were gone after three months of imatinib treatment, most likely due to compensatory mechanisms. We speculate that the SREBP transcriptional program of the target cell determines the phenotypic alteration induced by imatinib: In macrophages, imatinib has preferentially an immune-dampening effect, while in the liver also lipogenesis is affected. Thus, improvements in metabolic disease manifestations likely arise from a combination of the immune-dampening effect on macrophages and reduced lipogenesis induced by imatinib. Hence, in the long-term, reduced SREBP target gene expression upon imatinib was associated with reduced hepatic steatosis, systemic and adipose tissue inflammation and increased insulin sensitivity.

Another transcription factor involved in both inflammation and lipid metabolism is PPARγ[29]. In obesity and insulin resistance, PPARγ was shown to become phosphorylated at serine273 (pS273) with subsequent dysregulation of metabolically important genes[30].
Interestingly, a recent study showed that PPARγ-phosphorylation at serine273 was blocked by imatinib, thereby restoring dysregulated diabetes-genes and reducing insulin resistance[22]. However, in our time-resolved study the early immune-dampening effect on macrophages and the reduction in lipid levels clearly preceded restoration of PPARγ-phosphorylation-related genes in adipose tissue, indicating that restored PPARγ-phosphorylation might be a secondary phenomenon. Restoration of PPARγ-phosphorylation-related genes in adipose tissue potentially develops as less TNF-α is available to engage in PPARγ-phosphorylation and its deleterious metabolic downstream effects. A recent study demonstrated that imatinib interferes with the interaction between the histone H3 lysine 4 methyltransferase MLL4 and PPARγ, thereby dampening steatotic target genes in short-term experiments[31]. Thus, dampened SREBP transcriptional programs as observed in our study could ultimately be due to imatinib interfering with the MLL4-PPARγ axis with subsequently reduced transcription of SREBP target genes.

As a third potential mechanistic pathway, we assessed browning of adipose tissue by imatinib, however, we were not able to find consistent upregulation of cold-induced thermogenesis genes. This is in contrast to the publication by Choi and colleagues[22], which could be explained by differences in the experimental set-up (administration of imatinib i.p. versus oral; treatment duration and genetic background (C57BL/6J versus C57BL/6N)). The latter is insofar important as genetic variability is known to affect cold-induced thermogenesis[32].

6.7 Imatinib lowers pro-inflammatory activation in human monocytes, but hyperglycemia alters their responsiveness

To translate our findings to human disease, we probed the effect of imatinib on human monocytes. Especially, as previous studies showed a heightened inflammatory state in human myeloid cells with hyperglycemia[33, 34], diabetic patients could exhibit altered susceptibility to immune-modulatory drugs like imatinib. Human monocytes responded to imatinib treatment by down-regulation of pro-inflammatory markers also in a non-activated state. This is consistent with previous studies showing that monocytes have a “pre-activated” basal condition that requires only a single stimulation, while macrophages depend on a second signal to be

activated[35]. In activated monocytes, however, the immune-dampening effect of imatinib was lost with deranged glycemic control, suggesting altered susceptibility to the drug with hyperglycemia, this phenomenon could not be overcome with increasing doses of imatinib. Although the overstimulation as achieved by *ex vivo* LPS/IFNγ-stimulation might not represent the *in vivo* situation, it uncovers altered susceptibility to immune-modulation with hyperglycemia.

6.8 Strength and limitations

The strength of our study is that the long-term follow-up and time-resolved approach allowed us to distinguish early from later effects of imatinib on different cells and organs. Hence, it became clear that imatinib simultaneously affects inflammatory and lipogenic signals in macrophages and in the liver before reducing metabolic disease manifestations such as NAFLD, systemic and adipose tissue inflammation or insulin resistance. Our findings expand on previous literature by linking SREBP-signaling not only to lipogenesis, but also to innate immunity in the context of NAFLD. A more profound understanding of integrated pathways between inflammation and lipid metabolism could pave the way for the development of novel therapeutics in NAFLD. The limitation of the present study is that our models allowed us to study the impact of imatinib on the initiation stage (steatosis and inflammation), but not the progression stage of the disease. Therefore, using fibrosis/ cirrhosis models could help us to understand the impact of imatinib on innate immunity in the final stages of NAFLD.

6.9 Clinical Relevance

The clinical significance of our findings lies in the scarcity of therapeutic measures available for NAFLD patients. Imatinib has generally a mild adverse effect profile and a long-term safety record. In rare instances, however, imatinib has been associated with acute liver injury often in connection with hepatotoxic agents interfering with cytochrome P450 enzymes, leading to increased imatinib concentrations[36]. Thus, taking this into account, clinical trials could be envisaged in the context of NAFLD. Imatinib has already been tested in the setting of type 1 diabetes mellitus, however, the results have not yet been published[37]. In the light of our findings that imatinib exerts effects on both the innate immunity and lipid metabolism, clinical studies involving patients with metabolic disease – preferentially with chronic low-grade inflammation and NAFLD – could yield promising results in the future.

7. Conclusion

In brief, our findings show that imatinib improves NAFLD by modulating hepatic pro-inflammatory macrophages and lipid metabolism in the liver. In line with previous studies, the present study confirms the critical roles of TNF-α, hepatic macrophages and lipid accumulation in the initiation of NAFLD. In parallel, our data supports the concepts of targeting innate immunity and lipid metabolism during disease development. Thus, understanding the pathophysiological signaling between innate immunity and lipogenic pathway could be beneficial to develop novel therapeutic agents to attenuate or even prevent NAFLD in future.

8. References

1. Information, N.C.f.B., Vol. 2018 (2018, Nov, 10).
2. Guemes, M., Rahman, S.A. & Hussain, K. What is a normal blood glucose? *Archives of disease in childhood* 101, 569-574 (2016).
3. Aronoff, S.L., Berkowitz, K., Shreiner, B. & Want, L. Glucose Metabolism and Regulation: Beyond Insulin and Glucagon. *Diabetes Spectrum* 17, 183-190 (2004).
4. Jump, D.B., Clarke, S.D., Thelen, A. & Liimatta, M. Coordinate regulation of glycolytic and lipogenic gene expression by polyunsaturated fatty acids. *Journal of lipid research* 35, 1076-1084 (1994).
5. Kersten, S. Mechanisms of nutritional and hormonal regulation of lipogenesis. *EMBO Rep* 2, 282-286 (2001).
6. Eberle, D., Hegarty, B., Bossard, P., Ferre, P. & Foufelle, F. SREBP transcription factors: master regulators of lipid homeostasis. *Biochimie* 86, 839-848 (2004).
7. Han, S.J. & Boyko, E.J. The Evidence for an Obesity Paradox in Type 2 Diabetes Mellitus. *Diabetes Metab J* 42, 179-187 (2018).
8. Mokdad, A.H. *et al.* Prevalence of obesity, diabetes, and obesity-related health risk factors, 2001. *Jama* 289, 76-79 (2003).
9. Organization, W.H., Vol. 2018 (16 February 2018).
10. Ofei, F. Obesity - a preventable disease. *Ghana Med J* 39, 98-101 (2005).
11. Yki-Jarvinen, H. Ectopic fat accumulation: an important cause of insulin resistance in humans. *J R Soc Med* 95 Suppl 42, 39-45 (2002).
12. Fabbrini, E., Sullivan, S. & Klein, S. Obesity and nonalcoholic fatty liver disease: biochemical, metabolic, and clinical implications. *Hepatology* 51, 679-689 (2010).
13. Chen, Z., Yu, R., Xiong, Y., Du, F. & Zhu, S. A vicious circle between insulin resistance and inflammation in nonalcoholic fatty liver disease. *Lipids Health Dis* 16, 203 (2017).
14. Shoelson, S.E., Lee, J. & Goldfine, A.B. Inflammation and insulin resistance. *J Clin Invest* 116, 1793-1801 (2006).
15. Association, A.D. (2019).
16. Diagnosis and classification of diabetes mellitus. *Diabetes Care* 32 Suppl 1, S62-67 (2009).
17. American Diabetes, A. Diagnosis and classification of diabetes mellitus. *Diabetes Care* 33 Suppl 1, S62-69 (2010).
18. Donath, M.Y. & Shoelson, S.E. Type 2 diabetes as an inflammatory disease. *Nat Rev Immunol* 11, 98-107 (2011).
19. Robertson, R.P., Harmon, J., Tran, P.O. & Poitout, V. Beta-cell glucose toxicity, lipotoxicity, and chronic oxidative stress in type 2 diabetes. *Diabetes* 53 Suppl 1, S119-124 (2004).
20. Weir, G.C. & Bonner-Weir, S. Five stages of evolving beta-cell dysfunction during progression to diabetes. *Diabetes* 53 Suppl 3, S16-21 (2004).
21. Prentki, M. & Nolan, C.J. Islet beta cell failure in type 2 diabetes. *J Clin Invest* 116, 1802-1812 (2006).
22. Hull, R.L., Westermark, G.T., Westermark, P. & Kahn, S.E. Islet amyloid: a critical entity in the pathogenesis of type 2 diabetes. *J Clin Endocrinol Metab* 89, 3629-3643 (2004).
23. Harding, H.P. & Ron, D. Endoplasmic reticulum stress and the development of diabetes: a review. *Diabetes* 51 Suppl 3, S455-461 (2002).
24. Hotamisligil, G.S. & Erbay, E. Nutrient sensing and inflammation in metabolic diseases. *Nat Rev Immunol* 8, 923-934 (2008).
25. Donath, M.Y. Targeting inflammation in the treatment of type 2 diabetes: time to start. *Nature reviews. Drug discovery* 13, 465-476 (2014).
26. Farrell, G.C., Wong, V.W. & Chitturi, S. NAFLD in Asia--as common and important as in the West. *Nature reviews. Gastroenterology & hepatology* 10, 307-318 (2013).
27. Younossi, Z.M. *et al.* Global epidemiology of nonalcoholic fatty liver disease-Meta-analytic assessment of prevalence, incidence, and outcomes. *Hepatology* 64, 73-84 (2016).
28. Yang, K.C. *et al.* Association of Non-alcoholic Fatty Liver Disease with Metabolic Syndrome Independently of Central Obesity and Insulin Resistance. *Scientific reports* 6, 27034 (2016).
29. Wong, R.J. *et al.* Nonalcoholic steatohepatitis is the second leading etiology of liver disease among adults awaiting liver transplantation in the United States. *Gastroenterology* 148 (2015).

30. Tarantino, G., Savastano, S. & Colao, A. Hepatic steatosis, low-grade chronic inflammation and hormone/growth factor/adipokine imbalance. *World journal of gastroenterology* 16, 4773-4783 (2010).
31. Kleiner, D.E. *et al.* Design and validation of a histological scoring system for nonalcoholic fatty liver disease. *Hepatology* 41, 1313-1321 (2005).
32. Hubscher, S.G. Histological assessment of non-alcoholic fatty liver disease. *Histopathology* 49, 450-465 (2006).
33. Paschos, P. & Paletas, K. Non alcoholic fatty liver disease and metabolic syndrome. *Hippokratia* 13, 9-19 (2009).
34. Milic, S., Lulic, D. & Stimac, D. Non-alcoholic fatty liver disease and obesity: biochemical, metabolic and clinical presentations. *World journal of gastroenterology* 20, 9330-9337 (2014).
35. Williamson, R.M. *et al.* Prevalence of and risk factors for hepatic steatosis and nonalcoholic Fatty liver disease in people with type 2 diabetes: the Edinburgh Type 2 Diabetes Study. *Diabetes Care* 34, 1139-1144 (2011).
36. Vanjiappan, S., Hamide, A., Ananthakrishnan, R., Periyasamy, S.G. & Mehalingam, V. Nonalcoholic fatty liver disease in patients with type 2 diabetes mellitus and its association with cardiovascular disease. *Diabetes & metabolic syndrome* 12, 479-482 (2018).
37. Targher, G. *et al.* Nonalcoholic fatty liver disease is independently associated with an increased incidence of cardiovascular events in type 2 diabetic patients. *Diabetes Care* 30, 2119-2121 (2007).
38. Targher, G. *et al.* Increased risk of CKD among type 2 diabetics with nonalcoholic fatty liver disease. *Journal of the American Society of Nephrology : JASN* 19, 1564-1570 (2008).
39. Patel, A. & Harrison, S.A. Hepatitis C virus infection and nonalcoholic steatohepatitis. *Gastroenterol Hepatol (N Y)* 8, 305-312 (2012).
40. Rockstroh, J.K. Non-Alcoholic Fatty Liver Disease (NAFLD) and Non-Alcoholic Steatohepatitis (NASH) in HIV. *Current HIV/AIDS reports* 14, 47-53 (2017).
41. Nishizawa, H. *et al.* Nonalcoholic fatty liver disease in adult hypopituitary patients with GH deficiency and the impact of GH replacement therapy. *European journal of endocrinology* 167, 67-74 (2012).
42. Yan, M. *et al.* The Relationship Between Tamoxifen-associated Nonalcoholic Fatty Liver Disease and the Prognosis of Patients With Early-stage Breast Cancer. *Clinical breast cancer* 17, 195-203 (2017).
43. Shetty, A., Cho, W., Alazawi, W. & Syn, W.K. Methotrexate Hepatotoxicity and the Impact of Nonalcoholic Fatty Liver Disease. *The American journal of the medical sciences* 354, 172-181 (2017).
44. Asrih, M. & Jornayvaz, F.R. Inflammation as a potential link between nonalcoholic fatty liver disease and insulin resistance. *The Journal of endocrinology* 218, R25-36 (2013).
45. Buzzetti, E., Pinzani, M. & Tsochatzis, E.A. The multiple-hit pathogenesis of non-alcoholic fatty liver disease (NAFLD). *Metabolism: clinical and experimental* 65, 1038-1048 (2016).
46. Li, X.L. *et al.* Gene polymorphisms associated with non-alcoholic fatty liver disease and coronary artery disease: a concise review. *Lipids Health Dis* 15, 53 (2016).
47. Ma, J., Zhou, Q. & Li, H. Gut Microbiota and Nonalcoholic Fatty Liver Disease: Insights on Mechanisms and Therapy. *Nutrients* 9 (2017).
48. Boutari, C., Perakakis, N. & Mantzoros, C.S. Association of Adipokines with Development and Progression of Nonalcoholic Fatty Liver Disease. *Endocrinology and metabolism (Seoul, Korea)* 33, 33-43 (2018).
49. Neuschwander-Tetri, B.A. Non-alcoholic fatty liver disease. *BMC Medicine* 15, 45 (2017).
50. Dharmalingam, M. & Yamasandhi, P.G. Nonalcoholic Fatty Liver Disease and Type 2 Diabetes Mellitus. *Indian journal of endocrinology and metabolism* 22, 421-428 (2018).
51. Fon Tacer, K. & Rozman, D. Nonalcoholic Fatty liver disease: focus on lipoprotein and lipid deregulation. *Journal of lipids* 2011, 783976 (2011).
52. Jornayvaz, F.R. *et al.* Thyroid hormone receptor-alpha gene knockout mice are protected from diet-induced hepatic insulin resistance. *Endocrinology* 153, 583-591 (2012).
53. Jornayvaz, F.R. & Shulman, G.I. Diacylglycerol activation of protein kinase Cepsilon and hepatic insulin resistance. *Cell metabolism* 15, 574-584 (2012).
54. Laplante, M. & Sabatini, D.M. mTORC1 activates SREBP-1c and uncouples lipogenesis from gluconeogenesis. *Proceedings of the National Academy of Sciences of the United States of America* 107, 3281-3282 (2010).
55. Pettinelli, P. & Videla, L.A. Up-regulation of PPAR-gamma mRNA expression in the liver of obese patients: an additional reinforcing lipogenic mechanism to SREBP-1c induction. *J Clin Endocrinol Metab* 96, 1424-1430 (2011).

56. Moon, Y.A. The SCAP/SREBP Pathway: A Mediator of Hepatic Steatosis. *Endocrinology and metabolism (Seoul, Korea)* 32, 6-10 (2017).
57. Tilg, H. & Moschen, A.R. Evolution of inflammation in nonalcoholic fatty liver disease: the multiple parallel hits hypothesis. *Hepatology* 52, 1836-1846 (2010).
58. Yamaguchi, K. *et al.* Inhibiting triglyceride synthesis improves hepatic steatosis but exacerbates liver damage and fibrosis in obese mice with nonalcoholic steatohepatitis. *Hepatology* 45, 1366-1374 (2007).
59. Feldstein, A.E. *et al.* Free fatty acids promote hepatic lipotoxicity by stimulating TNF-alpha expression via a lysosomal pathway. *Hepatology* 40, 185-194 (2004).
60. Mari, M. *et al.* Mitochondrial free cholesterol loading sensitizes to TNF- and Fas-mediated steatohepatitis. *Cell metabolism* 4, 185-198 (2006).
61. Del Campo, J.A., Gallego, P. & Grande, L. Role of inflammatory response in liver diseases: Therapeutic strategies. *World journal of hepatology* 10, 1-7 (2018).
62. Hundertmark, J., Krenkel, O. & Tacke, F. Adapted Immune Responses of Myeloid-Derived Cells in Fatty Liver Disease. *Front Immunol* 9, 2418 (2018).
63. Arrese, M., Cabrera, D., Kalergis, A.M. & Feldstein, A.E. Innate Immunity and Inflammation in NAFLD/NASH. *Digestive diseases and sciences* 61, 1294-1303 (2016).
64. Miura, K., Seki, E., Ohnishi, H. & Brenner, D.A. Role of toll-like receptors and their downstream molecules in the development of nonalcoholic Fatty liver disease. *Gastroenterology research and practice* 2010, 362847 (2010).
65. Martinon, F., Burns, K. & Tschopp, J. The inflammasome: a molecular platform triggering activation of inflammatory caspases and processing of proIL-beta. *Molecular cell* 10, 417-426 (2002).
66. Tilg, H. & Diehl, A.M. Cytokines in alcoholic and nonalcoholic steatohepatitis. *N Engl J Med* 343, 1467-1476 (2000).
67. Guilliams, M. *et al.* Unsupervised High-Dimensional Analysis Aligns Dendritic Cells across Tissues and Species. *Immunity* 45, 669-684 (2016).
68. Krenkel, O. & Tacke, F. Liver macrophages in tissue homeostasis and disease. *Nat Rev Immunol* 17, 306-321 (2017).
69. Duarte, N. *et al.* How Inflammation Impinges on NAFLD: A Role for Kupffer Cells. *BioMed research international* 2015, 984578 (2015).
70. Sica, A., Invernizzi, P. & Mantovani, A. Macrophage plasticity and polarization in liver homeostasis and pathology. *Hepatology* 59, 2034-2042 (2014).
71. Nguyen-Lefebvre, A.T. & Horuzsko, A. Kupffer Cell Metabolism and Function. *Journal of enzymology and metabolism* 1 (2015).
72. Kazankov, K. *et al.* The role of macrophages in nonalcoholic fatty liver disease and nonalcoholic steatohepatitis. *Nature reviews. Gastroenterology & hepatology* (2018).
73. Alisi, A. *et al.* The Role of Tissue Macrophage-Mediated Inflammation on NAFLD Pathogenesis and Its Clinical Implications. *Mediators of inflammation* 2017, 8162421 (2017).
74. Gadd, V.L. *et al.* The portal inflammatory infiltrate and ductular reaction in human nonalcoholic fatty liver disease. *Hepatology* 59, 1393-1405 (2014).
75. Huang, W. *et al.* Depletion of liver Kupffer cells prevents the development of diet-induced hepatic steatosis and insulin resistance. *Diabetes* 59, 347-357 (2010).
76. Neyrinck, A.M. *et al.* Critical role of Kupffer cells in the management of diet-induced diabetes and obesity. *Biochemical and biophysical research communications* 385, 351-356 (2009).
77. Tosello-Trampont, A.C., Landes, S.G., Nguyen, V., Novobrantseva, T.I. & Hahn, Y.S. Kuppfer cells trigger nonalcoholic steatohepatitis development in diet-induced mouse model through tumor necrosis factor-alpha production. *The Journal of biological chemistry* 287, 40161-40172 (2012).
78. Krenkel, O. *et al.* Therapeutic inhibition of inflammatory monocyte recruitment reduces steatohepatitis and liver fibrosis. *Hepatology* 67, 1270-1283 (2018).
79. Tacke, F. Targeting hepatic macrophages to treat liver diseases. *J Hepatol* 66, 1300-1312 (2017).
80. Ju, C. & Tacke, F. Hepatic macrophages in homeostasis and liver diseases: from pathogenesis to novel therapeutic strategies. *Cell Mol Immunol* 13, 316-327 (2016).
81. Chen, L. *et al.* Selective depletion of hepatic Kupffer cells significantly alleviated hepatosteatosis and intrahepatic inflammation induced by high fat diet. *Hepato-gastroenterology* 59, 1208-1212 (2012).
82. Lanthier, N. Targeting Kupffer cells in non-alcoholic fatty liver disease/non-alcoholic steatohepatitis: Why and how? *World journal of hepatology* 7, 2184-2188 (2015).

83. Baeck, C. *et al.* Pharmacological inhibition of the chemokine CCL2 (MCP-1) diminishes liver macrophage infiltration and steatohepatitis in chronic hepatic injury. *Gut* 61, 416-426 (2012).
84. Tamura, Y. *et al.* Inhibition of CCR2 ameliorates insulin resistance and hepatic steatosis in db/db mice. *Arterioscler Thromb Vasc Biol* 28, 2195-2201 (2008).
85. Kanda, H. *et al.* MCP-1 contributes to macrophage infiltration into adipose tissue, insulin resistance, and hepatic steatosis in obesity. *J Clin Invest* 116, 1494-1505 (2006).
86. Miura, K., Yang, L., van Rooijen, N., Ohnishi, H. & Seki, E. Hepatic recruitment of macrophages promotes nonalcoholic steatohepatitis through CCR2. *Am J Physiol Gastrointest Liver Physiol* 302, G1310-1321 (2012).
87. Lefebvre, E. *et al.* Antifibrotic Effects of the Dual CCR2/CCR5 Antagonist Cenicriviroc in Animal Models of Liver and Kidney Fibrosis. *PLoS One* 11, e0158156 (2016).
88. Zhang, X. *et al.* CXC chemokine receptor 3 promotes steatohepatitis in mice through mediating inflammatory cytokines, macrophages and autophagy. *J Hepatol* 64, 160-170 (2016).
89. Zhang, X. *et al.* CXCL10 plays a key role as an inflammatory mediator and a non-invasive biomarker of non-alcoholic steatohepatitis. *J Hepatol* 61, 1365-1375 (2014).
90. Wehr, A. *et al.* Pharmacological inhibition of the chemokine CXCL16 diminishes liver macrophage infiltration and steatohepatitis in chronic hepatic injury. *PLoS One* 9, e112327 (2014).
91. Park, E.J. *et al.* Dietary and genetic obesity promote liver inflammation and tumorigenesis by enhancing IL-6 and TNF expression. *Cell* 140, 197-208 (2010).
92. Tomita, K. *et al.* Tumour necrosis factor alpha signalling through activation of Kupffer cells plays an essential role in liver fibrosis of non-alcoholic steatohepatitis in mice. *Gut* 55, 415-424 (2006).
93. Rivera, C.A. *et al.* Toll-like receptor-4 signaling and Kupffer cells play pivotal roles in the pathogenesis of non-alcoholic steatohepatitis. *J Hepatol* 47, 571-579 (2007).
94. Friedman, S.L. *et al.* A randomized, placebo-controlled trial of cenicriviroc for treatment of nonalcoholic steatohepatitis with fibrosis. *Hepatology* 67, 1754-1767 (2018).
95. Harrison, S.A. *et al.* Randomised clinical study: GR-MD-02, a galectin-3 inhibitor, vs. placebo in patients having non-alcoholic steatohepatitis with advanced fibrosis. *Alimentary pharmacology & therapeutics* 44, 1183-1198 (2016).
96. Traber, P.G. & Zomer, E. Therapy of experimental NASH and fibrosis with galectin inhibitors. *PLoS One* 8, e83481 (2013).
97. McNelis, J.C. & Olefsky, J.M. Macrophages, immunity, and metabolic disease. *Immunity* 41, 36-48 (2014).
98. Feng, X. *et al.* Chrysin attenuates inflammation by regulating M1/M2 status via activating PPARgamma. *Biochemical pharmacology* 89, 503-514 (2014).
99. Luo, W., Xu, Q., Wang, Q., Wu, H. & Hua, J. Effect of modulation of PPAR-gamma activity on Kupffer cells M1/M2 polarization in the development of non-alcoholic fatty liver disease. *Scientific reports* 7, 44612 (2017).
100. Odegaard, J.I. *et al.* Alternative M2 activation of Kupffer cells by PPARdelta ameliorates obesity-induced insulin resistance. *Cell metabolism* 7, 496-507 (2008).
101. Boettcher, E., Csako, G., Pucino, F., Wesley, R. & Loomba, R. Meta-analysis: pioglitazone improves liver histology and fibrosis in patients with non-alcoholic steatohepatitis. *Alimentary pharmacology & therapeutics* 35, 66-75 (2012).
102. Rizos, C.V., Elisaf, M.S., Mikhailidis, D.P. & Liberopoulos, E.N. How safe is the use of thiazolidinediones in clinical practice? *Expert Opin Drug Saf* 8, 15-32 (2009).
103. He, S. *et al.* Pioglitazone prescription increases risk of bladder cancer in patients with type 2 diabetes: an updated meta-analysis. *Tumour biology : the journal of the International Society for Oncodevelopmental Biology and Medicine* 35, 2095-2102 (2014).
104. Floyd, Z.E. & Stephens, J.M. Controlling a master switch of adipocyte development and insulin sensitivity: covalent modifications of PPARgamma. *Biochimica et biophysica acta* 1822, 1090-1095 (2012).
105. Choi, S. *et al.* PPARgamma antagonist Gleevec improves insulin sensitivity and promotes the browning of white adipose tissue. *Diabetes* (2016).
106. Choi, J.H. *et al.* Anti-diabetic drugs inhibit obesity-linked phosphorylation of PPARgamma by Cdk5. *Nature* 466, 451-456 (2010).
107. Hantschel, O., Rix, U. & Superti-Furga, G. Target spectrum of the BCR-ABL inhibitors imatinib, nilotinib and dasatinib. *Leukemia & lymphoma* 49, 615-619 (2008).

108. Cavnar, M.J. *et al.* KIT oncogene inhibition drives intratumoral macrophage M2 polarization. *The Journal of experimental medicine* 210, 2873-2886 (2013).
109. Klawitter, J. *et al.* Time-dependent effects of imatinib in human leukaemia cells: a kinetic NMR-profiling study. *British journal of cancer* 100, 923-931 (2009).
110. Wolf, A.M. *et al.* The kinase inhibitor imatinib mesylate inhibits TNF-{alpha} production in vitro and prevents TNF-dependent acute hepatic inflammation. *Proceedings of the National Academy of Sciences of the United States of America* 102, 13622-13627 (2005).
111. Breccia, M., Muscaritoli, M., Aversa, Z., Mandelli, F. & Alimena, G. Imatinib mesylate may improve fasting blood glucose in diabetic Ph+ chronic myelogenous leukemia patients responsive to treatment. *Journal of clinical oncology : official journal of the American Society of Clinical Oncology* 22, 4653-4655 (2004).
112. Agostino, N.M. *et al.* Effect of the tyrosine kinase inhibitors (sunitinib, sorafenib, dasatinib, and imatinib) on blood glucose levels in diabetic and nondiabetic patients in general clinical practice. *Journal of oncology pharmacy practice : official publication of the International Society of Oncology Pharmacy Practitioners* 17, 197-202 (2011).
113. Morita, S. *et al.* Targeting ABL-IRE1alpha Signaling Spares ER-Stressed Pancreatic beta Cells to Reverse Autoimmune Diabetes. *Cell metabolism* 25, 883-897.e888 (2017).
114. Hagerkvist, R., Sandler, S., Mokhtari, D. & Welsh, N. Amelioration of diabetes by imatinib mesylate (Gleevec): role of beta-cell NF-kappaB activation and anti-apoptotic preconditioning. *Faseb j* 21, 618-628 (2007).
115. Han, M.S. *et al.* Imatinib mesylate reduces endoplasmic reticulum stress and induces remission of diabetes in db/db mice. *Diabetes* 58, 329-336 (2009).
116. Van den Bossche, J., Baardman, J. & de Winther, M.P. Metabolic Characterization of Polarized M1 and M2 Bone Marrow-derived Macrophages Using Real-time Extracellular Flux Analysis. *J Vis Exp* (2015).
117. Kleiner, D.E. *et al.* Design and validation of a histological scoring system for nonalcoholic fatty liver disease. *Hepatology* 41, 1313-1321 (2005).
118. Calabrese, D. & Wieland, S.F. Highly Sensitive Detection of HBV RNA in Liver Tissue by In Situ Hybridization. *Methods in molecular biology (Clifton, N.J.)* 1540, 119-134 (2017).
119. Azizi, G. & Mirshafiey, A. Imatinib mesylate: an innovation in treatment of autoimmune diseases. *Recent patents on inflammation & allergy drug discovery* 7, 259-267 (2013).
120. Leder, C., Ortler, S., Seggewiss, R., Einsele, H. & Wiendl, H. Modulation of T-effector function by imatinib at the level of cytokine secretion. *Experimental hematology* 35, 1266-1271 (2007).
121. Erridge, C., Attina, T., Spickett, C.M. & Webb, D.J. A high-fat meal induces low-grade endotoxemia: evidence of a novel mechanism of postprandial inflammation. *The American journal of clinical nutrition* 86, 1286-1292 (2007).
122. Stephens, R.S., Johnston, L., Servinsky, L., Kim, B.S. & Damarla, M. The tyrosine kinase inhibitor imatinib prevents lung injury and death after intravenous LPS in mice. *Physiological reports* 3 (2015).
123. Artyomov, M.N., Sergushichev, A. & Schilling, J.D. Integrating immunometabolism and macrophage diversity. *Semin Immunol* 28, 417-424 (2016).
124. Choi, S.S. *et al.* PPARgamma Antagonist Gleevec Improves Insulin Sensitivity and Promotes the Browning of White Adipose Tissue. *Diabetes* 65, 829-839 (2016).
125. Leroux, A. *et al.* Toxic lipids stored by Kupffer cells correlates with their pro-inflammatory phenotype at an early stage of steatohepatitis. *J Hepatol* 57, 141-149 (2012).
126. Montecucco, F. & Mach, F. Does non-alcoholic fatty liver disease (NAFLD) increase cardiovascular risk? *Endocrine, metabolic & immune disorders drug targets* 8, 301-307 (2008).
127. Seggewiss, R. *et al.* Imatinib inhibits T-cell receptor-mediated T-cell proliferation and activation in a dose-dependent manner. *Blood* 105, 2473-2479 (2005).
128. Carulli, G. *et al.* Reduced circulating B-lymphocytes and altered B-cell compartments in patients suffering from chronic myeloid leukaemia undergoing therapy with Imatinib. *Hematological oncology* 33, 250-252 (2015).
129. Napier, R.J. *et al.* Low doses of imatinib induce myelopoiesis and enhance host anti-microbial immunity. *PLoS pathogens* 11, e1004770 (2015).
130. Fon Tacer, K., Kuzman, D., Seliskar, M., Pompon, D. & Rozman, D. TNF-alpha interferes with lipid homeostasis and activates acute and proatherogenic processes. *Physiological genomics* 31, 216-227 (2007).

131. Chen, X., Xun, K., Chen, L. & Wang, Y. TNF-alpha, a potent lipid metabolism regulator. *Cell biochemistry and function* 27, 407-416 (2009).
132. Endo, M., Masaki, T., Seike, M. & Yoshimatsu, H. TNF-alpha induces hepatic steatosis in mice by enhancing gene expression of sterol regulatory element binding protein-1c (SREBP-1c). *Experimental biology and medicine (Maywood, N.J.)* 232, 614-621 (2007).
133. Lau, J.K., Zhang, X. & Yu, J. Animal models of non-alcoholic fatty liver disease: current perspectives and recent advances. *The Journal of pathology* 241, 36-44 (2017).
134. Chatrath, H., Vuppalanchi, R. & Chalasani, N. Dyslipidemia in patients with nonalcoholic fatty liver disease. *Semin Liver Dis* 32, 22-29 (2012).
135. Nepali, S. *et al.* Euphorbia supina extract results in inhibition of highfatdietinduced obesity in mice. *International journal of molecular medicine* 41, 2952-2960 (2018).
136. Liu, Z. *et al.* High-fat diet induces hepatic insulin resistance and impairment of synaptic plasticity. *PLoS One* 10, e0128274 (2015).
137. Schaffler, A., Scholmerich, J. & Buchler, C. Mechanisms of disease: adipocytokines and visceral adipose tissue--emerging role in nonalcoholic fatty liver disease. *Nature clinical practice. Gastroenterology & hepatology* 2, 273-280 (2005).
138. Hagerkvist, R., Jansson, L. & Welsh, N. Imatinib mesylate improves insulin sensitivity and glucose disposal rates in rats fed a high-fat diet. *Clinical science (London, England : 1979)* 114, 65-71 (2008).
139. Shao, W. & Espenshade, P.J. Expanding roles for SREBP in metabolism. *Cell Metab* 16, 414-419 (2012).
140. Im, S.S. *et al.* Linking lipid metabolism to the innate immune response in macrophages through sterol regulatory element binding protein-1a. *Cell Metab* 13, 540-549 (2011).
141. Varga, T., Czimmerer, Z. & Nagy, L. PPARs are a unique set of fatty acid regulated transcription factors controlling both lipid metabolism and inflammation. *Biochimica et biophysica acta* 1812, 1007-1022 (2011).
142. Kim, D.H. *et al.* Critical Roles of the Histone Methyltransferase MLL4/KMT2D in Murine Hepatic Steatosis Directed by ABL1 and PPARgamma2. *Cell reports* 17, 1671-1682 (2016).
143. Guerra, C., Koza, R.A., Yamashita, H., Walsh, K. & Kozak, L.P. Emergence of brown adipocytes in white fat in mice is under genetic control. Effects on body weight and adiposity. *J Clin Invest* 102, 412-420 (1998).
144. Gonzalez, Y. *et al.* High glucose concentrations induce TNF-alpha production through the down-regulation of CD33 in primary human monocytes. *BMC Immunol* 13, 19 (2012).
145. Lee, H.M. *et al.* Upregulated NLRP3 inflammasome activation in patients with type 2 diabetes. *Diabetes* 62, 194-204 (2013).
146. Netea, M.G. *et al.* Differential requirement for the activation of the inflammasome for processing and release of IL-1beta in monocytes and macrophages. *Blood* 113, 2324-2335 (2009).
147. Tonyali, O. *et al.* Imatinib mesylate-induced acute liver failure in a patient with gastrointestinal stromal tumors. *Med Oncol* 27, 768-773 (2010).
148. https://clinicaltrials.gov/ct2/show/NCT01781975?term=imatinib+and+diabetes&rank=1.